Structural studies of IPK1: how molecular turtles are made

By

Varin Gosein

Department of Pharmacology and Therapeutics
McGill University
Montreal, Québec, Canada

December 2013

A thesis submitted to McGill University in partial fulfillment of the requirements of the degree of Doctor of Philosophy

For my parents,

whose unwavering love and support have made this possible

Abstract

Inositol phosphates (IPs) are signaling molecules implicated in a variety of cellular processes, notably, cell survival signaling and vesicular trafficking, which underlie diseases such as cancer and diabetes. The specific roles of many IPs in disease states have yet to be determined. Inositol phosphate kinases (IPKs) phosphorylate inositol 1,4,5-trisphosphate (IP_3) on different positions of its inositol ring to yield an array of unique IPs. Control of IP production at different stages of the IP metabolic pathway could be used as an approach to determine the functional roles of each IP. In this thesis, we focus on inositol 1,3,4,5,6-pentakisphosphate 2-kinase (IPK1), which phosphorylates IP_5 to IP_6. These two IPs regulate apoptosis *in vitro* and *in vivo*, revealing a role for IPK1 in cell death, but their precise mechanisms of action remain unresolved. Our overall goal was to structurally and biochemically characterize IPK1 to identify how it selects its substrates, how it is regulated, and how it may be targeted with small molecules to be used as tools to study IPK1 function. We determined the IP-free crystal structure of IPK1, which revealed that the N-lobe of IPK1 is unstable in the absence of substrate. Based on this observation, we hypothesized that IPK1 uses a mechanism of IP-induced stabilization to select IP_5 as its substrate: IP_5 is initially recognized by IPK1 through the 4-, 5-, and 6-phosphates, and then, the 1- and 3-phosphates induce N-lobe stabilization, thereby allowing IPK1 activation only when the appropriate IP is bound. The key interaction between R130 and the 1-phosphate of the IP stabilizes the N-lobe for subsequent kinase activation. To validate our hypothesis, we evaluated the role of each IP phosphate for IP binding and kinase activation. We determined that the 5- and 6-phosphates were more important for IP binding, while the 1- and 3-phosphates were more important for IPK1 activation. Moreover, we demonstrated that IPs lacking the 1- or 3-phosphates were unable to stabilize IPK1 to the same extent as IP_5, and that artificial stabilization of the N-lobe by engineered disulfide bonds altered IPK1 substrate specificity, by reducing the need for N-lobe interactions with substrate. We also characterized PKRnc and Catechin Gallate as leads for the development of small molecule inhibitors of IPK1. Taken together, our studies provide a basis for the development of selective inhibitors for IPK1 to investigate the roles of IPs that modulate apoptotic signaling pathways. Moreover, IP-induced stabilization distinguishes IPK1 from other IPKs and

provides important considerations for the selective inhibition of each IPK. Uncovering the role of IPs in different cellular processes may ultimately lead to novel treatments for diseases whose underlying mechanisms are mediated by IP signaling.

Résumé

Inositol phosphates (IPs) représentent une classe de molécules de signalisation qui sont impliqués dans différents processus cellulaires, en particulier dans la signalisation de la survie cellulaire et le trafic vésiculaire, qui sont la base des maladies telles que le cancer et le diabète. Les rôles spécifiques de plusieurs IPs dans des états pathologiques n'ont pas encore été déterminés. Inositol phosphates kinases (IPKs) catalysent la phosphorylation de inositol 1,4,5-trisphosphate (IP_3) sur différentes positions de son cycle d'inositol pour créer de nouveaux IPs qui sont uniques. Le control de la production des IPs à différentes étapes de la voie métabolique des IPs pourrait être utilisé pour découvrir les rôles fonctionnels de chaque IP. Dans cette thèse, nous nous concentrons sur inositol 1,3,4,5,6-pentakisphosphate 2-kinase (IPK1), qui catalyse la formation de IP_6 à partir de IP_5. Ces deux IPs régulent l'apoptose *in vitro* et *in vivo* et dévoilent un rôle pour IPK1 dans la mort cellulaire, mais leurs mécanismes d'actions précises ne fut résolus. Notre objectif était de caractériser IPK1, en démontrant sa structure et sa biochimie, pour déterminer comment celle-ci choisit ses substrats, de quel façon il est réglementé, et comment il peut être ciblé pour étudier sa fonction cellulaire. Nous avons obtenu la structure cristallographique de IPK1 sans que IP soit présent, qui révéla que le N-lobe de IPK1 est deséquilibré dans l'absence de IP. D'après cette observation, nous avons supposé que IPK1 utilise un mécanisme de 'stabilisation induit par IP' pour sélectionner IP_5 comme son substrat natif: Initialement, le 4-, 5-, et 6-phosphate de IP_5 sont reconnus par IPK1, et par ensuite, le 1- et 3-phosphate de IP_5 induisent la stabilisation du N-lobe, qui permit l'activation de IPK1 seulement quand le IP correspondant est attaché. L'interaction entre R130 et le 1-phosphate du IP stabilise le N-lobe pour l'activation de la kinase. Pour valider notre hypothèse, nous avons évalué le rôle de chaque phosphate du IP pour l'engagement de IPK1 et l'activation de IPK1. Nous démontrâmes que le 5- et 6-phosphate sont plus importants pour engager IPK1 tandis que le 1- et 3-phosphate sont plus importants pour l'activation de IPK1. De plus, nous avons démontré que les IPs qui manquent le 1- et 3-phosphate ont été incapable de stabiliser IPK1 dans la même mesure que IP_5, et que la stabilisation artificielle du N-lobe a modifié la spécificité de substrat de IPK1, en réduisant la nécessité pour les interactions entre le N-lobe et le substrat. Nous avons également

caractérisé PKRnc et Catechin Gallate comme des pistes pour le développement d'inhibiteurs pour IPK1. Nos études fournissent une base importante pour le développement d'inhibiteurs sélectifs pour IPK1 pour enquêter sur les rôles des IPs qui modulent les voies de signalisation apoptotiques. Pour ajouter, la 'stabilisation induit par IP' distingue IPK1 d'autres IPKs et fournit des considérations importantes pour l'inhibition sélective de chaque IPK. En découvrant les rôles des IPs dans différents processus cellulaires, on peut finalement conduire de nouveaux traitements pour les maladies dont les mécanismes sous-jacents sont médiés par la signalisation IP.

Table of Contents

List of Figures and Tables

FIGURES

TABLES

List of Abbreviations

1,3,4,5-IP_4	inositol 1,3,4,5-tetrakisphosphate
1,3,4,6-IP_4	inositol 1,3,4,6-tetrakisphosphate
1,3,4-IP_3	inositol 1,3,4-trisphosphate
1,4,5,6-IP_4	inositol 1,4,5,6-tetrakisphosphate
1,5-PP_2-IP_4	1,5-diphosphoinositol 2,3,4,6-tetrakisphosphate
3,4,5.6-IP_4	inositol 3,4,5,6-tetrakisphosphate
1-PP-IP_5	1-diphosphoinositol 2,3,4,5,6-pentakisphosphate
5-PP-IP_4	5-diphosphoinositol 3,4,5,6-tetrakisphosphate
5-PP-IP_5	5-diphosphoinositol 1,2,3,4,6-pentakisphosphate
ADP	adenosine diphosphate
Akt	protein kinase B
AMPPNP	adenosine 5'-β,γ-imido triphosphate
ArgR	arginine repressor
ATP	adenosine triphosphate
C	catechin
Ca^{2+}	calcium ion
CaM	Ca^{2+}/calmodulin
CaMKII	Ca^{2+}/calmodulin-dependent protein kinase II
CF	cystic fibrosis
CFTR	cystic fibrosis transmembrane conductance regulator
CG	catechin gallate
CK2	casein kinase II
Cl^-	chloride ion
ClC-3	chloride channel 3
COI-1	coronatine-insensitive protein 1
DAG	diacylglycerol
Dbp5	DEAD-box protein 5
DIPP	diphosphoinositol-polyphosphate diphosphatase
DMSO	dimethyl sulfoxide
DNA	deoxyribonucleic acid
DSF	differential scanning fluorimetry
DTT	dithiothreitol

EC	epicatechin
ECG	epicatechin gallate
EGC	epigallocatechin
EGCG	epigallocatechin gallate
EGFR	epidermal growth factor receptor
ER	endoplasmic reticulum
ERFD	early renal function decline
ERK	extracellular signal-regulated kinase
Fz	frizzled
$GAP1^{IP4BP}$	GTPase-activating protein 1
$GAP1^{m}$	Ras GTPase-activating protein 2
GC	gallocatechin
GI	gastrointestinal tract
G-loop	glycine rich loop
GPI	glycosylphosphatidylinositols
GSK3β	glycogen synthase kinase 3
Hb	hemoglobin
HDAC	histone deacetylase
HEPES	4-(2-hydroxyethyl)-1-piperazineethanesulfonic acid
HRM	high resolution melt
IFN-β	interferon-β
IP	inositol phosphate
IP_3	inositol 1,4,5-trisphosphate
IP_3K	inositol 1,4,5-trisphosphate 3-kinase
IP_4	inositol tetrakisphosphate
IP_5	inositol 1,3,4,5,6-pentakisphosphate
IP_6	inositol 1,2,3,4,5,6-hexakisphosphate
IP_6K	inositol 1,2,3,4,5,6-hexakisphosphate kinase
IPK	inositol phosphate kinase
IPK1	inositol 1,3,4,5,6-pentakisphosphate 2-kinase
IPK2	yeast inositol phosphate multikinase
IPMK	inositol phosphate multikinase
IPTG	isopropyl β-D-1-thiogalactopyranoside
ITC	isothermal titration calorimetry

ITPK1	inositol 1,3,4-trisphosphate 5/6-kinase
KPO_4	potassium phosphate
Mcm1	minichromosome maintenance protein 1
MES	2-(N-morpholino)ethanesulfonic acid
$MgCl_2$	magnesium chloride
MTA1	metastasis-associated protein
NCOR2	nuclear receptor corepressor 2
NPC	nuclear pore complex
NIH	National Institutes of Health
O_2	oxygen
PDB	Protein Data Bank
PDK1	phosphoinositide-dependent kinase-1
PEG	polyethylene glycol
PH	pleckstrin homology
Pho5	repressible acid phosphatase
PI	phosphatidylinositides
PI3K	phosphoinositide 3-kinase
PIP_2	phosphatidylinositol 4,5-bisphosphate
PIP_3	phosphatidylinositol 3,4,5-trisphosphate
PK	protein kinase
PKA	protein kinase A
PKC	protein kinase C
PKR	protein kinase RNA-activated
PKRnc	protein kinase RNA-activated negative control
PLC	phospholipase C
PO_4	phosphate
PP-IP	diphosphoinositol phosphate
$PPIP_5K$	5-diphosphoinositol 1,2,3,4,6-pentakisphosphate kinase
PTEN	phosphatase and tensin homolog
RAF	rapidly accelerated fibrosarcoma
RASA3	Ras GTPase-activating protein 3
RMSD	root mean squared deviation
RNA	ribonucleic acid
RNAi	RNA interference

rRNA	ribosomal ribonucleic acid
SARs	structure-activity relationships
SKOV-3	human ovarian carcinoma continuous cell line
SopB	inositol phosphate phosphatase
STS	staurosporine
TCEP	tris-2-carboxyethyl phosphine
TCOF1	treacle protein
THF	3',4',7',8'-tetrahydroxyflavone
TNF	tumor necrosis factor
UBF	nucleolar transcription factor 1
Wnt	wingless-related integration site

Statement of Contributions

This dissertation is in a manuscript-based format in accordance with the Guidelines for Thesis Preparation from the Graduate and Postdoctoral Studies Office of McGill University. This thesis is comprised of three published manuscripts and one manuscript in preparation. The contribution of each author is described below.

Chapter 2: Inositol phosphate-induced stabilization of inositol 1,3,4,5,6-pentakisphosphate 2-kinase and its role in substrate specificity.
Protein Science. 2012. 21(5):737-742.
Varin Gosein, Ting-Fung Leung, Oren Krajden, Gregory J. Miller

All experiments were performed by Varin Gosein, Ting-Fung Leung, and Oren Krajden.
Varin Gosein purified IPK1, optimized the IPK1 crystals, collected and processed X-ray diffraction data, determined and refined the structure of IPK1, and performed the limited proteolysis assay. Ting-Fung Leung optimized IPK1 purification and grew initial IPK1 crystals. Oren Krajden expressed and purified IPK1.
The manuscript was prepared by Varin Gosein and Gregory J. Miller.

Chapter 3: Roles of phosphate recognition in inositol 1,3,4,5,6-pentakisphosphate 2-kinase substrate binding and activation.
Journal of Biological Chemistry. 2013. 288(37):26908-26913.
Varin Gosein and Gregory J. Miller

All experiments were performed by Varin Gosein.
The manuscript was prepared by Varin Gosein and Gregory J. Miller.

Chapter 4: Conformational stability of inositol 1,3,4,5,6-pentakisphosphate 2-kinase dictates its substrate selectivity.
Journal of Biological Chemistry. 2013. doi: 10.1074/jbc.M113.512731.
Varin Gosein and Gregory J. Miller

All experiments were performed by Varin Gosein.
The manuscript was prepared by Varin Gosein and Gregory J. Miller.

Chapter 5: Identification of small molecule inhibitors of inositol 1,3,4,5,6-pentakisphosphate 2-kinase.
Manuscript In Preparation.
Varin Gosein and Gregory J. Miller

All experiments were performed by Varin Gosein.
The manuscript was prepared by Varin Gosein and Gregory J. Miller.

Contributions to Original Knowledge

1. Inositol phosphate-induced stabilization of inositol 1,3,4,5,6-pentakisphosphate 2-kinase and its role in substrate specificity. Varin Gosein, Ting-Fung Leung, Oren Krajden, Gregory J. Miller. Protein Science. 2012. 21(5):737-742.

This study is the first to show that IPK1 adopts multiple conformational states during its catalytic cycle. We also showed that the stability of IPK1 is dependent on the binding of the IP substrate. Moreover, we solved the first crystal structure of IPK1 in the absence of IP (Protein Data Bank code: 3UDS) and compared it to a crystal structure of IPK1 bound to IP (Protein Data Bank code: 3UDZ), which demonstrates that the N-lobe of IPK1 is unstable in the absence of IP. These findings provided the initial evidence to allow us to propose a two-step model of IP-induced stabilization of IPK1 whereby the IP is first recognized by the stable C-lobe, and then specific interactions between the IP and the N-lobe fully stabilize IPK1. Our model is the first proposal put forth to explain how IPK1 selects its IP substrate.

2. Roles of phosphate recognition in inositol 1,3,4,5,6-pentakisphosphate 2-kinase substrate binding and activation. Varin Gosein and Gregory J. Miller. Journal of Biological Chemistry. 2013. 288(37):26908-26913.

This is the first study to employ different IPs to systematically test the effect of each substrate phosphate group on binding and activation of an IPK. We also developed a simple and effective approach based on luminescence for measuring activity of IPK1, avoiding the use of more complicated experimental procedures using HPLC or radio-labeled substrates. Our findings indicate that each phosphate group of the IP plays a distinct role in binding or activation of IPK1 and there are only three critical residues that important for IPK1 activation, supporting in part our proposed model. Understanding the mechanism of IP recognition of IPK1 could ultimately lead to the development of selective inhibitors for IPK1.

3. Conformational stability of inositol 1,3,4,5,6-pentakisphosphate 2-kinase dictates its substrate selectivity. Varin Gosein and Gregory J. Miller. Journal of Biological Chemistry. 2013. doi: 10.1074/jbc.M113.512731.

This study is the first to employ differential scanning fluorimetry to directly measure the overall stability of an IPK. We systematically tested IPs with different phosphate profiles to demonstrate how phosphates of the IP stabilize the N-lobe of IPK1. This proves for the first time that IPK1 substrate specificity is linked to IPK1 stability. Furthermore, we describe how we can manipulate the substrate specificity of IPK1 through introduction of disulfide bonds that artificially stabilize the N-lobe of IPK1. We solved the crystal structure of an IPK1 disulfide mutant (Protein Data Bank code: 4LV7), which shows the disulfide bond present. Altogether, these findings fully support our model of IP-induced stabilization for IPK1, a novel mechanism of IP recognition for IPKs.

4. Identification of small molecule inhibitors of inositol 1,3,4,5,6-pentakisphosphate 2-kinase. Varin Gosein and Gregory J. Miller. In preparation.

This work represents the first inhibitor screening of IPK1. We tested the sensitivity of IPK1 to polyphenolic inhibitors, kinase inhibitors and other structurally diverse compounds. In total, we identified >40 novel inhibitors of IPK1 that partially or fully inhibit IPK1. We demonstrate that IPK1 is sensitive to the polyphenol EGCG, describe structure-activity relationships of EGCG analogs, and identified a highly potent analog, CG. We also identified PKRnc amongst kinase inhibitors as a promising inhibitor of IPK1. Furthermore, our work reveals for the first time that IPK1 is not sensitive to most kinase inhibitors, even though IPK1 and protein kinases are structurally similar. Finally, we describe the type of competitive inhibition for CG and PKRnc, which suggests a novel allosteric binding site on IPK1. Collectively, these findings provide numerous opportunities for the development of selective inhibitors of IPK1 for future study of higher inositol phosphate signaling and the role of IPK1 in mammals.

Publications

Inositol phosphate-induced stabilization of inositol 1,3,4,5,6-pentakisphosphate 2-kinase and its role in substrate specificity
Varin Gosein, Ting-Fung Leung, Oren Krajden, Gregory J. Miller
Protein Science. 2012. 21(5):737-742.

Roles of phosphate recognition in inositol 1,3,4,5,6-pentakisphosphate 2-kinase substrate binding and activation
Varin Gosein and Gregory J. Miller
Journal of Biological Chemistry. 2013. 288(37):26908-26913.

Conformational stability of inositol 1,3,4,5,6-pentakisphosphate 2-kinase dictates its substrate selectivity
Varin Gosein and Gregory J. Miller
Journal of Biological Chemistry. 2013. doi: 10.1074/jbc.M113.512731.

"Click" dendrimers as anti-inflammatory agents: with insights into their binding from molecular modeling studies.
Kevin Neibert*, Varin Gosein*, Anjali Sharma, Mohidus Khan, Michael A. Whitehead, Dusica Maysinger, Ashok Kakkar
Molecular Pharmaceutics. 2013. 10(6):2502-2508.
*indicates shared first-authorship

Acknowledgements

First and foremost, I would like to express my sincere thanks to my supervisor, **Dr. Gregory Miller**, for his guidance, patience, and support over the course of my doctoral studies. I am especially grateful for his continued enthusiasm under difficult circumstances and his respect for my intellectual freedom, both of which were paramount in helping me to complete my thesis. Thank you very much for allowing me to work with you and learn from you. Your intensity and work ethic always motivated me to strive for excellence.

I would like to express a special thanks to my advisor, **Dr. Dan Bernard**, for his counsel and motivational support over the years. I also thank my committee members, **Dr. Albert Berghuis** and **Dr. Uri Saragovi**, for their enthusiasm about my work and for their constructive recommendations at committee meetings. I would also like to thank **Dr. Dusica Maysinger** for a positive research collaboration and a rewarding teaching opportunity.

I would like to thank a special friend and colleague, **Dr. Hatem Dokainish**. Your professional guidance, moral support, and true friendship gave me the strength I needed to get through tough times.

I thank a longtime friend and colleague, **Sebastien Boridy**. We have shared many memorable moments together throughout our academic careers. I have always appreciated your selflessness, positive energy, and work ethic. We have both come a very long way and I am proud that we have made the journey together.

I sincerely thank my longtime and closest friends: **Khashayar Afshar**, **Moneesh Jhamb**, **Amir Kahnamouee**, **Shawn Lennox**, **Yvonne Quan**, and **Jason Tan**. Throughout my studies, you have all been there for me. You guys have been an infinite source of moral support. We have shared a lifetime of laughter together. I cannot thank you enough.

Thank you to past and present members of the Miller Lab: **Gayane Machkalyan, Elizabeth Andrews, Vanessa Libasci, David Sterling**, and **Ting Feung Lung**. You have all been a pleasure to work with and I am fortunate to call all of you both colleagues and friends. I sincerely thank you for your helpful discussions, your positive encouragement, and your professionalism. I could not have completed my studies without you.

Thank you to members of the Maysinger Lab, who have "adopted" me over the years: **Angela Choi, Armen Khatchadourian, Manasi Jain**, and **Kevin Neibert**; and thank you to two other colleagues, **Catherine Ho** and **Raminder Gill**. I am very grateful for the support all of you have given me throughout the years, especially when I was the only student in the lab. I am sincerely thankful to have befriended all of you and I thank you for lightening the mood during my graduate school experience.

I would also like to thank the administrative staff in the Department of Pharmacology and Therapeutics: **Hélène Duplessis, Chantal Grignon, David Kalant, Tina Tremblay,** and **Heidi Cheung**. I appreciate your patience, your help, and all that did in the background to facilitate my graduate school experience.

Thank you to the **McGill Chemical Biology Scholarships** (2008, 2009) and **McGill Excellence Fellowships** (2007, 2009, 2011) for their financial support.

Finally, I would like to express my deepest gratitude towards my family: my mother and father, **Norma** and **Sona**, and my two brothers, **Adesh** and **Satyanand**. You have loved me unconditionally. You have given me everything I need to succeed in my education and in life. You have demonstrated the meaning of hard work, ambition, perseverance, strength, duty, and especially, patience. I am so fortunate to have you as my family and I deeply appreciate all that you have done for me.

Chapter 1. General Introduction

1.1 Statement of the purpose of the investigation

Cellular signaling is a complex system comprised of receptors, enzymes, scaffolding machinery, and small molecules that coordinate the basic functions of the cell. This field grows in complexity with our understanding of different signaling systems and their regulation. The interest in this field is driven by the underlying principal that disruptions in cellular signaling contribute to diseases such as cancer and diabetes and the discovery of a new receptor, ligand, signaling event, signaling pathway, or its regulation leads us one step closer to effective treatments for these diseases.

During the 1980s, the inositol phosphate, inositol 1,4,5-trisphosphate (IP_3), was recognized as a second messenger for calcium release. Over the next 30 years, it was discovered that IP_3 is metabolized into many other inositol phosphates (IPs), together, comprising a new class of signaling molecules. Since the early 1990s, the enzymes that carry out these metabolic reactions have been identified and their actions studied.

Despite the wealth of knowledge on cellular signaling, how IP signaling affects cellular events remains poorly understood. There has been much success in measuring changes in IP levels during a variety of cellular processes; however, the specific roles of many of the IPs in those processes remain unclear: With what do they interact? How do they modulate the activity of cellular receptors? More importantly, can we identify new IP targets and approaches to regulate disruptions in cellular signaling in disease states? The answers to these questions are plagued by the lack of tools to attenuate production of specific IPs to discover their functional importance.

In this thesis, we open up a new avenue to explore the functional roles of higher IPs that are implicated in cell death. We focus on the enzyme, inositol 1,3,4,5,6-pentakisphosphate 2-kinase (IPK1), which is uniquely positioned at a bottleneck in the pathways for the production of higher IPs. In our first three aims, we structurally and biochemically characterize IPK1 to distinguish it from related enzymes. In our last aim, we identify novel small molecule inhibitors of IPK1. Taken together, these aims provide a basis for the selective targeting of IPK1, which could be used for the future study of higher IPs.

1.2 Inositol

Inositol is a carbohydrate that consists of a cyclohexane core with one hydroxyl group positioned on each carbon of the ring. Inositol was first isolated from muscle extracts by Scherer in 1850 and was named for the Greek word for 'muscle' (Posternak, 1965). Although the chemical structure of inositol appears very simple, inositol possesses complex stereochemistry that ultimately serves as the basis for the production of a myriad of derivatives. In theory, each of the six hydroxyl groups on the cyclohexane ring can be oriented with axial or equatorial stereochemistry resulting in nine different stereoisomers of inositol (Murthy, 2006). For example, the six hydroxyl groups are positioned equatorially in *scyllo*-inositol, while *myo*-inositol possesses five equatorial hydroxyl groups and one axial hydroxyl group. The *allo*-, *cis*-, and *muco*-isomers each have three axial hydroxyl groups, while the *epi*- and *neo*-isomers each have two axial hydroxyl groups. The *chiro*-isomer also has two axial hydroxyl groups as well, but are positioned such that two chiral enantiomers exist, the D-*chiro*-inositol and L-*chiro* inositol forms. To date, six of these isomers have been discovered in nature: *myo*-, *muco*-, *neo*-, D-*chiro*-, L-*chiro*-, and *scyllo*-isomers (Murthy, 2006). More importantly, *myo*-inositol is the most abundant stereoisomer in nature and occupies a central role in cellular metabolism and signal transduction (Loewus and Murthy, 2000; Murthy, 2006). *myo*-Inositol serves as the basis for the biosynthesis of inositol phosphates (IPs), phosphatidylinositides (PIs), and glycosylphosphatidylinositols (GPIs) (Murthy, 2006).

1.3 Nomenclature of inositol

In 1976, the International Union of Pure and Applied Chemistry (IUPAC) issued recommendations for the assignment of the stereochemistry (D or L) and carbon numbering to be used for the nomenclature for inositol and its derivatives (IUPAC, 1976). When *myo*-inositol is drawn as a horizontal projection, there are two sets of hydroxyl groups: one set positioned above the ring (C1, C2, C3, and C5); and one set positioned below the ring (C4 and C6). IUPAC rules state that C1 should be assigned to an enantiotopic carbon in the set that contains the most number of substituents. Numbering then proceeds towards the next carbon in that

set. If carbon numbering proceeds counterclockwise, then the D-stereochemical assignment is used in the nomenclature of the IP. If numbering proceeds clockwise, then the L-stereochemical assignment is used. *myo*-inositol possesses internal symmetry, in which two enantiotopic carbons may be assigned C1, so it is possible to use either numbering scheme. In this thesis, the D-numbering scheme will be used for all nomenclature of IPs, as it is most widely used in modern literature (Shears, 2004) (Figure 1.1). In the D-stereochemical configuration, the axial hydroxyl of *myo*-inositol is on the second carbon (C2) of the inositol ring. A frequently used metaphor for this numbering derives from the similarity of the thermodynamically stable chair configuration of D-*myo*-inositol to a turtle (Agranoff, 1978) (Figure 1.1). The head represents the axial hydroxyl on the second carbon, and the four limbs and tail represent the five equatorial hydroxyl groups. The right hand limb is the 1-position, the left hand limb is the 3-position, and carbon numbering proceeds counterclockwise.

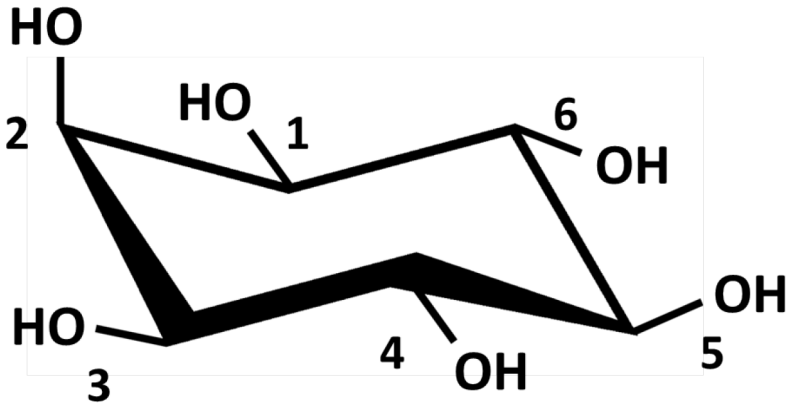

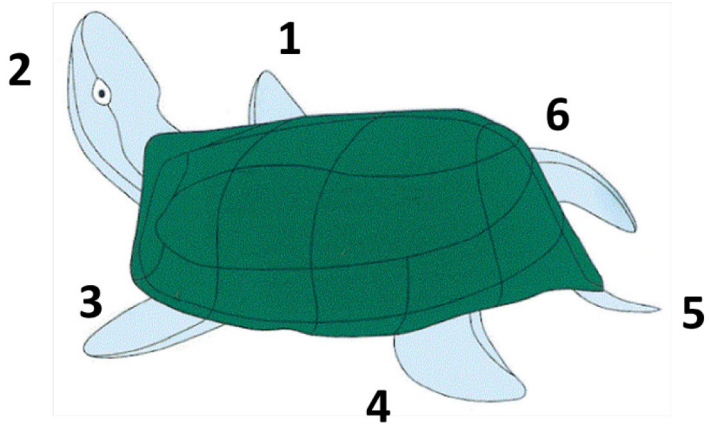

Figure 1.1. Stereochemistry of D-*myo*-inositol.

Adapted from Shears, 2004, in accordance with The Biochemical Society.

1.4 Inositol phosphates

One of the aforementioned derivatives of inositol are IPs, which are obtained by the addition of a phosphate moiety to any of the hydroxyl groups of the inositol ring (Murthy, 2006). Unlike their inositol-containing lipid counterparts, IPs are water-soluble compounds. The further addition of a phosphate moiety to an already phosphorylated position of the inositol ring yields derivatives known as diphosphoinositol phosphates (PP-IPs). Linkage of a diacylglycerol (DAG) moiety on the 1-hydroxyl of an IP creates other derivatives known as phosphatidylinositols (PIs), which are not water-soluble. IPs were initially discovered in 1919 in plants and were thought to be part of a phosphate storage mechanism (Posternak, 1919). In 1983, IP_3 was identified as a second messenger that mobilized Ca^{2+} release and the notion of IPs as signaling molecules was established (Streb et al., 1983). Over the next 30 years, the role of IPs in cellular signaling was reinforced as the identification and study of IP_3s, IP_4s, IP_5s, IP_6, and PP-IPs was conducted in mammals, plants, and other species (Irvine and Schell, 2001). However, key questions remain unanswered: What are the physiological roles of each of these identified IPs? What are their mechanisms of action? How are these IPs produced and metabolized? What roles, if any, do these IPs play in known human diseases? The answers to these questions are further complicated by the fact that over 30 IPs have been identified within the cell, multiple metabolic pathways can regulate the levels of IPs, and individual IPs can regulate multiple cellular processes (Shi et al., 2006).

1.5 IP metabolic pathways

In all eukaryotes, the most abundant IPs are created by the phosphorylation of IP_3 at different positions of the inositol ring to yield an array of IPs (Figure 1.2). These phosphorylation reactions are carried out by a family of enzymes known as inositol phosphate kinases (IPKs) (Shears, 2004). Dephosphorylation of IPs may also occur by a series of phosphatases (Irvine and Schell, 2001). In all eukaryotes, IP_3 and DAG are obtained by cleavage of phosphatidylinositol 4,5-bisphosphate (PIP_2) by phospholipase C (PLC). Those IP metabolic pathways in yeast, plants, and mammals that are currently understood to be the most important will be

outlined, however, there exists many more IP interconversions that will not be mentioned here (Irvine and Schell, 2001).

1.5.1 IP metabolism in yeast and plants

In yeast and in plants, IP_3 is first phosphorylated on the 6-position of the inositol ring to yield inositol 1,4,5,6-tetrakisphosphate (1,4,5,6-IP_4), and subsequently on the 3-position to yield inositol 1,3,4,5,6-pentakisphosphate (IP_5). Both phosphorylation reactions are carried out separately by inositol phosphate multikinase (IPMK) (Odom et al., 2000; Stevenson-Paulik et al., 2002; Saiardi et al., 2000a). IP_5 is then phosphorylated on the 2-position by inositol 1,3,4,5,6-pentakisphosphate 2-kinase (IPK1) to yield inositol 1,2,3,4,5,6-hexakisphosphate (IP_6), also known as phytic acid (York et al., 1999; Ives et al., 2000). IP_6 is further phosphorylated by IP_6 kinase (IP_6K) on the 5-position resulting in the formation of 5-diphosphoinositol 1,2,3,4,6-pentakisphosphate (5-PP-IP_5) (Saiardi et al., 1999). IP_6K can also phosphorylate IP_5 on the 5-position to yield 5-diphosphoinositol 3,4,5,6-tetrakisphosphate (5-PP-IP_4) in yeast, but not plants (Saiardi et al., 2000b). 5-PP-IP_5 can be further phosphorylated on the 1-position by PP-IP_5 kinase ($PPIP_5K$) to yield 1,5-diphosphoinositol 2,3,4,6-tetrakisphosphate (1,5-PP_2-IP_4) (Mulugu et al., 2007; Lin et al., 2009). PP-IPs can be converted back to IP_6 by the cleavage of the pyrophosphate moieties by diphosphoinositol-polyphosphate diphosphatases (DIPPs) (Barker et al., 2009).

1.5.2 IP metabolism in mammals

In mammals, several intermediates exist between IP_3 and IP_5, but the conversion of IP_5 to IP_6 and higher IPs remains identical to yeast and plants. In mammals, IP_3 is first phosphorylated on the 3-position by inositol 1,4,5-trisphosphate 3-kinase (IP_3K) to yield inositol 1,3,4,5-tetrakisphosphate (1,3,4,5-IP_4) (Batty et al., 1985; Irvine et al., 1986). Then, a 5-phosphatase dephosphorylates 1,3,4,5-IP_4 to inositol 1,3,4-trisphosphate (1,3,4-IP_3) (Connolly et al., 1987). 1,3,4-IP_3 is then phosphorylated on the 6-position by inositol 1,3,4-trisphosphate 5/6-kinase (ITPK1) to yield inositol 1,3,4,6-tetrakisphosphate (1,3,4,6-IP_4) (Shears et al., 1987; Balla et al., 1987; Stephens et al., 1988). Finally,

a homolog of IPMK phosphorylates the 5-position of 1,3,4,6-IP_4 to obtain IP_5 (Nalaskowski et al., 2002; Chang et al., 2002). In a branch of this pathway, 1,4,5,6-IP_4 can be phosphorylated by IPMK on the 3-position to yield IP_5 (Chang et al., 2002). Dephosphorylation of IP_5 on the 3-position can occur by the phosphatase PTEN to obtain 1,4,5,6-IP_4 (Caffrey et al., 2001). In a deadend branch of this pathway, dephosphorylation of IP_5 on the 1-position by ITPK1 yields inositol 3,4,5,6-tetrakisphosphate (3,4,5,6-IP_4) (Chamberlain et al., 2007), which undergoes cycles of phosphate addition and removal to create and eliminate a signaling molecule. Further phosphorylation of IP_5 is achieved using the same set of enzymes in mammals as in yeast and plants (Saiardi et al., 1999; Saiardi et al., 2001b; Schell et al., 1999). Thus, IPK1 acts as a gatekeeper for IP_6 and higher IPs in all three species and IP_5 serves as a metabolic 'hub' for higher IPs (Irvine and Schell, 2001).

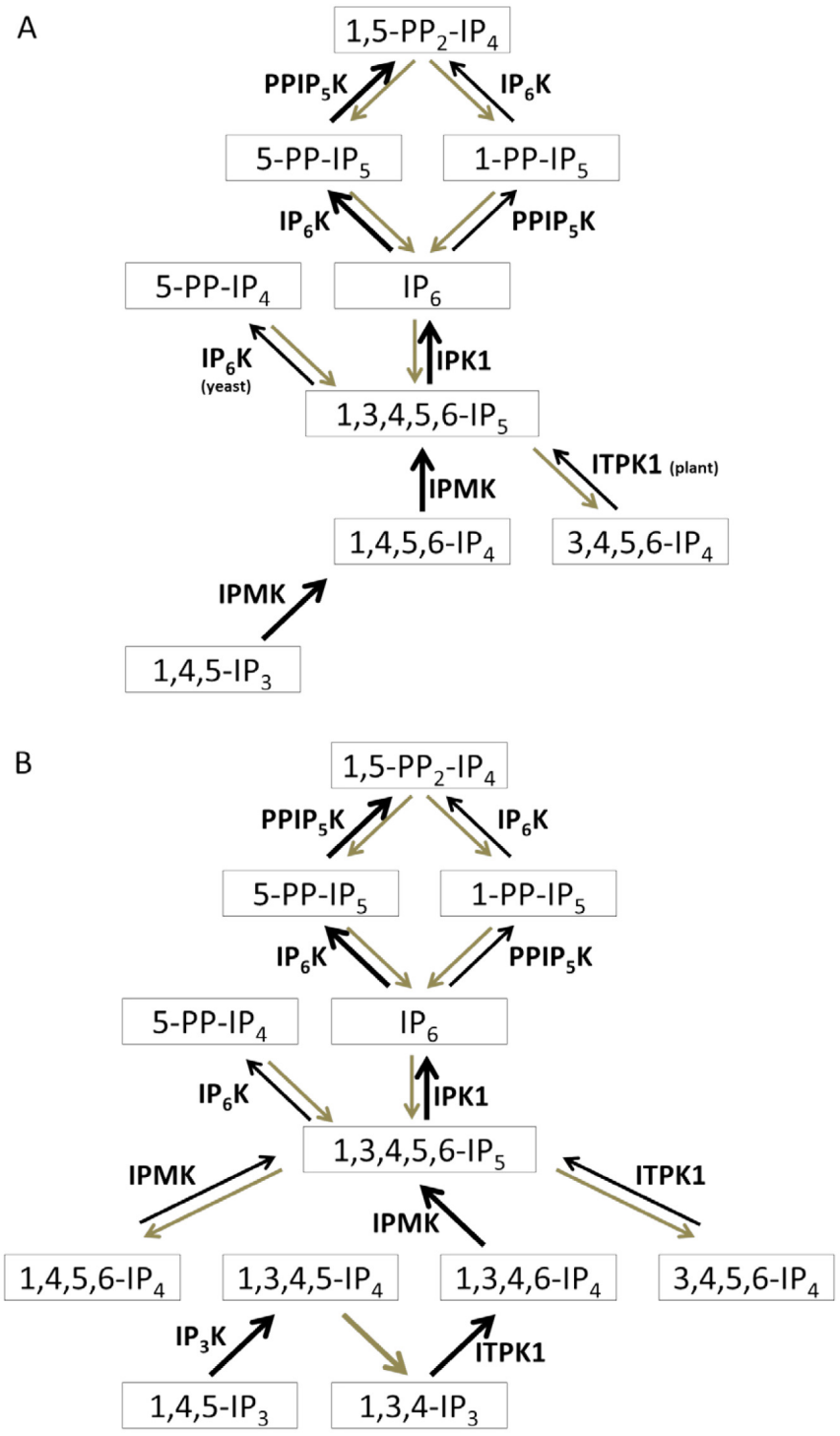

Figure 1.2. IP metabolic pathways in (A) yeast and plants and (B) mammals. Black arrows indicate phosphorylation reactions by IPKs, as labeled. Grey arrows indicate dephosphorylation reactions by phosphatases (labels omitted for clarity).

1.6 IP cellular roles

The diversity of IPs in different species and the energy required to create and maintain these phosphorylated molecules suggests there are important cellular roles for many IPs in the IP synthetics pathways; however, the complexity of IP metabolism continues to hinder the ability to ascertain the functional roles of some IPs that are pivotal in the IP metabolic pathway, such as IP_5.

1.6.1 IP_3 roles

The most studied IP is IP_3. In eukaryotic cells, IP_3 signaling is an important regulator of Ca^{2+} homeostasis (Michell et al., 1981). External ligands bind to G-protein coupled receptors that are linked to a Gq heterotrimeric G protein. The α-subunit of Gq activates the isozyme PLC-β, which cleaves insoluble PIP_2 to produce soluble IP_3 and DAG. The isozyme PLC-γ can also cleave PIP_2, but is activated by receptor tyrosine kinase pathways that are activated by external growth factors (Berridge, 1993). The second messenger IP_3 diffuses away from the membrane and into the cytoplasm where it encounters and binds to the IP_3 receptor, a ligand gated Ca^{2+} ion channel, on the endoplasmic reticulum (ER), or sarcoplasmic reticulum in muscle cells, which triggers the release of intracellular Ca^{2+} (Berridge, 1993).

There is currently no role known for 1,3,4-IP_3 other than a metabolic intermediate, however, the conversion of 1,3,4-IP_3 to 1,3,4,6-IP_4 by ITPK1 is the rate-limiting step in the IP metabolic pathway (Verbsky et al., 2005a).

The IP_3 receptor is highly concentrated in the cerebellum (Worley et al., 1989) and defects in IP_3 signaling are linked with two neurological diseases. In Huntington's disease, a genetic mutation in Huntingtin-1 results in the production of a modified Huntingtin-1 with an extra 35 glutamate residues on its N-terminus, which sensitizes the IP_3 receptor to IP_3. Thus, there is an over release of Ca^{2+} from the ER that leads to degeneration of the medium spiny neurons in the striata (Bezprozvanny and Hayden, 2004). Disruptions in Ca^{2+} signaling caused by mutations in presenilin and amyloid precursor protein genes can lead to Alzheimer's disease. Increased IP_3-mediated Ca^{2+} release from the ER has been caused by mutations in presenilin-1 in several animal models (Stutzmann, 2005).

Ca^{2+} channel blockers have also been somewhat effective in the treatment of Alzheimer's disease (Goodison et al., 2012).

1.6.2 IP_4 roles

1.6.2.1 1,3,4,5-IP_4

There is much debate about the role of 1,3,4,5-IP_4 in cellular signaling (Shears et al., 2012). Initial reports suggested that 1,3,4,5-IP_4 is involved with Ca^{2+} entry (Irvine, 1986) as stimulus-dependent increases in IP_3 also resulted in increased levels of 1,3,4,5-IP_4 (Batty et al., 1985). Subsequent studies for the last 20 years have produced conflicting data to validate the role of 1,3,4,5-IP_4 in Ca^{2+} mobilization (Schell, 2010) attributed to irreproducible results (Irvine and Moor, 1987; Crossley et al., 1988; Hill et al., 1988; Boynton et al., 1990), varying model systems used (Putney, 1992; Irvine, 1992; Smith et al., 2000; Brough et al., 2005), and physiologically irrelevant concentrations during experimentation (Luckhoff and Clapham, 1992; Hermosura et al., 2000; Bird and Putney, 1996). It has been proposed that the molecular actions of 1,3,4,5-IP_4 may be cell-specific, dependent on the strength of receptor activation, localization of IPKs which metabolize 1,3,4,5-IP_4, or other unknown regulatory factors (Shears et al., 2012).

More recently, studies have implicated 1,3,4,5-IP_4 in immune cell development (Sauer and Cooke, 2010). IP_3K null mice, which cannot generate 1,3,4,5-IP_4, exhibited a complete block in T cell development in the thymus (Pouillon et al., 2003), and T-cell receptor signaling was severely compromised as a result (Huang and Sauer, 2010). Furthermore, splenic B cell development and B cell function was also defective (Pouillon et al., 2003). 1,3,4,5-IP_4 was identified to bind with high affinity to $GAP1^{IP4BP}$, also known as RASA3 (Cozier et al., 2000), a Ras-GTPase that shares homology with $GAP1^{m}$, which binds to PIP_3, an inositol lipid with a head group very similar to 1,3,4,5-IP_4 (Cullen et al., 1995). RASA3 also regulates the ERK signaling pathway, through which T-cell receptor and B-cell receptor signaling occurs, which may explain the lack of immune cell development in IP_3K null mice (Pouillon et al., 2003). Binding of 1,3,4,5-IP_4 to RASA3 occurs through the pleckstrin homology (PH) domain of RASA3 (Fukuda and Mikoshiba, 1996). COS-7 cells overexpressing IP_3K or treated with 1,3,4,5-IP_4

resulted in translocation of RASA3 away from the plasma membrane to the cytosol, indicating the role of 1,3,4,5-IP_4 in controlling RASA3 membrane localization (Marechal et al., 2007). 1,3,4,5-IP_4 has also been shown to be an inhibitory signal for neutrophil function by binding to the PH domain of Akt thereby preventing plasma membrane recruitment of Akt (Jia et al., 2007).

1.6.2.2 1,3,4,6-IP_4

There is currently no specific physiological role known for 1,3,4,6-IP_4 in mammalian cells. Early studies indicated that 1,3,4,6-IP_4 may be involved with Ca^{2+} homeostasis in Xenopus because treatment of oocytes with 1,3,4,6-IP_4 evoked Ca^{2+}-dependent membrane currents through liberation of intracellular Ca^{2+} (Ivorra et al., 1991). It was proposed that 1,3,4,6-IP_4 acts through IP_3 receptors, however, the exact mechanism of action has not been elucidated. Thus, 1,3,4,6-IP_4 is mainly considered a metabolic intermediate between 1,3,4-IP_3 and IP_5, and is preferentially phosphorylated by IPMK on the 5-position (Chang et al., 2002). However, 1,3,4,6-IP_4 may also be generated by ITPK1 through a complex, ADP-dependent phosphotransferase mechanism involving both 1,3,4-IP_3 and 3,4,5,6-IP_4 (Chamberlain et al., 2007) (see section 1.7.2).

1.6.2.3 3,4,5,6-IP_4

There is substantial evidence to indicate that 3,4,5,6-IP_4 is a secondary messenger, like IP_3 (Shears et al., 2012). Upon PLC activation, the cellular level of 1,3,4-IP_3 increases, which in turn controls 3,4,5,6-IP_4 synthesis through ITPK1 activation (Batty et al., 1998; Batty and Downes, 1994). The concentration of 3,4,5,6-IP_4 increases from 1 μM in resting cells to 5-10 μM upon stimulus-dependent PLC activation, which requires action of numerous enzymes in the biosynthetic pathway (Ho and Shears, 2002). 3,4,5,6-IP_4 inhibits CaMKII-activated Cl^- channels in a concentration-dependent manner and this effect does not occur with any other IPs (Xie et al., 1996; Xie et al., 1998; Ismailov et al., 1996; Ho et al., 2001). These Cl^- channels regulate salt and fluid secretion in the lungs, GI tract, and exocrine glands (Petersen, 1992). Thus, the physiological role of 3,4,5,6-IP_4 is regulation of epithelial salt and fluid secretion by action upon Cl^-

transport (Vajanaphanich et al., 1994; Carew et al., 2000). It was recently identified that the ClC-3 receptor is specifically modulated by 3,4,5,6-IP_4 (Mitchell et al., 2008), however, 3,4,5,6-IP_4 does not act as a direct channel blocker (Ho et al., 2001), nor does it directly inhibit CaMKII activity (Ho and Shears, 2002). It is presumed that an intermediary protein is mediating the action of 3,4,5,6-IP_4 on Cl^- channels (Shears et al., 2012).

The role of 3,4,5,6-IP_4 in the regulation of salt and fluid secretion has important implications for patients with cystic fibrosis (CF) (Ismailov et al., 1996). The majority of patients with CF have a mutation in the cyclic AMP-regulated chloride channel CFTR, which impairs Cl^- transport (Modiano et al., 2005); ClC-3 is likely the most active channel remaining (Rudolf et al., 2003) and its activity was found to be enhanced in CF patients (Leung et al., 1995). Blocking the inhibitory effect of 3,4,5,6-IP_4 on ClC-3 could restore trans-epithelial Cl^- secretion (Rudolf et al., 2003), which is compromised in CF patients.

1.6.2.4 1,4,5,6-IP_4

In yeast and plants, 1,4,5,6-IP_4 is obtained by phosphorylation of IP_3 by IPMK (known as IPK2 in yeast) (Odom et al., 2000; Saiardi et al., 2001a). As such, 1,4,5,6-IP_4 is an important metabolite along the main axis of IP metabolism in yeast and plants. However, in mammals, 1,4,5,6-IP_4 is primarily produced through dephosphorylation of IP_5 and is not part of the main axis of IP metabolism from IP_3. Consequently, most investigations of 1,4,5,6-IP_4 roles have been conducted in yeast and implicate 1,4,5,6-IP_4 in transcriptional regulation. Using *ipk2*Δ yeast cells, it was shown that the synthesis of 1,4,5,6-IP_4 was necessary for the function of the ArgR-Mcm1 transcriptional complex that regulates ornithine transaminase gene expression (Odom et al., 2000). Furthermore, IPK2 kinase activity regulates transcription of Pho5, the main acid phosphatase responsible for phosphate metabolism in yeast, via chromatin remodeling (He et al., 2012; Steger et al., 2003). It has been proposed that 1,4,5,6-IP_4 stimulates nucleosome sliding, which exposes regulatory elements for transcription (Shen et al., 2003). Very recently, the crystal structure of the complex between human HDAC3 and a co-repressor, human NCOR2 was solved (Watson et al., 2012). The structure revealed that 1,4,5,6-IP_4 acted as a scaffold between the two proteins and complex

formation, stabilization and activation of HDAC3, were all dependent on 1,4,5,6-IP_4. A second structure of the complex between HDAC1 and MTA1 co-repressor was also solved and revealed a binding pocket for 1,4,5,6-IP_4 (Millard et al., 2013). Functional assays indicated that both HDAC1 and HDAC3 complex assembly and activity were regulated by 1,4,5,6-IP_4, further implicating 1,4,5,6-IP_4 as a transcriptional regulator (Millard et al., 2013).

The role of 1,4,5,6-IP_4 as an HDAC regulator may have implications for the underlying mechanisms that lead to cancer. One of the most commonly mutated proteins in human cancers is the tumor suppressor gene PTEN, which is most often considered an antagonist of PI3K signaling, so its mutation and inactivation allows PI3K-directed survival signaling to run unregulated (Di Cristofano and Pandolfi, 2000). However, PTEN also possesses 3-phosphatase activity and can dephosphorylate IP_5 to produce 1,4,5,6-IP_4 (Caffrey et al., 2001). PTEN is also highly active in the nucleus and contributes to chromosome stability (Di Cristofano and Pandolfi, 2000). Thus, PTEN mutations may contribute to oncogenesis by disrupting HDAC complex formation (Watson et al., 2012).

Lastly, elevated levels of 1,4,5,6-IP_4 were observed during *Salmonella dublin* invasion of epithelial cells (Eckmann et al., 1997). This leads to an inhibition of EGFR-stimulated PI3K signaling and increased salt and fluid secretion. It was later determined that the Salmonella virulence factor, SopB, required for the pathogen's virulence, is a phosphatase that can convert IP_5 to 1,4,5,6-IP_4 (Norris et al., 1998; Zhou et al., 2001). Ectopic expression of SopB in mammalian cells stimulates Cl^- influx (Feng et al., 2001), but SopB also shows specificity for PIs *in vitro* (Norris et al., 1998), so it still unclear whether Cl^- influx is mediated by 1,4,5,6-IP_4 or an inositol lipid mediator. Taken together, it is unknown if there are physiological roles for 1,4,5,6-IP_4 in fluid secretion or it is simply a pathological consequence of Salmonella invasion (Eckmann et al., 1997).

1.6.3 IP_5 roles

IP_5 (1,3,4,5,6-IP_5) is the predominant isomer of inositol pentakisphosphates in many types of mammalian cells where it is often measured to be at concentrations exceeding 30 μM (Stephens et al., 1991; Oliver et al., 1992; Pittet et al., 1989). Other isomers are also found at high concentrations, but with

cell-type specificity. Jurkat T cells and T5-1B cells have considerable amounts of 1,2,4,5,6-IP_5 and 2,3,4,5,6-IP_5, respectively, but how the synthesis of these isomers fit into the biosynthetic IP pathways has not been explored (Guse and Emmrich, 1991; McConnell et al., 1991).

In nucleated erythrocytes from several animal species, it was observed that IP_5 decreases the affinity of hemoglobin (Hb) for O_2 (Coates, 1975; Riera et al., 1991). This role for IP_5 may be species specific or characteristic of developmental isoforms of Hb, such as embryonic Hb (Isaacks et al., 1978; Isaacks et al., 1987). Interestingly, the South American arapaima, a fully aquatic fish that ultimately requires surface air to breathe later in life, shows a 7-fold increase in IP_5 concentration and a 50% reduction in ATP and GTP concentration in erythrocytes during this time (Val et al., 1992). IP_5 is a more potent effector of Hb-O_2 affinity than ATP and GTP, so low levels of IP_5, early in life, may ensure that Hb-O_2 affinity is high to extract O_2 from water, while high levels of IP_5, later in life, lowers Hb-O_2 affinity since air is O_2-rich (Val et al., 1992).

More recent studies have linked IP_5 to downstream signaling of Frizzled (Fz) receptors in the Wnt/β-catenin pathway, which regulates embryonic development and adult tissue homeostasis (Kim et al., 2013). Activation of Fz receptors by Wnt ligands activates casein kinase 2 (CK2) and inhibits glycogen synthase kinase 3β (GSK3β), positive and negative modulators, of Wnt/β-catenin signaling (Gao and Wang, 2006; Song et al., 2003; MacDonald et al., 2009); however, it is unclear how CK2 and GSK3β are regulated downstream by Fz receptor activation. Wnt ligands also induce PLC activation and IP accumulation (Slusarski et al., 1997), so it was suggested that IPs may play a role in regulating CK2 and GSK3β activity. When Fz receptors were stimulated by Wnt3a, levels of IP_5 increased 2.5-fold, resulting in the activation of CK2 and inhibition of GSK3β, which were dependent on IP_5 accumulation (Gao and Wang, 2007). These experiments were performed *in vitro*, but the effective concentrations of IP_5 for CK2 activation and GSK3β inhibition were within normal cellular concentrations of IP_5 (Oliver et al., 1992; Pittet et al., 1989). Interestingly, IP_5 can activate liver-purified CK2 *in vitro*, but not bacterially purified, recombinant CK2; thus, it was hypothesized that IP_5 acts by antagonizing an uncharacterized, heat-stable inhibitor of CK2 (Solyakov et al., 2004). However, it is generally accepted that CK2 is constitutively active with no requirement to be stimulated, which raises the

concern that this may not be a physiologically relevant observation (Ruzzene et al., 2010). Further study will be required to ascertain the mechanism of action of IP_5 on CK2 activation.

Likewise, Wnt3a-mediated accumulation of IP_5 and inhibition of GSK3β is poorly understood. GSK3β inhibition requires IP_5; treatment of cells with IP_3, 1,3,4,5-IP_4, or IP_6 had no effect on GSK3β activity (Gao and Wang, 2007), and RNA interference (RNAi) of IP_3K and IPMK, which substantially reduces IP_5 synthesis, also prevented Wnt3a-mediated inhibition of GSK3β (Gao and Wang, 2007). Purified GSK3β was not inhibited by IP_5, therefore, an intermediary must be required (Gao and Wang, 2007). Interestingly, the link between IP_5 and the Wnt/β-catenin pathway, which regulates embryonic development, may explain the embryonic lethality of IPK1 null mice (Verbsky et al., 2005b). Further studies will be needed to characterize the role of IP_5 in the Wnt/β-catenin pathway.

IP_5 has also been reported to play a role in the PI3K/Akt pathway. Akt regulates a myriad of cellular processes, including cell survival, growth, and proliferation (Manning and Cantley, 2007). Treatment of ovarian, lung, and breast cancer cells with IP_5 *in vitro* prevented phosphorylation and activation of Akt (Piccolo et al., 2004), while treatment of IP_5 inhibited tumor growth in SKOV-3 xenografted nude mice that express a high level of constitutively activated Akt *in vivo* (Maffucci et al., 2005; Sain et al., 2006). It is still unclear how IP_5 regulates the PI3K/Akt pathway. IP_5 can bind to the PH domain of phosphoinositide-dependent kinase-1 (PDK1) (Komander et al., 2004), which is normally recruited to the plasma membrane via PIP_3 binding to its PH domain (Stokoe et al., 1997). Co-localization of PDK1 and Akt enables Akt phosphorylation and activation by PDK1 (Stephens et al., 1998; Currie et al., 1999). Thus, PDK1 may bind IP_5 in the cytosol, thereby preventing Akt activation.

IP-PH domain interactions have been observed for IP_3 (Kavran et al., 1998), 1,3,4,5-IP_4 (Cozier et al., 2000; Fukuda and Mikoshiba, 1996; Jia et al., 2007; Anraku et al., 2011), IP_5 (Komander et al., 2004; Jackson et al., 2011) and have been postulated for PP-IPs (see section 1.6.5). Given that IPs are structurally similar to the headgroup of PIs, IP-PH domain interactions likely represent a common mechanism of action for how individual IPs can elicit their functional roles. Although PH domains are one of the most common domains in the proteome, only 10% of PH domains bind to PIs with high affinity and specificity;

the remaining 90% have poor affinity for PIs and are hypothesized to function as protein binding domains (Lemmon, 2007). PH domains that have poor affinity for PIs can still form high affinity IP-PH interactions (Rosen et al., 2012), and can discriminate between specific IPs (Jackson et al., 2011), suggesting that IPs can differentially regulate PH domain interactions to modulate protein function.

1.6.4 IP_6 roles

Since its early discovery in plants, IP_6 has been considered a phosphate store for seeds (Posternak, 1919). It is now known that IP_6 is ubiquitously present in all mammalian cells (Heslop et al., 1985) and is likely the most abundant IP (Shi et al., 2006). The intracellular concentration of IP_6 in mammalian cells is 10-60 μM, although the local concentration available to interact with its partners is unmeasured (Pittet et al., 1989; Szwergold et al., 1987). Early proposed functions of IP_6 in mammals included inhibition of protein phosphatases (Larsson et al., 1997), activation of PKC (Efanov et al., 1997), or as an antioxidant (Hawkins et al., 1993; Spiers et al., 1996).

A series of studies have also linked IP_6 to vesicle trafficking in pancreatic β-cells (Barker et al., 2009), binding to clathrin assembly proteins AP2 and AP180 (Theibert et al., 1991; Chadwick et al., 1992), and inhibition of clathrin cage assembly (Norris et al., 1995; Ye et al., 1995). As supporting evidence for this, IP_6K1 knockout mice exhibited decreased insulin release from pancreatic β-cells (Bhandari et al., 2008), which might be related to the complex role of IP_6 in regulating endocytotic and exocytotic function in β-cells (Hoy et al., 2002). Moreover, a putative disruption of the IP_6K1 gene has also been detected in a family with Type II diabetes (Kamimura et al., 2004), which may contribute to their reduced insulin exocytosis.

The discovery that IP_6 (York et al., 1999) and later, IPK1 (Brehm et al., 2007) are concentrated at the nucleus focused attention on nuclear roles of IP_6 (Monserrate and York, 2010). Subsequent studies revealed the requirement of IP_6 for nuclear mRNA export (York et al., 1999; Feng et al., 2001; Alcazar-Roman et al., 2006), DNA repair by non-homologous end-joining (Hanakahi et al., 2000; Cheung et al., 2008) and chromatin remodeling (Shen et al., 2003). IP_6 is also a co-factor for ADAR2, an adenosine deaminase involved in RNA editing and localized

within the nucleolus, by binding within the protein core and promoting correct protein folding (Macbeth et al., 2005).

Among the most compelling roles that have emerged for IP_6 is its role in controlling apoptosis. Induction of apoptosis was observed in cultured prostate carcinoma cells line, PC-3 (Shamsuddin and Yang, 1995), TRAMP-C1 (Sharma et al., 2003), and DU145 (Agarwal et al., 2003), when treated with IP_6. Since these early reports, many cancer cell lines including breast, colon, liver, lung, skin, and other cells lines have been shown to exhibit inhibited growth when treated with pharmacological (1-2 mM) or physiological concentrations (50-100 μM) of IP_6 (Vucenik and Shamsuddin, 2003; Shi et al., 2006). In some cases, IP_6 administration in combination with chemotherapeutic agents such as tamoxifen, has enhanced their anti-proliferative effects (Tantivejkul et al., 2003), indicating that IP_6 mediates cell death signaling pathways. Furthermore, rat and mice models for colon, liver, lung, breast, prostate, and skin cancers have been treated with IP_6, either through diet or injection, and have exhibited reduced tumor growth (Vucenik and Shamsuddin, 2006). IP_6K2 knockout mice have also displayed increased incidence of aerodigestive tract carcinoma when exposed to the carcinogen 4-nitroquinoline 1-oxide compared to wild-type mice, further revealing the role of IP_6 in promoting cell death (Morrison et al., 2009).

The underlying molecular mechanisms of the anticancer effect of IP_6 are poorly understood. Studies in different cell lines reveal that IP_6 can reduce the phosphorylation of PI3K, PDK1, Akt, and GSK3β (Jagadeesh and Banerjee, 2006; Gu et al., 2010), but whether or not these actions explain the anticancer activities of IP_6 requires further study.

It is possible that IP_6 may not elicit all of its anti-cancer effects directly, and IP_6 may be metabolized to other signaling molecules that control cell proliferation and apoptosis. IP_6K2, which phosphorylates IP_6 to higher IPs, mediates growth suppressive and apoptotic effects of interferon-β (IFN-β) in ovarian carcinoma cells (Morrison et al., 2001), which indicates more highly phophorylated forms of IPs other than IP_6 are the active agents in this pathway. Furthermore, increased activity of IP_6K2 also enhanced the cytotoxic effects of cisplatin, staurosporine, hydrogen peroxide, and hypoxia (Nagata et al., 2005), while knockdown of IP_6K2 using RNAi protected cells from apoptotic-inducing IFN-β, γ-irradiation, cisplatin, and etoposide (Morrison et al., 2002).

There is conflicting evidence for the roles of IP_5, IP_6, and the enzymes that regulate their levels in controlling cell proliferation and survival signaling. On one hand, either IPK1 overexpression or RNAi of IP_6K2 are both protective, which suggests that cellular accumulation of IP_6 protects cells from cell death, while RNAi of IPK1 or overexpression of IP_6K2 sensitize cells to apoptosis, indicating depletion of IP_6 is pro-apoptotic. On the other hand, treatments of cells with either IP_5 and IP_6 are pro-apoptotic. In the IP metabolic pathway, IPK1 is positioned between IP_5 and IP_6 and thus plays a significant role in regulating the levels of these IPs. An inhibitor of IPK1 would prove valuable to differentiate the roles of both these IPs.

1.6.5 PP-IP roles

Diphosphoinositol phosphates (PP-IPs) were discovered by two separate groups in 1993 and represent the most recently defined class of IPs (Menniti et al., 1993; Stephens et al., 1993). PP-IPs are found ubiquitously in all eukaryotic cells, from fungi to humans (Bennett et al., 2006). They are characterized by their pyrophosphate moieties, located on either one (5-PP-IP_5) or two (1,5-PP_2-IP_4) positions of the inositol ring. These moieties contain a high-energy phosphate bond, whose free-energy of hydrolysis is similar to that found in ATP, which led to the suggestion that PP-IPs might be regulators of cellular energy metabolism (Laussmann et al., 1996; Szijgyarto et al., 2011); however, the abundance of ATP (mM) compared to PP-IPs (μM range) suggests otherwise. This hypothesis has evolved, and it has been proposed that PP-IPs are energy sensors, rather than regulators (Wilson et al., 2013).

PP-IPs are thought to elicit their effects through two mechanisms. First, PP-IPs may bind to proteins such as those containing PH domains, which has been previously demonstrated for other IPs, and second, by protein pyrophosphorylation, whereby PP-IPs, non-enzymatically donate the β-phosphate of the pyrophosphate moiety to pre-phosphorylated serine residue (Shears, 2001; Saiardi et al., 2004; Bhandari et al., 2007). So far, strong and direct experimental evidence to support these mechanisms of action has been lacking. For example, the concentration of 5-PP-IP_5 required to displace PIP_3 in the PH domain of Akt *in vitro* implies 5-PP-IP_5 is constitutively bound to Akt *in vivo* (Wilson et al., 2013).

The protein pyrophosphorylation signaling model is further challenged by the absence of conservation between human, yeast, and slime mold proteins that can be pyrophosphorylated *in vitro*, which is unexpected considering that PP-IPs are found in all three groups. Furthermore, there is no direct biophysical evidence that supports the hypothesis that this type of protein modification occurs *in vivo* (Azevedo et al., 2009; Shears, 2010; Wilson et al., 2013). Thus, the mechanisms of action of PP-IPs require further study.

PP-IPs have been implicated in a diverse range of cellular processes (Barker et al., 2009). These include exocytosis, endocytosis, apoptosis, telomere maintenance, and vesicle trafficking (Barker et al., 2009; Saiardi et al., 2002; Nagata et al., 2005; Saiardi et al., 2005). Many of these studies that suggest roles for PP-IPs have identified both IP_6 and PP-IPs as signals in these processes, which have confounded the roles of IP_6 and higher IPs (Barker et al., 2009). PP-IP concentrations are significantly lower than IP_6 in mammalian cells, ranging from 0.5-1.3 μM (Albert et al., 1997), which would indicate that IP_6 is the likely signal if both IP_6 and PP-IP interact with their targets with similar affinities. Although their concentrations remain constant, PP-IP turnover is very rapid, with 20% of the pool of IP_5 and 50% of the pool of IP_6 being metabolized to PP-IPs every hour (Menniti et al., 1993; Glennon and Shears, 1993). Thus, an inhibitor of IPK1 would substantially compromise PP-IP production from IP_6 and could offer a new tool to probe for the specific functions of PP-IPs. An inhibitor for IP_6K has been identified, but lacks specificity for IP_6K over other IPKs (Padmanabhan et al., 2009; Wilson et al., 2013).

1.7 IPK1 biology

There have been very few studies of IPK1 function in animals. Most studies have employed over-expression or RNAi knockdown in cultured mammalian cells in an effort to understand the role of IPK1; however, these approaches do not discriminate between the impact of the catalytic functions of IPK1 – production of IP_6, and higher IPs – and non-catalytic functions of IPK1. Moreover, some specific roles for IPK1 have emerged in yeast and in plants, but whether these functions are conserved in mammalian cells remains to be determined.

1.7.1 *Saccharomyces cerevisiae* IPK1

A series of studies have revealed that *S. cerevisiae* IPK1 mediates nuclear mRNA export. The essential nuclear pore complex (NPC)- associated factor Gle1, uses IP_6 as a co-factor, and together, Gle1-IP_6 stimulates Dbp5 ATPase activity at the NPC, which is required for efficient nuclear mRNA export (Miller et al., 2004; Alcazar-Roman et al., 2006). The localization of IPK1 at the nucleus with the NPC likely facilitates production of IP_6 where it is needed for Gle1 function (Odom et al., 2000). Accordingly, *ipk1Δ Schizosaccharomyces pombe* (fission yeast) also exhibited defects in mRNA export, as well as defects in polarized growth, cell morphology, endocytosis, and cell separation (Sarmah and Wente, 2009). These studies were performed using *ipk1Δ* yeast strains and have yet to be replicated using IPK1 knockouts of mammalian cells to show that the role of IPK1 in mRNA export is conserved among eukaryotes.

1.7.2 IPK1 in plants

IPK1 was characterized in the plant *Arabidopsis thaliana* (Sweetman et al., 2006) to show strong tissue-specific expression in the male and female organs of the flower bus, but the significance of the tissue-specific expression of IPK1 is unknown. Specific accumulation of IPK1 in various tissues in maize has also been reported (Sun et al., 2007).

Recently, a role for IPK1 in plant immunity has emerged. Plants with kinase dead IPK1 were hyper-susceptible to infection from several viruses, bacterial pathogens, and fungi (Murphy et al., 2008). IP_6 is known to be a co-factor for some plant F-box proteins, which are involved in wound healing upon plant injury (Tan et al., 2007); however, it was recently determined that IP_5, not IP_6, is the modulator of the F-box protein COI1 (Mosblech et al., 2011). Interaction between COI1 and its target, jasmonic acid, was increased in *ipk1Δ* yeast that exhibit elevated levels of IP_5 (Mosblech et al., 2011), suggesting that competition between IP_5 and IP_6 as co-factors could be a regulatory mechanism employed by F-box proteins.

1.7.3 IPK1 in animals

The IPK1 gene was identified to be located on human chromosome 9 and the gene has been isolated for biochemical characterization (Verbsky et al., 2002). IPK1 primarily uses IP_5 as its substrate with a K_M = 0.4 μM and V_{MAX} = 31 nmol/min/mg. Expression of human IPK1 in an *ipk1Δ* yeast strain restored IP_6 production and rescued a *gle1* lethal phenotype, demonstrating functional conservation of IPK1 across species (Verbsky et al., 2002).

Human IPK1 expression is predominantly in brain, heart, placenta and testes (Verbsky et al., 2002), but there is a spatial micro-heterogeneity in its intracellular localization (Brehm et al., 2007). In the cytoplasm, IPK1 is concentrated in stress granules. In the nucleus, IPK1 is concentrated with euchromatin, mRNA, and in the nucleoli. It has been hypothesized that the localization of IPKs can contribute to different IP metabolic profiles within different compartments of the cell (Brehm et al., 2007); however, artificial localization of IPK1 to the plasma membrane allowed nuclear export of mRNA, which is lost when IPK1 is inactivated, suggesting that IPK1 products diffuse through the cell to their sites of action (Miller et al., 2004). Very recently, a non-catalytic role was identified for IPK1 in the nucleolus. IPK1 acts as a scaffold for three proteins that regulate rRNA synthesis: CK2, TCOF1, and UBF (Brehm et al., 2013). When rRNA synthesis was compromised under serum starved conditions, IPK1 did not localize to the nucleolus (Brehm et al., 2013), suggesting that IPK1 is critical for the regulation of rRNA synthesis, and consequently, ribosome biogenesis.

IPK1 also plays an important role in development. RNAi knockdown of IPK1 prevented the normal establishment of left-right asymmetry in zebrafish embryos, resulting in randomized organ placement during development (Sarmah et al., 2005). This is likely due to reduced Ca^{2+} flux that was detected in the ciliated Kupffer's vesicle, the organ responsible for left-right asymmetry, thereby inhibiting ciliary beating and length (Sarmah et al., 2005; Sarmah et al., 2007). Moreover, IPK1 null mice are embryonic lethal by 8.5 days, but the underlying molecular mechanisms are still unknown (Verbsky et al., 2005b).

IPK1 may also possess a role in early renal function decline (ERFD) as increased expression of IPK1 has been detected in renal biopsies of Type I diabetes

patients with early nephropathy (Merchant et al., 2009). IPK1 also co-localized with stress granules in the cytoplasm of isolated cells *in vivo*, consistent with previous *in vitro* observations (Brehm et al., 2007). Although, the functional significance of IPK1 in nephropathy is still unknown, IPK1 peptides were detected in the urinary peptidome of diabetic patients with ERFD, suggesting that IPK1 could be a candidate biomarker in the urinary peptidome for progressive renal function decline (Merchant et al., 2009).

As mentioned previously, IP_5 and IP_6 promote apoptosis (see section 1.6.3 and 1.6.4), and likewise, alterations in IPK1 can alter cell death signaling responses. Overexpression of IPK1 protected HEK293 cells from TNFα-mediated and Fas-induced apoptosis, while RNAi knockdown of IPK1 sensitized cells to TNFα-mediated apoptosis (Verbsky and Majerus, 2005). It is still unclear how overexpression of IPK1, which results in production of IP_6, protects cells, but these observations clearly indicate IPK1 is key for tuning cell responses via IP_5 and IP_6 (Verbsky and Majerus, 2005).

1.8 Structural biology of IPKs

IPKs are currently organized into three subfamilies according to their sequence similarity and structural homology: 1) the inositol polyphosphate kinase subfamily (IPMK, IP_3Ks and IP_6Ks); 2) the ATP-grasp fold subfamily (ITPK, $PPIP_5K$); and 3) the IPK1 subfamily (IPK1) (Irvine and Schell, 2001; Wang et al., 2012) (Figure 1.3). The crystal structures for the kinase domains of each IPK, except IP_6K, have been solved, however, the mechanisms of substrate selectivity have not been described for all IPKs.

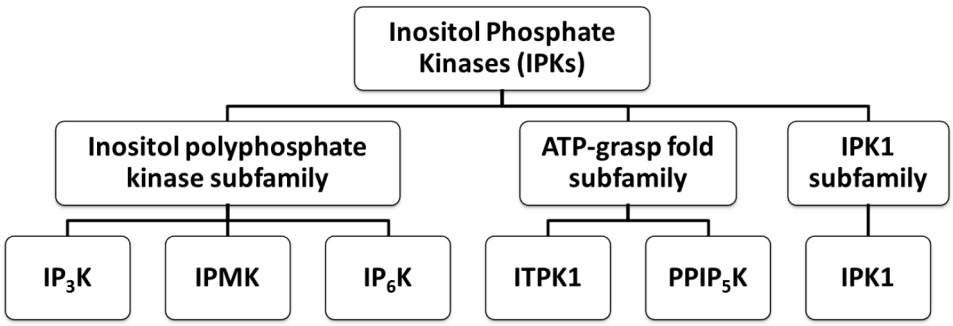

Figure 1.3. Classification of IPKs.

1.8.1 IP_3K

IP_3Ks are members of the inositol polyphosphate kinase subfamily. Members of this subfamily possess a conserved catalytic C-terminal region and a variable N-terminal region involved in targeting and regulation. In addition, there are three characteristic sequence motifs that are shared among inositol polyphosphate kinases, SSLL, IDFG, and PxxxDxKxG, that are collectively involved in nucleotide binding, metal co-factor coordination, and catalysis. Inositol polyphosphate kinases also possess structural features similar to those of protein kinases (PKs) that will be described.

Animals express three isoforms of IP_3Ks, which differ in intracellular distribution, regulation, and sensitivity to Ca^{2+}, due to the CaM domains that are uniquely present in IP_3Ks amongst IPKs (Dewaste et al., 2003; Pattni and Banting, 2004; Communi et al., 1995).

The first crystal structures of an IPK were that of the conserved catalytic core of IP_3K-A from human (Gonzalez et al., 2004) and from rat (Miller and Hurley, 2004). The catalytic core consists of an N-lobe and a C-lobe, connected by a hinge, and an IP-lobe that is an independent structural lobe inserted into the C-lobe sequence (Figure 1.4a). The N-lobe is formed by 4 anti-parallel β-strands and an α-helix in an α+β fold. The C-lobe is formed by 5 anti-parallel β-strands and three α-helices, also in an α+β fold. The IP-lobe consists of 4 α-helices in a coil arrangement (Gonzalez et al., 2004). The three lobes fold such that the ATP binding site is sandwiched between the N-lobe and the C-lobe, while the IP binding site is contained between the IP-lobe and edge of the N- and C-lobe sandwich. The ATP and IP are bound such that the γ-phosphate of ATP is positioned in close proximity to the 3-hydroxyl of IP_3. The adenine and ribose groups of the nucleotide are bound in a hydrophobic pocket formed by L251 and L252 of the hinge region, F198 of the N-lobe, L401 of the SSLL motif and I415 of the IDFG motif. The ribose oxygens form hydrogen bonds with K336, and D262 of the PxxxDxKxG motif. D416, from the IDFG motif, coordinates the ATP phosphates through the metal ion co-factor, which is, in turn, coordinated by S399 of the SSLL motif, through an ordered water molecule.

The IP_3 ligand is coordinated by seven residues from the IP-lobe and two residues from the C-lobe (Gonzalez et al., 2004). The 3-hydroxyl of IP_3 is

positioned near the γ-phosphate of ATP, which facilitates a direct in-line transfer of the γ-phosphate of ATP to the IP while being coordinated by K264 of the PxxxDxKxG motif. Moreover, many of the residues that coordinate IP_3 are basic, forming a positively charged pocket that recognizes the acidic IP ligand (Miller and Hurley, 2004; Gonzalez et al., 2004). To selectively phosphorylate IP_3, IP_3K apparently uses a mechanism of substrate selectivity based on shape complementarity. The IP binding site is restrictive, providing sufficient space for the phosphate groups at the 1-, 4-, and 5-positions, but only hydroxyl groups at the 2-, 3-, and 6-positions. For example, phosphate groups cannot occupy the 2- and 6-positions because steric clashes would occur with M316 and M288, respectively (Gonzalez et al., 2004). Furthermore, a phosphate at the 3-position would clash with the γ-phosphate of ATP. Also, IP_3K cannot phosphorylate PIP_2, the insoluble PI with a head group analagous to IP_3, because the lipid moiety on the 1-position would clash with residues of the IP-lobe (Bird et al., 1992). In effect, the IP-lobe acts as a surrogate membrane, blocking access of membrane-bound PIs to the active site (Miller and Hurley, 2004). Thus, the shape of the IP binding site confers high specificity of IP_3K towards a single substrate, IP_3 (Shears, 2004).

As the first IPK to be structurally characterized, IP_3K has been rigorously compared to PKs. Overall, their topology is very similar, as both possess an N-lobe and a C-lobe connected by a hinge, but IP_3K also possesses a separate IP-lobe. Both N-lobes adopt a α+β fold and there is an intermolecular salt bridge within the N-lobe (L209-E215 in IP_3K equivalent to K72-E91 in PKA). In IP_3Ks, this salt bridge is broken by the IP upon substrate binding and the newly bound IP assumes the role of this bridge. In PKA, this salt bridge stabilizes the active conformation of PKA (Huse and Kuriyan, 2002). Both IP_3K and PKA possess a glycine rich loop (G-loop) that coordinates the nucleotide. This loop is highly mobile in both enzymes (Gonzalez et al., 2004; Madhusudan et al., 1994). In the apo-form of IP_3K, the G-loop connects to an N-terminal α-helix that occupies the ATP binding site. The reorientation of this α-helix by the CaM domain likely plays a role in the regulation of IP_3K (Gonzalez et al., 2004; Madhusudan et al., 1994). The C-lobes of IP_3K and PKA greatly differ in overall fold as the C-lobe of IP_3K contains a large β-sheet and the C-lobe of PKA is α-helical. However, an alignment of IP_3K and PKA indicates that the IDFG motif is topologically equivalent to the DFG

motif in PKA (Gonzalez et al., 2004) and both aspartate residues coordinate the γ-phosphate of the ATP. In PKA, there is a catalytic loop that contains a DxKxxNLL motif, wherein the lysine residue neutralizes the negative charge developed during phosphoryl transfer (Madhusudan et al., 2002). This catalytic loop is replaced by a β-strand in IP_3K that contains the PxxxDxKxG motif, which possesses a conserved lysine residue that neutralizes charges during phosphoryl transfer. Thus, the IP_3K active site contains the equivalent of the most critical residues found in PKA, which coordinate the adenine and phosphates of ATP (Miller and Hurley, 2004).

1.8.2 ITPK1

ITPK1 is a 5/6-kinase that catalyzes the phosphorylation of 1,3,4-IP_3 to either 1,3,4,5-IP_4 or 1,3,4,6-IP_4. ITPK1 plays a key role in the IP metabolic pathway as it is the rate-limiting enzyme for the synthesis of highly phosphorylated IPs (Verbsky et al., 2005a). ITPK1 also phosphorylates 3,4,5,6-IP_4 on the 1-position to IP_5 (Tan et al., 1997; Yang and Shears, 2000), and dephosphorylates 1,3,4,5-IP_4 and 1,3,4,6-IP_4 to 1,3,4-IP_3, and IP_5 to 3,4,5,6-IP_4, in more complex mechanisms (Ho et al., 2002; Chamberlain et al., 2007; Saiardi and Cockcroft, 2008). Thus, ITPK1 possesses catalytic pleiotrophy.

The crystal structures of ITPK1 from *Entamoeba histolytica* (Miller et al., 2005) and human (Chamberlain et al., 2007) reveal a globular fold for ITPK1, consisting of three domains surrounding the ATP binding cleft: an N-terminal domain, C-terminal domain, and a central domain (Miller et al., 2005) (Figure 1.4c). Each domain possesses a β-sheet core surrounded by α-helices. The β-sheets of the C-terminal domain and the central domain envelope the nucleotide, coordinated by numerous hydrophobic residues and polar contacts (Miller et al., 2005). A structural comparison of ITPK1 to known structures indicated that ITPK1 is closely related to the ATP-grasp family based on domain topology, the ATP binding cleft, and conserved residues that bind ATP and the metal co-factor (Artymiuk et al., 1996; Miller et al., 2005).

The substrate-bound structure of ITPK1 reveals that numerous hydrogen bonds and salt bridges are coordinating the 1-, 3-, and 4-phosphate groups of 1,3,4-IP_3, however, the 2-, 5-, and 6-hydroxyl groups have no direct contact with ITPK1 (Miller et al., 2005). Thus, the IP binding site is quite large and potentially able to

accommodate a large number of IPs (Miller et al., 2005). The product-bound structure containing 1,3,4,6-IP_4 revealed additional interactions with the 6-phosphate (Miller et al., 2005). Thus, ITPK1 uses a mechanism of substrate selectivity that is dictated by the phosphate groups of the IP (Miller et al., 2005). This is a stark contrast to the interactions between the IP and IP_3K (Gonzalez et al., 2004). In ITPK1, the γ-phosphate of ATP is equidistant from the 5- and 6-hydroxyl of the IP and two different oxygen atoms of the γ-phosphate are coordinated by separate magnesium ions for phosphorylation of either the 5- or 6-position. Steric hindrance in this region of the active site prevents phosphorylation of both 5- and 6-positions (Miller et al., 2005).

Occupancy of specific positions in the IP binding site reveals the structural basis for ITPK1 catalytic pleiotrophy and how it can phosphorylate 3,4,5,6-IP_4 on the 1-position (Yang et al., 2006). The large IP binding site and lack of contacts at every position allows 3,4,5,6-IP_4 to be reoriented. If the key phosphate binding sites are accommodated while a hydroxyl group is positioned at the active site, then an IP can be recognized as a substrate. In the case of 3,4,5,6-IP_4, its 3-, 4-, 5-, and 6-phosphates occupy positions filled by the 4-phosphate, 3-phosphate, 2-hydroxyl, and 1-phosphate of 1,3,4-IP_3, respectively. In this orientation, both the 1- and 2-hydroxyls of 3,4,5,6-IP_4 are positioned to be phosphorylated, however, the equatorial 1-hydroxyl is preferred due to its stereochemistry (Miller et al., 2005).

1.8.3 IPMK

IPMK displays catalytic versatility, like ITPK1, catalyzing the formation of multiple IPs from multiple substrates (Resnick and Saiardi, 2008). In humans and plants, IPMK acts primarily as a 5-kinase, with some 3-kinase and 6-kinase activity (Chang et al., 2002; Saiardi et al., 2001a; Nalaskowski et al., 2002; Chang and Majerus, 2006). The yeast homolog acts as a 6- and 3-kinase with no 5-kinase activity (Odom et al., 2000).

The structure of IPMK is very similar to IP_3K, with an RMSD of 1.3 Å, even though IMPK and IP_3K only share 17% sequence identity (Holmes and Jogl, 2006). IPMK consists of an N-lobe, C-lobe, and IP-lobe (Figure 1.4b). The N- and C-lobes adopt an α+β fold like in IP_3K, but the IP-lobe in IPMK comprises two α-helices compared to four in IP_3K. The ATP binding site in IPMK is located

between the N- and C-lobes. ATP forms contacts with L260 of the SSLL motif and I324 of the IDFG motif, among others, the ribose group forms a hydrogen bond with D131 of the PxxxDxKxG motif, and phosphoryl transfer of the γ-phosphate to the 3-position is mediated by K133 of the PxxxDxKxG motif (Holmes and Jogl, 2006). Overall, the coordination of the nucleotide and metal ion co-factor through an aspartate residue remains similar in both IMPK and IP_3K.

IPMK has not yet been co-crystallized with IP (Holmes and Jogl, 2006; Endo-Streeter et al., 2012), however, an alignment of IPMK and IP_3K has enabled modeling of IP_3 into the IP binding site of yeast IPMK (Holmes and Jogl, 2006). The smaller IP-lobe of IPMK compared to IP_3K provides a less restrictive pocket for IPs to bind. When IP_3 is bound for 3-phosphorylation, IPMK side-chains interact directly with the 1-, 4-, and 5-phosphates of IP_3. A phosphate moiety cannot occupy the axial 2-position because it would be sterically hindered by M151, as seen with M316 in IP_3K (Gonzalez et al., 2004), and 3-phosphate would clash with the γ-phosphate of ATP. However, IPMK possesses an R150, instead of the M288 seen in IP_3K, which does not preclude binding of a phosphate group at the 6-position (Holmes and Jogl, 2006). 1,4,5,6-IP_4 can also bind in the same orientation as IP_3 and would be phosphorylated to IP_5. Furthermore, the unrestrictive IP binding pocket allows IP_3 to bind in alternate orientation (Holmes and Jogl, 2006). A 180° flip of IP_3 allows the 6-hydroxyl to occupy the 3-hydroxyl that is favorable for 6-phosphorylation of IP_3. Although the 1-phosphate would now occupy the 2-position, the 1-phosphate is equatorial and is not sterically hindered by M151, instead forming contacts with other side-chains. 1,3,4,5-IP_4 can also bind in the alternate orientation of IP_3 and be phosphorylated to IP_5.

More recently, the crystal structure of plant IPMK has revealed that an IP phosphate motif may be recognized by IPMK, which may explain the 6/3/5-kinase activities of IPMK (Endo-Streeter et al., 2012). Modeling of IPs into the active site of the plant IPMK crystal structure suggests that the 5-kinase activity of human and plant IPMK may be elicited via the reorientation of 1,3,4,6-IP_4 in the IP binding site, such that the 5-hydroxyl of 1,3,4,6-IP_4 is occupying the same position as the 3-hydroxyl of IP_3 or 1,4,5,6-IP_4. Thus, in this new orientation, the 5-hydroxyl of 1,3,4,6-IP_4 is positioned for phosphorylation (Chang and Majerus, 2006; Endo-Streeter et al., 2012).

Small inter-species residue changes likely contribute to changes in kinase specificity observed between different subspecies of IMPK, however, all IPMKs discriminate their substrates based on a combination of steric exclusions and phosphate occupancies (Endo-Streeter et al., 2012). Thus, IPMK's mechanism of substrate selectivity retains features of both IP_3K, which it shares structural homology, and ITPK1, which also displays catalytic versatility.

1.8.4 $PPIP_5K$

$PPIP_5K$ phosphorylates the 1-phosphate of IP_6 or 5-PP-IP_5 to yield 1-PP-IP_5 or 1,5-PP_2-IP_4, respectively (Draskovic et al., 2008; Lin et al., 2009), but shows negligible activity toward 1-PP-IP_5, IP_5, or 5-PP-IP_4, which indicates the dense phosphate profile of the substrates is critical for recognition (Wang et al., 2012). Thus, $PPIP_5K$ is a highly specific 1-kinase and must accommodate highly negative pyrophosphate moieties.

Recently, the crystal structure of human $PPIP_5K$ was solved and revealed it largely resembles ITPK1, even though they only share 11% sequence identity (Wang et al., 2012) (Figure 1.4d). Two anti-parallel β-sheets surround the nucleotide, representative of the ATP-grasp fold (Wang et al., 2012). Although the ATP binding sites of $PPIP_5K$ and ITPK1 are similar, the IP binding site shows considerable structural differences. In $PPIP_5K$, arginine and lysine residues strongly interact with every phosphate of IP_6 or 1-PP-IP_5, whereas in ITPK1, non-basic glycine and glutamine residues line the IP binding site, resulting in only three phosphates and none of the hydroxyls of IP_3 being directly coordinated (Miller et al., 2005). Mutations of most of the $PPIP_5K$ residues in the IP binding site reduced enzymatic activity by 90% revealing their importance for IP recognition (Wang et al., 2012), which is consistent with its highly specific substrate recognition. Moreover, the IP binding site in $PPIP_5K$ is precisely shaped to accommodate the stereochemistry of six or more phosphates, whereas the IP binding site in ITPK1 is relatively wide for different substrate orientations, which confers catalytic versatility (Miller et al., 2005). The crystal structures of $PPIP_5K$ reveal that IP_6 and 5-PP-IP_5 bind in the same orientation (Wang et al., 2012). Finally, the inositol ring of the IP is positioned perpendicular to the ATP phosphates, which avoids electrostatic clashes with the non-reacting oxygen atoms of the 1-phosphate and

steric clashes with the axial 2-phosphate that faces the opposite direction. Thus, $PPIP_5K$ employs a hybrid shape-affinity mechanism of substrate selectivity. Steric occlusion of the axial 2-phosphate prevents reorientation of 1-PP-IP_5, such that the pyrophosphate occupies the 5-position (180° flip across the 3'-6' axis), while the heavily basic IP binding site promotes high affinity to highly phosphorylated IP substrates, like IP_6 and 5-PP-IP_5, over IP_5 and PP-IP_4, and presumably, IP_3s and monophosphorylated IP_4s.

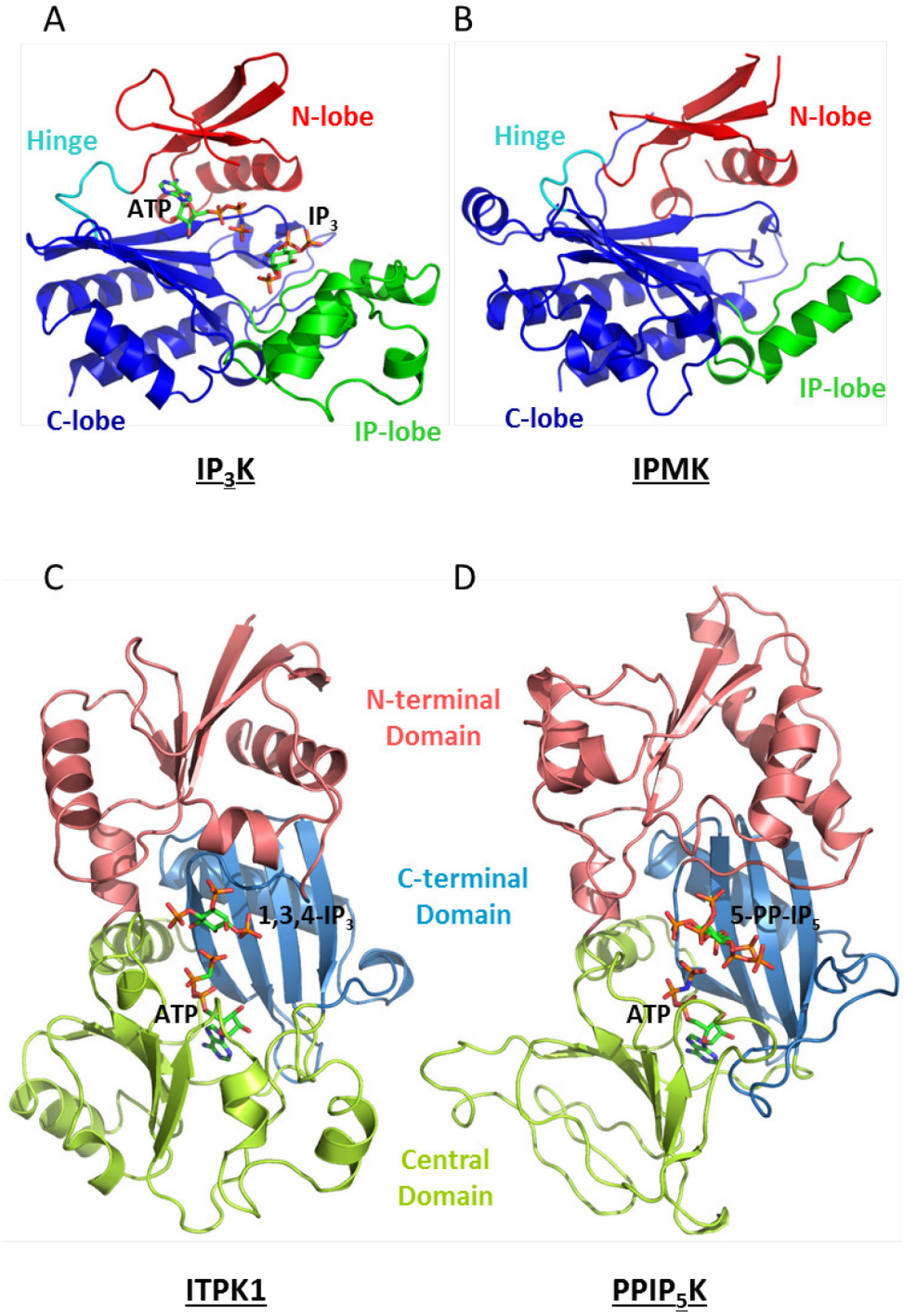

Figure 1.4. Structure and fold of IPKs. (A) IP_3K and (B) IPMK belong to the inositol polyphosphate kinase subfamily. (C) ITPK1 and (D) $PPIP_5K$ belong to the ATP-grasp fold subfamily.

1.8.5 IPK1

IPK1 is the putative member of a third subfamily of IPKs. IPK1 has been characterized from various sources including soybean (Phillippy et al., 1994), yeast (Ives et al., 2000), human (Verbsky et al., 2002), plant (Sweetman et al., 2006), and maize (Sun et al., 2007). Remarkably, there is very low sequence homology for IPK1 from yeast to mammals (11%), yet every IPK1 phosphorylates the 2-hydroxyl of IP_5 to yield IP_6 (Sweetman et al., 2006). Moreover, IPK1 shows kinase specificity for the axial 2-hydroxyl, distinguishing IPK1 among all other IPKs, which phosphorylate equatorially oriented hydroxyl groups of the inositol ring (Stephens et al., 1991). Consequently, IPK1 is very different from other IPKs. The sequence of IPK1 does not contain any signature motifs of the inositol polyphosphate subfamily and secondary structure predictions do not detect any conserved β-sheets representative of the ATP grasp subfamily (Cheek et al., 2005). Thus, the structure of IPK1 was expected to adopt a novel fold.

Concurrent to our studies, the crystal structure of plant IPK1 was solved (Gonzalez et al., 2010), which revealed IPK1 possesses a bi-lobed structure with a hinge that connects the N-lobe and C-lobe as they fold over the active site, which contains both IP and nucleotide. In IP_3K and IPMK, the N- and C-lobes fold over the ATP binding cleft, but a separate IP-lobe contributes to inositide binding. In contrast, the C-lobe of IPK1 possesses a defined region, termed the C_{IP}-lobe, which is the major region involved in inositide binding and encompasses almost half of the protein (Gonzalez et al., 2010). In ITPK1 and $PPIP_5K$, two domains surround the active site containing both IP and ATP. Thus, the overall structure of IPK1 has some similarities and differences with previously crystallized IPKs.

Gonzalez et al. co-crystallized IPK1 in four complexes, with either IP_5 or IP_6 (binary complexes), and AMPPNP+IP_5 or ADP+IP_6 (ternary complexes) (Gonzalez et al., 2010). The ATP binding site is formed by numerous residues on the N- and C-lobe, which create a hydrophobic environment for the adenine and ribose of the nucleotide. A G-loop on the N-lobe coordinates the phosphates of ATP, as seen with IP_3K and PKA. Like all other IPKs, an aspartate residue, D368, coordinates the metal ion, and a lysine residue, K168, neutralizes the negative charge during phosphoryl transfer.

These four structures also described the IP binding site. Electrostatic maps of the surface of IPK1 show a very large, basic, and solvent exposed pocket where the IP binds. Of the 13 interactions with the IPK1 and IP, 11 occur on the C-lobe, while only 2 occur on the N-lobe. The 4-, 5-, and 6-phosphates are exclusively coordinated by the C-lobe, while the 1- and 3-phosphates are coordinated by the N-lobe. Many of these residues are highly basic lysine and arginine residues, however, there are some acidic and polar residues as well. The plane of the IP is perpendicular to ATP such that the γ-phosphate is positioned for transfer to the axial 2-hydroxyl of the IP. Both D368 and K168 coordinate the 2-hydroxyl and mutations of these residues rendered IPK1 inactive (Gonzalez et al., 2010).

There were no apparent differences between the two IP-bound, substrate-bound, and product-bound structures of IPK1. Superposition of these four structures of IPK1 yielded an RMSD of only 0.48 Å (Gonzalez et al., 2010). These structures depict how nucleotide and inositide bind in the active site, but they do not describe the catalytic cycle of IPK1. Moreover, it is not clear how IPK1 shows specificity for IP_5 over IP_4s and IP_3s. The IP binding site presents no steric occlusions in each of the phosphate binding regions, as seen in ITPK1, and the IP binding site is not specifically shaped for IP_5 over other IPs, as seen with IP_3 in IP_3K. Thus, the mechanism of substrate selectivity employed by IPK1 remains undefined.

1.9 Rationale of the Thesis

Given that a) IP_5, IP_6, and PP-IPs have all been implicated in cell death, b) IPK1 plays a significant role in regulating the levels of higher IPs, and c) IPKs are structurally diverse, the overall goal of this thesis work is to structurally and biochemically characterize IPK1.

The specific objectives of this work are to:

1. identify conformational states of IPK1, which reveals the mechanism of IP recognition for IPK1;
2. define the roles of phosphate recognition in IP binding and IPK1 activation, which validates the IP recognition mechanism of IPK1;
3. describe the conformational changes and kinase activation of IPK1, which distinguishes IPK1 activation from other kinases; and
4. identify novel small molecule inhibitors of IPK1, which provides a basis for the structural determinants of IPK1 inhibitor specificity.

Our work lays the foundation to develop selective inhibitors for IPK1 to be used as a tool to i) further our understanding of the functional roles of higher IPs, ii) validate the IP signaling axis as a target for inducing cell death, and iii) explore new avenues to treat diseases associated with dysregulated cell death signaling. In addition, characterization of IPK family members reveals similarities and differences that can be exploited to target other IPKs and further our understanding of diverse IP signaling pathways.

Connecting Text

Substrate recognition is an important component for the catalytic mechanism of any enzyme. Information on the IP recognition mechanisms for some IPKs has been described, but remain elusive for others, such as IPK1 (Gonzalez et al., 2004; Holmes and Jogl, 2006; Miller et al., 2005; Wang et al., 2012) . The initial crystal structures of IPK1 showed how IPK1 phosphorylates IP_5 to yield IP_6, but did not reveal how IPK1 selectively recognizes IP_5 (Gonzalez et al., 2010).

In Chapter 2, we describe experiments revealing that IPK1 adopts multiple conformational states in solution, which are not appreciated from previous static crystal structures. These conformational states were identified by performing limited proteolysis of IPK1 in the apo-, substrate-, and product-bound form. Furthermore, we determined the crystal structure of IPK1 in complex with nucleotide only, which reveals that a significant portion of the N-lobe is unstable in the absence of IP.

The data from Chapter 2 allows us to propose a two-step model of IP recognition for IPK1. In this model, IP_5 is initially recognized by the 4-, 5-, and 6-phosphates. Then, the 1-phosphate stabilizes the N-lobe and engages IPK1 into the active state. Our model of IP recognition for IPK1 is unique among IPKs and provides further insight into the catalytic mechanisms for all kinases.

Chapter 2. Inositol phosphate-induced stabilization of inositol 1,3,4,5,6-pentakisphosphate 2-kinase and its role in substrate specificity

Varin Gosein, Ting-Fung Leung, Oren Krajden, Gregory J. Miller

Protein Science. 2012. 21(5):737-742.

Abstract

Inositol phosphate kinases (IPKs) sequentially phosphorylate inositol phosphates (IPs) on their inositol rings to yield an array of signaling molecules. IPKs must possess the ability to recognize their physiological substrates from among a pool of over 30 cellular IPs that differ in numbers and positions of phosphates. Crystal structures from IPK subfamilies have revealed structural determinants for IP discrimination, which vary considerably between IPKs. However, recent structures of inositol 1,3,4,5,6-pentakisphosphate 2-kinase (IPK1) did not reveal how IPK1 selectively recognizes its physiological substrate, IP_5, while excluding others. Here, we report that limited proteolysis has revealed the presence of multiple conformational states in the IPK1 catalytic cycle, with notable protection from protease only in the presence of IP. Further, a 3.1 Å crystal structure of IPK1 bound to ADP in the absence of IP revealed decreased order in residues 110–140 within the N-lobe of the kinase compared with structures in which IP is bound. Using this solution and crystallographic data, we propose a model for recognition of IP substrate by IPK1 wherein phosphate groups at the 4-, 5-, and 6-positions are recognized initially by the C-lobe with subsequent interaction of the 1-position phosphate by R130 that stabilizes this residue and the N-lobe. This model explains how IPK1 can be highly specific for a single IP substrate by linking its interactions with substrate phosphate groups to the stabilization of the N- and C-lobes and kinase activation.

Keywords: inositol phosphate; kinase activation; substrate recognition; enzyme specificity

Introduction

Inositol phosphate kinases (IPKs) sequentially phosphorylate inositol phosphates (IPs) on their inositol rings to yield an array of unique signaling molecules with diverse cellular functions (Majerus, 1992; Shears, 1998). Among these functions, IPs are implicated in a variety of diseases such as cancer and diabetes (Piccolo et al., 2004; Irvine, 2005; Shi et al., 2006). IPKs must discriminate between IPs with different numbers and positions of phosphates to recognize specifically their physiological substrates. Crystal structures from each of the IPK subfamilies have revealed structural determinants for IP discrimination, which vary considerably between IPKs. Strict specificity of inositol 1,4,5-trisphosphate 3-kinase (IP_3K) relies upon shape complementarity with the sparsely phosphorylated IP_3 substrate, and it binds to both precisely positioned phosphate and hydroxyl groups (Gonzalez et al., 2004). In contrast, the active site of inositol 1,3,4-trisphosphate 5/6-kinase (ITPK1) exhibits little shape complementarity with its varied substrates and its affinity for them is dictated by contacts with phosphates alone, thereby permitting promiscuous substrate recognition (Miller et al., 2005). Inositol 1,3,4,5,6-pentakisphosphate 2-kinase (IPK1) is uniquely specific for a single highly phosphorylated IP, inositol 1,3,4,5,6-pentakisphosphate (IP_5), which demands use of a mechanism distinct from those used by IP_3K or ITPK1 to achieve selectivity.

The recently determined crystal structures of IPK1 in its IP substrate- and product-bound forms revealed extensive contacts with phosphate groups of IPs and the mechanism through which the axial 2-hydroxyl of its substrate is selectively phosphorylated (Gonzalez et al., 2010). These four structures are highly similar with no significant differences (RMSD = 0.48 Å) suggesting IPK1 adopts the same conformation regardless of whether it is substrate- or product-bound (Figure 2.1a). However, it was not clear from these similar structures how IPK1 recognizes IP_5 while excluding other IPs with similar stereochemistry at the 2-hydroxyl and phosphate groups. We hypothesized that this selectivity is defined by a previously unrecognized conformational change triggered by binding of an IP with a specific phosphate profile.

Materials and Methods

Protein Expression and Purification

A. thaliana IPK1 was previously cloned into a pET28a vector containing a 6xHis tag and expressed in Bl-21 AI cells (Invitrogen). Cells were grown in Terrific broth with kanamycin at 37 °C to an OD_{600} = 1.5 and protein over-expression was induced with 0.5 mM IPTG and 0.1% L-arabinose at 18 °C for 20 h. Cells were harvested at 5000xg and were lysed for 1 h using a sonicator in 10 mM Tris-HCl (pH 8.0), 250 mM NaCl and 50% glycerol. Supernatant was separated from lysate using centrifugation. The supernatant was then diluted 5-fold using 20 mM Tris-HCl (pH 8.0) and 500 mM NaCl and then 25 mM imidazole was added. IPK1 was purified by applying the diluted supernatant to a Ni-NTA column followed by washing with 20-column volumes of 50 mM KPO_4 (pH 8.0), 800 mM NaCl, 1% Triton X-100, 1.7 mM β-mercaptoethanol. Protein was eluted using 10-column volumes of 250 mM imidazole in 20 mM Tris-HCl (pH 8.0), 300 mM NaCl buffer and subsequently dialyzed into 50 mM Tris-HCl (pH 8.0), 50 mM NaCl, and 1 mM DTT. Next, the protein was applied to a 5 mL Heparin SP FF column. The column was washed with 10-column volumes of dialysis buffer and IPK1 was eluted over an increasing NaCl concentration gradient. Fractions containing purified protein were analyzed by SDS-PAGE and pooled accordingly. Finally, the pooled sample was applied to a S-300 Sephacryl gel filtration column equilibrated in 50 mM Tris-HCl (pH 8.0), 150 mM NaCl, and 2.5 mM DTT. Fractions containing IPK1 were analyzed by SDS-PAGE and pooled accordingly. The protein was concentrated to 20 mg/mL and stored at 4 °C. A summary of the purification of IPK1 is provided in Figure S2.1.

Protein Crystallization

All crystals grew at 20 °C within 6-72 h using the sitting-drop vapour-diffusion method. All ligand solutions were pH 8.0 prior to incubating with protein for 30 min at 4 °C. IP_6 was purchased from Sigma-Aldrich. IP_5 was purchased from Cayman Chemical Company. IPK1 (5 mg/mL) crystallized with 5 mM ADP/IP_6/$MgCl_2$ in 0.08 M MES (pH 6.5), 19.85% PEG 3000, 0.17 M NaCl, 2.35% benzamidine HCl. For the substrate-bound state, IPK1 (5 mg/mL) crystallized with 2 mM ADP/IP_5, 4 mM $MgCl_2$ in 0.09 M MES (pH 6.5), 18% PEG4000, 0.54 M

NaCl, 0.01 M Trimethylamine HCl. For the ADP-only bound state, IPK1 (10 mg/mL) crystallized with 5 mM ADP/$MgCl_2$ in 0.18 M $CaCl_2$, 0.1 M Tris-HCl (pH 8.0), 18.18% PEG6000, 0.01 M TCEP. Crystals of IPK1 in complex with different ligands are shown in Figure S2.2.

Data collection

X-ray diffraction data for all complexes were collected on a Rigaku MicroMax-007 HF microfocus X-ray generator fitted with Varimax X-ray optics and a Saturn 944+ CCD detector. All data were measured under cryogenic conditions, cryoprotected with reservoir solution including 5-10% PEG400, and processed with HKL2000 software (Otwinowski and Minor, 1997).

Structure Determination and Refinement

Diffraction data was analyzed and processed with HKL2000 software and refined with Phenix (Adams et al., 2010) and Coot (Emsley and Cowtan, 2004). Molecular replacement was performed with Protein Data Bank code: 2XAM. All model images were created using PyMol (DeLano Scientific).

Limited Proteolysis

Limited proteolysis of IPK1 was performed in 50 mM Tris-HCl (pH 8.0), 150 mM NaCl, and 2.5 mM DTT buffer in separate 1.5 mL microfuge tubes. 80 μg of IPK1 was incubated with 2 mM $MgCl_2$, 2 mM of nucleotide (ATP, ADP, AMPPNP) and/or 2 mM of IP (IP_5 or IP_6) for 20 min at 4 °C. 0.08 μg of trypsin was added resulting in a final volume of 200 μL. The reactions were incubated at 20 °C and 50 μL samples were taken at 1 h, 5 h, 9 h, 16 h. Samples were analyzed by SDS-PAGE and stained with Coomassie blue. For N-terminal sequencing, a duplicate gel was run and bands were transferred to a PVDF membrane. The blot was submitted to the Sheldon Biotechnology Centre (McGill University, Montreal, QC) for N-terminal sequencing of the fragments.

B-factor Analysis

B-factors were extracted from PDB files using the online tool NIH StrucTools. Mainchain B-factors from the ADP+IP_5 structure were subtracted from the ADP structure and ADP+IP_6 structure to provide a baseline for B-factor

comparison between ADP and ADP+IP_6 complexes. Calculated B-factor differences were plotted using GraphPad Prism (GraphPad Software Inc.)

Results and Discussion

To confirm the presence of different conformational states in the IPK1 catalytic cycle, we performed limited proteolysis of IPK1 in its free state, bound to nucleotides or to a nucleotide analog (ATP, ADP, or AMPPNP), IP (IP_5 or IP_6), and in ternary complexes (AMPPNP+IP_5 or ADP+IP_6) (Figure 2.1b). Trypsin digests were performed at 20 °C for 9 hours and the resulting proteolytic patterns were compared on SDS gels to detect distinct conformations. Differences in the digestion patterns were evident, indicating that IPK1 adopts a series of conformations in solution. In the apo state, IPK1 is extensively digested to small fragments indicating that free IPK1 is protease labile and suggesting that it is flexible in solution. Nucleotides alone exhibited modest protection of IPK1 from proteolysis but the digestion pattern revealed no protection of stable domains. IP_6 binding also provided little protection from protease. This is in contrast to IP_5, which protected a 37 kDa fragment not protected in the apo state, which is indicative of IP-induced stabilization of IPK1. N-terminal sequencing revealed that this 37 kDa-protected fragment resulted from trypsin cleavage between R130 and V131 while all residues C-terminal to R130 remained intact, thereby demonstrating stabilization of the C-lobe of the kinase but not the N-lobe. No differences were reported between the IP_5- and IP_6-bound IPK1 crystal structures, indicating that there are differences in conformational dynamics in different ligand-bound states that may not be detectable in static crystal structures. Finally, we observed synergistic protection in the ternary complexes. Here, when bound also by nucleotides, both IP_5 and IP_6 protected IPK1 from cleavage at R130, albeit to different extents. The additional 46 kDa fragment stabilized in the ternary complexes is cleaved by trypsin at K52 while the remainder of the protein remains intact, including the site at R130. This synergistic protection of R130 revealed stabilization of both the N- and the C-lobes of the kinase, which has been reported to be a critical step in kinase activation (Knighton et al., 1991; Sicheri et al., 1997; Ozkirimli and Post, 2006).

To further explore the conformational changes IPK1 undergoes during IP binding, we determined the nucleotide-bound structure of IPK1 in the absence and presence of its IP substrate and compared features of these structures to identify the mechanism by which IPK1 transitions into its catalytically active state.

Here, we present the 3.1 Å crystal structure of IPK1 bound to ADP in the absence of IP (Table S2.1). Overall, this structure is very similar to the previously solved crystal structures of IP-bound IPK1 with and without nucleotides and our own structure of IPK1 bound to ADP+IP_6. There are no gross conformational differences between the IP-bound and free structures in the C-lobe (RMSD = 0.40 Å) of the kinase and no differences in positions or B-factors of the residues that bind the 4-, 5-, and 6-phosphates of the IP. In this structure, IP-binding residues, including K411, R415, Y419, K170, R192, H196, K200 and N238, are all positioned as they are in the IP-bound states (Figure 2.2a). These residues are likely held in place by water molecules that create a network of interactions in the absence of IP, but this supposition is speculative as the resolution of the structure (3.1 Å) was too low to confirm positions of solvent molecules. Between the ADP-bound state and all IP-bound structures, there is a notable difference in the orientation of the residue that interacts with the 1-phosphate of the IP (Figure 2.2a,b). The sidechain for R130 cannot be modeled in the ADP-alone state, suggesting that this residue becomes ordered only upon occupancy of the active site by the correct substrate.

To identify regions of decreased order in the ADP-bound state, we compared B-factors among ADP+IP_6-bound-, ADP+IP_5-bound-, and the ADP-bound-IPK1 structures (Figure 2.2c). Only modest differences were detectable between the ADP+IP_5- and ADP+IP_6-bound states (blue line), but compared to either of these structures, there were substantial localized increases in B-factors in the ADP-bound state (red line). Specifically, marked differences in B-factors were observed for residues 110 to 140 in the N-lobe of the kinase when the ADP+IP_6 and the ADP-bound structures were compared. Consistent with the limited proteolysis in solution where IPK1 is cleaved at R130 in the absence of IP, we see a destabilization of the region surrounding R130 in the IP-free crystal structure, which appears to be shared with much of the N-lobe of the kinase (Figure 2.2d).

Our limited proteolysis and IP-free crystal structure indicate that IPK1 adopts multiple conformational states not appreciated from previous crystal structures. Here, the decreased order in the crystal structure is consistent with the protease sensitivity in solution supporting our use of the crystal structure to propose dynamics of the N-lobe of the kinase in the absence of IP substrate. The different extents of protease protection in these states suggest that conformational

dynamics may play a more significant role in the IPK1 catalytic cycle than previously thought.

Consistent with these observations, we propose a model for recognition of IP substrate by IPK1 wherein phosphate groups at the 4-, 5- and 6-positions are required for initial recognition of IP_5 by the residues K411, R415, Y419, K170, R192, H196, K200 and N238, which are poised for binding IP_5 in the IP-free state (Figure 2.3a). Subsequently, interaction of a 1-position phosphate with R130 stabilizes this residue and the N-lobe. In this two-step model for substrate recognition and activation, contacts at the 4-, 5-, and 6-positions are needed for initial recognition and the 1-phosphate is required for IPK1 subsequently to adopt an active conformation. In this model, the 4-, 5-, and 6-phosphates share the role for mediating initial substrate contact with the enzyme, while the 1-phosphate plays the subsequent, but critical role of stabilizing the N-lobe of the kinase, an essential step for kinase activation (Figure 2.3b). This model – including the critical role of the 1-phosphate – is consistent with the report that IPK1 exhibits some activity toward 1,3,4,6-IP_4, but no activity towards 3,4,5,6-IP_4, which lacks the 1-phosphate (Sweetman et al., 2006).

Conclusion

Knockout of the IPK1 gene in mice is embryonic lethal (Verbsky et al., 2005b) and RNAi of IPK1 in zebrafish exhibit developmental defects (Sarmah et al., 2005) which suggest an important physiological role for IPK1. Characterizing the mechanism IPK1 uses for substrate recognition opens up new avenues for selectively targeting IPK1 as the similarity among IP substrates has previously hindered the development of specific inhibitors for IPKs.

Acknowledgements

We thank Dr. Charles. A. Brearley (University of East Anglia) for his gift of the AtIPK1-pET28 vector, Dr. Jing Hu (McGill University) for performing N-terminal sequencing, Dmitry Rodionov (McGill University) for assistance in crystal diffraction and Anne W. Coventry for critical reading of the manuscript.

This work was supported by a Canadian Institutes of Health Research Operating Grant MOP-93687, a CIHR New Investigator Award, and a CIHR Strategic Training Initiative in Chemical Biology.

Figure 2.1. Limited proteolysis of IPK1. (A) Cartoon representation of product-bound IPK1 depicting overall topology: N-lobe (red), C-lobe (blue), hinge (cyan), C_{IP}-lobe (green) with ADP (purple) and IP_6 (orange); Protein Data Bank code: 3UDZ. Dashed lies indicate untraceable regions. **(B)** IPK1 (55 kDa) was incubated with trypsin in numerous conditions with nucleotides and/or inositides. Two fragments were protected in multiple conditions. N-terminal sequencing identified one fragment to be cleaved after K52 (46 kDa) and the other to be cleaved after R130 (37 kDa). Both residues are shown in yellow in (A) (R130, sticks; K52, rectangle).

A

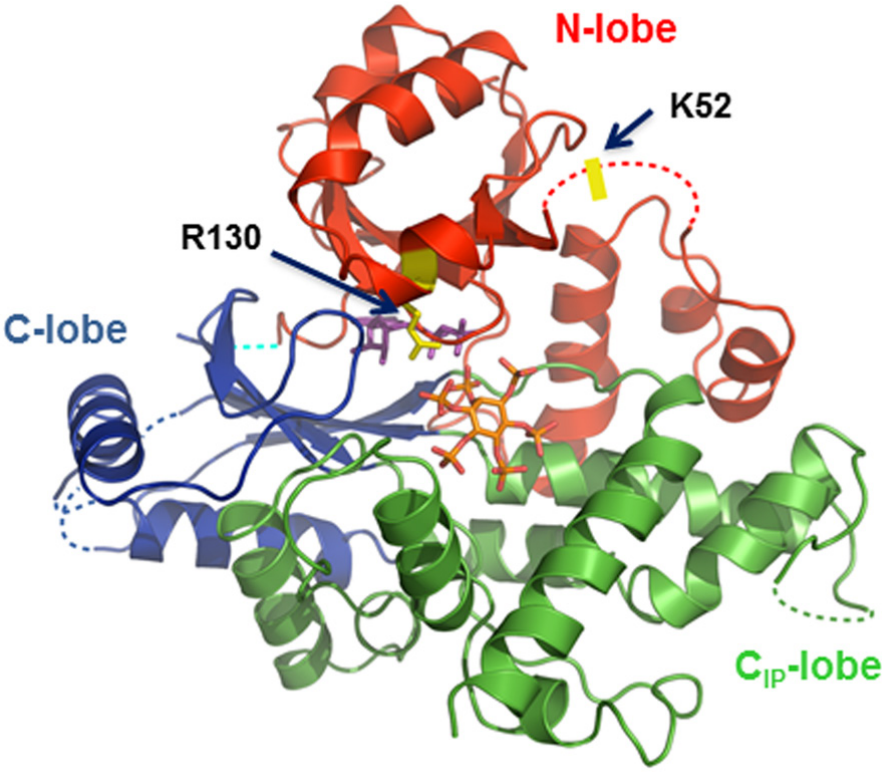
N-lobe
K52
R130
C-lobe
C$_{IP}$-lobe

B

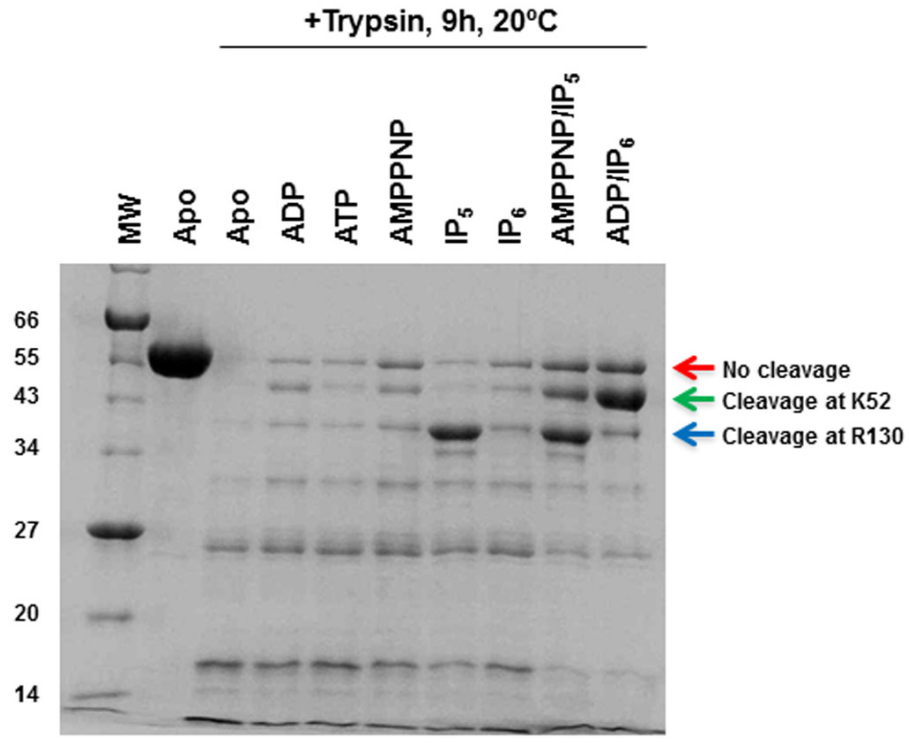
+Trypsin, 9h, 20°C
MW
Apo
Apo
ADP
ATP
AMPPNP
IP$_5$
IP$_6$
AMPPNP/IP$_5$
ADP/IP$_6$
66
55
43
34
27
20
14
No cleavage
Cleavage at K52
Cleavage at R130

Figure 2.1.

Figure 2.2. IPK1 exhibits localized disorder of the N-lobe in the absence of substrate. Electron density of substrate binding residues (2Fo-Fc (1.8σ)) is shown for crystal structures of IPK1 bound to **(A)** ADP+IP_6 and **(B)** ADP. **(C)** B-factor analysis of residues in ADP-bound state (red) and ADP+IP_6-bound state (blue). **(D)** Cartoon representation of ADP-bound crystal structure colored by B-factor differences between ADP-bound state and ADP+IP_6-bound states. Blue represents no difference while red represents highest differences.

A
ADP+IP6
R130
K411
R415
Y419
K170
R192
H196
N238
K200
B
ADP
R130
K411
R415
Y419
K170
R192
H196
N238
K200
C
R130
Δ B-factors (Å²)
60
40
20
0
-20
0
100
200
300
400
Residue
D
N-lobe
C-lobe
R130

Figure 2.2.

Figure 2.3. Proposed model of IPK1 activation. (A) In the inactive state, IPK1 remains an open "clamshell" (1) which closes slightly upon binding of ATP (2). IP_5 is then initially recognized at the 4-, 5- and 6-positions (3). Finally, with IP_5 bound, interactions between R130 and 1-phosphate stabilize the N-lobe of the kinase into the active state. **(B)** Two classes of interactions with IP substrate are necessary for IPK1 activity. The 4-, 5- and 6-positions of IP_5 are required for initial recognition, while the 1- and 3-positions are required for N-lobe stabilization. IP-binding residues from an alignment of the ADP-bound structure of IPK1 (purple), the ADP+IP_5-bound structure of IPK1 (blue), and the ADP+IP_6-bound structure of IPK1 (teal) are shown.

A

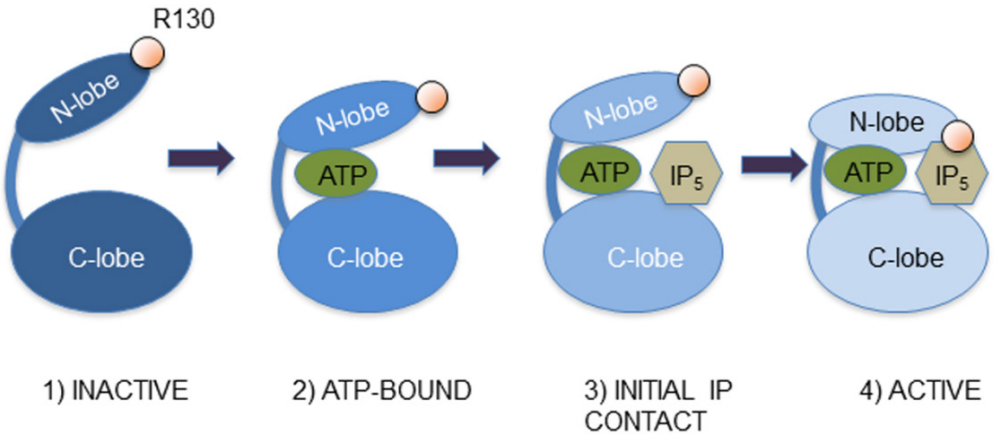
R130
N-lobe
C-lobe
N-lobe
ATP
C-lobe
N-lobe
ATP
IP5
C-lobe
N-lobe
ATP
IP5
C-lobe
1) INACTIVE
2) ATP-BOUND
3) INITIAL IP CONTACT
4) ACTIVE

B

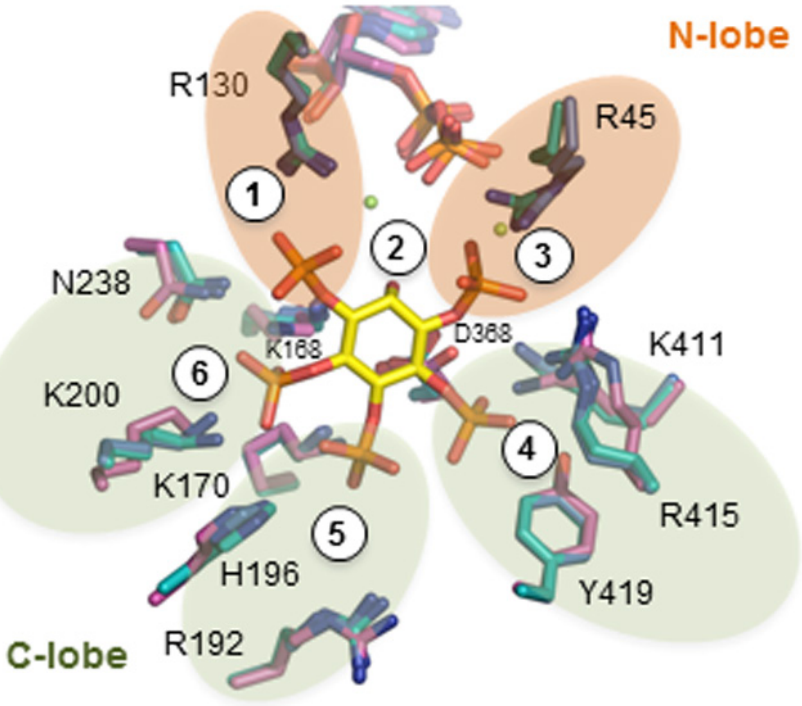
N-lobe
R130
R45
1
2
3
N238
K168
D368
K411
6
K200
4
K170
R415
5
H196
Y419
C-lobe
R192

Figure 2.3.

Figure S2.1. Purification of IPK1. (A) Samples of eluate after each purification step: immobilized metal affinity chromatography (IMAC) using Ni-NTA column, ion exchange (IEX) using Heparin SP FF column, gel filtration (GF) using S-300 Sephacryl column. The large band at 55 kDa is IPK1. **(B)** Chromatograph of IMAC. **(C)** Chromatograph of IEX (blue) overlayed with increasing NaCl gradient (green). **(D)** Chromatograph of GF (blue), overlayed with MW standards (red). Comparison of eluate volume with MW standards indicates that IPK1 is a monomer in solution and possesses a molecular weight of 55 kDa.

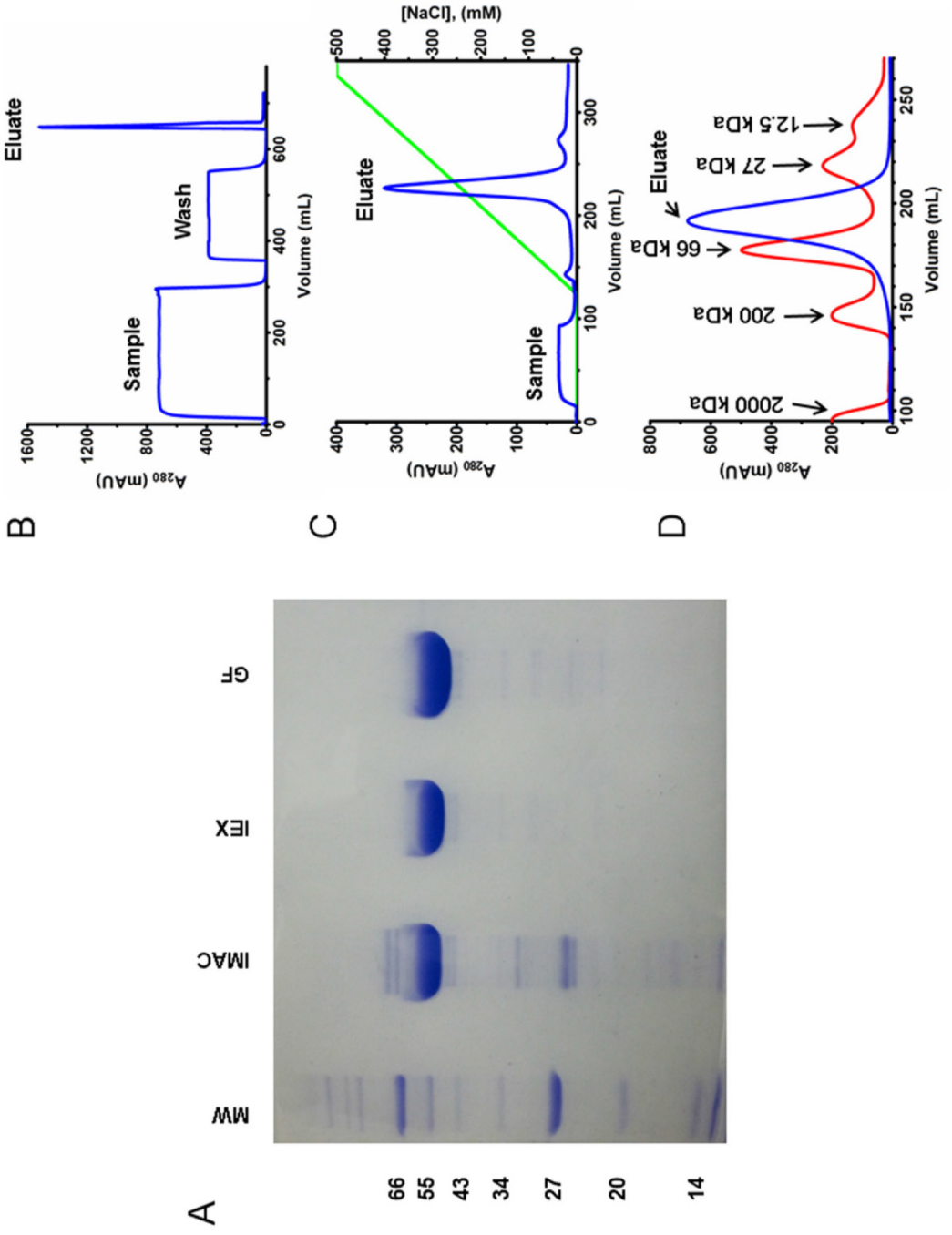
A
MW
IMAC
IEX
GF
66
55
43
34
27
20
14
B
Eluate
Wash
Sample
A280 (mAU)
Volume (mL)
C
[NaCl], (mM)
Eluate
Sample
A280 (mAU)
Volume (mL)
D
Eluate
2000 kDa
200 kDa
66 kDa
27 kDa
12.5 kDa
A280 (mAU)
Volume (mL)

Figure S2.1.

Figure S2.2. IPK1 crystal complexes. (A) ADP+IP_6. 5 mg/mL of IPK1 crystallized with 5 mM ADP/IP_6/$MgCl_2$ in 0.08 M MES (pH 6.5), 19.85% PEG 3000, 0.17 M NaCl, 2.35% benzamidine HCl. **(B)** ADP+IP_5. 5 mg/mL of IPK1 crystallized with 2 mM ADP/IP_5 in 4 mM $MgCl_2$, 0.09 M MES (pH 6.5), 18% PEG4000, 0.54 M NaCl, 0.01 M Trimethylamine HCl. **(C)** ATP. 5 mg/mL of IPK1 crystallized with 5 mM ATP/$MgCl_2$ in 0.18 M $CaCl_2$, 0.1 M Tris-HCl (pH 8.0), 18.18% PEG6000, 0.01M sodium bromide. **(D)** ADP. 10 mg/mL of IPK1 crystallized with 5 mM ADP/$MgCl_2$ in 0.18 M $CaCl_2$, 0.1 M Tris-HCl (pH 8.0), 18.18% PEG6000, 0.01 M TCEP. All crystals were grown 20 °C and ranged from 0.1-0.5 mm in size.

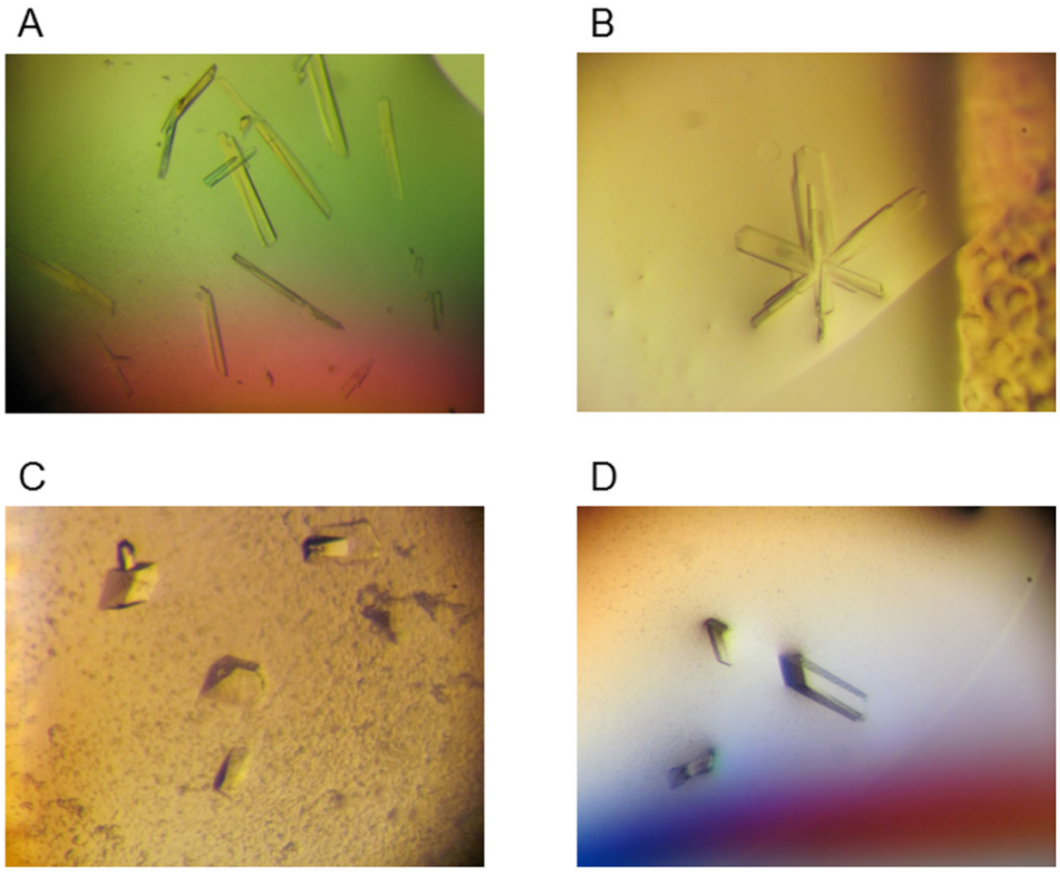

Figure S2.2.

Table S2.1. Data collection and refinement statistics.

(molecular replacement with PDB ID: 2XAM)

	ADP (PDB ID: 3UDS)	ADP+IP_5 (PDB ID: 3UDT)	ADP+IP_6 (PDB ID: 3UDZ)
Data collection			
Space group	P1	P1	P1
Cell dimensions			
a, *b*, *c* (Å)	58.29, 59.88, 82.91	59.36, 59.91, 83.14	59.06, 59.39, 82.75
α, β, γ (°)	83.40, 89.40, 65.30	90.02, 97.04, 116.81	89.84, 82.58, 63.36
Resolution (Å)	50.00-3.10 (3.29-3.10)**	50.00-3.10 (3.26-3.10)	50.00-2.50 (2.58-2.50)
R_{merge}	0.061 (0.134)	0.132 (0.218)	0.084 (0.152)
$I / \sigma I$	15.1 (7.7)	16.7 (7.0)	39.1 (15.8)
Completeness (%)	95.15 (90)	96.4 (95)	94.5 (91)
Redundancy (%)	3.9 (3.9)	3.9 (4.0)	3.7 (3.7)
Refinement			
Resolution (Å)	42.82-3.10	44.62-3.10	41.43-2.50
No. reflections	17,449	17,694	32,523
R_{work} / R_{free}	0.2370 / 0.3119	0.2098 / 0.2762	0.1890 / 0.2595
No. atoms	5,796	6,267	6,761
Protein	5,740	6,145	6,169
Ligand/ion	56	122	131
Water	0	0	461
B-factors (Å^2)			
Protein	64.31	26.26	35.28
Ligand/ion	65.12	36.02	27.81
Water	0	0	32.50
R.m.s. deviations			
Bond lengths (Å)	0.013	0.011	0.022
Bond angles (°)	1.319	1.287	1.229

*One single crystal used for each data collection.

**Values in parentheses are for highest-resolution shell.

Connecting Text

In Chapter 2, we proposed a two-step model of IP recognition for IPK1 whereby IP_5 is initially recognized at the 4-, 5-, and 6-positions, and then the 1-position phosphate stabilizes IPK1 into the active conformational state.

In Chapter 3, we describe experiments to support our model by defining the roles of the different phosphate groups of IP_5. We systematically tested IP_5 and a set of IP_4s that lacked phosphate groups at different positions in a binding assay and activity assay. With this strategy, we could elucidate the effect of each phosphate on IP binding to IPK1 and IPK1 activation. Furthermore, we tested the activity of a series of IPK1 mutants with point mutations for each residue that interacts with the IP substrate. Comparison of the activities of each mutant IPK1 to wild-type IPK1 highlights the role of each position phosphate for IPK1 activity.

The data from Chapter 3 show that the 5- and 6-phosphates are the most important for IP binding, and the 1- and 3-phosphates are the most important for IPK1 activation. These findings support in part our proposed IP recognition model for IPK1, but the role of the 1-phosphate in stabilizing IPK1 remains to be described.

Chapter 3. Roles of phosphate recognition in inositol 1,3,4,5,6-pentakisphosphate 2-kinase substrate binding and activation

Varin Gosein and Gregory J. Miller

Journal of Biological Chemistry. 2013. 288(37):26908-26913.

Abstract

Inositol phosphate kinases (IPKs) sequentially phosphorylate inositol phosphates (IPs) to yield a group of small signaling molecules involved in diverse cellular processes. Inositol 1,3,4,5,6-pentakisphosphate 2-kinase (IPK1) phosphorylates IP_5 to IP_6; however, the mechanism of IP recognition employed by IPK1 is currently unresolved. We previously demonstrated that IPK1 possesses an unstable N-lobe in the absence of IP, which led us to propose that the phosphate profile of the IP was linked to stabilization of IPK1. Here, we describe a systematic study to determine the roles of the 1, 3, 5, and 6 phosphate groups of IP_5 in IP binding and IPK1 activation. The 5- and 6-phosphate groups were the most important for IP binding to IPK1, and the 1- and 3-phosphate groups were more important for IPK1 activation than others. Moreover, we demonstrate that there are three critical residues (R130, K170, and K411) necessary for IPK1 activity. R130 is the only substrate-binding N-lobe residue that can render IPK1 inactive; its 1-phosphate is critical for full IPK1 activity and for stabilization of the active conformation of IPK1. Taken together, our results support the model for recognition of the IP substrate by IPK1 in which (i) the 4-, 5-, and 6-phosphates are initially recognized by the C-lobe and, subsequently, (ii) the interaction between the 1-phosphate and R130 stabilizes the N-lobe and activates IPK1. This model of IP recognition, believed to be unique among IPKs, could be exploited for selective inhibition of IPK1 in future studies that investigate the role of higher IPs.

Keywords: IPK1; IP_5; IP_6; inositol phosphates; phosphorylation; substrate recognition; kinase activation

Introduction

Inositol phosphates (IPs) are a group of small molecules that play critical roles in cellular signaling (Irvine and Schell, 2001). IP signaling regulates DNA editing and repair (Hanakahi et al., 2000), vesicle transport (Hilton et al., 2001), and ion channel regulation (Vajanaphanich et al., 1994) and has been implicated in diseases such as cancer and diabetes (Shi et al., 2006). IPs are produced by sequential phosphorylation of inositol 1,4,5-trisphosphate (IP_3) by a family of enzymes known as IP kinases (IPKs) (Irvine and Schell, 2001). Similarity between IPs, which sometimes differ by only one phosphate group on the inositol ring, demands that IPKs use mechanisms to recognize and phosphorylate specific positions of their IP substrates while excluding highly similar molecules. Crystal structures from each of the IPK subfamilies have revealed that the structural determinants for IP discrimination vary between IPKs. Inositol 1,4,5-trisphosphate 3-kinase (IP_3K) employs shape complementarity to recognize precisely positioned phosphate and hydroxyl groups of IP_3 (Gonzalez et al., 2004). In contrast, inositol 1,3,4-trisphosphate 5/6-kinase (ITPK1) discriminates among IPs using phosphate affinity and stereochemical features to establish contacts with phosphates that are sufficient for substrate recognition (Miller et al., 2005). Crystal structures of inositol 1,3,4,5,6-pentakisphosphate 2-kinase (IPK1) in its IP substrate- and product-bound forms reveal extensive contacts with all phosphate groups of the bound IPs (Gonzalez et al., 2010). These structures reveal how inositol 1,3,4,5,6-pentakisphosphate (IP_5) is phosphorylated on its axial 2-hydroxyl, yielding inositol 1,2,3,4,5,6-hexakisphosphate (IP_6), but they do not suggest a mechanism through which IPK1 selectively recognizes IP_5 as its substrate while excluding other highly phosphorylated IPs with free axial 2-hydroxyl groups. We recently determined the crystal structure of wild-type IPK1 in an IP-free state, which exhibited disorder within its N-lobe of the kinase, centered at R130 (Chapter 2) (Gosein et al., 2012). This IP-free structure suggests that binding of IP substrate plays a role in stabilization of the N- and C-lobes of the kinase, which is an important step in the activation of protein kinases (Knighton et al., 1991; Ozkirimli and Post, 2006; Sicheri et al., 1997).

Our current objective was to define the contributions of the individual phosphate groups of the IP to binding and to recognition of the bound IP as a substrate. The results demonstrate that each phosphate group of the IP plays a

different role in binding and activation of IPK1 and that there are three critical contacts formed between IPK1 and the IP that mediate IPK1 activation.

Materials and Methods

Generation of alanine mutants

Residues with interactions to IP_5, either directly or through solvent molecules, were identified using previous crystal structures (Gosein et al., 2012). Mutation of these residues to alanine was performed by site-directed mutagenesis using the quick-change method (Stratagene) and the sets of oligonucleotides shown in Table S3.1. A pET28a vector containing wild-type *A. thaliana* IPK1 and a hexahistidine tag was used as a template (a kind gift from Dr. C. Brearley). All mutations were verified by DNA sequencing.

Protein expression and purification

Wild-type IPK1 and alanine mutants were expressed in BL-21 AI cells (Invitrogen) that were grown in Terrific Broth to an OD_{600} = 1.5 and induced with 0.5 mM IPTG and 0.1% L-arabinose at 18 ºC for 20 h. Cells were lysed in 10 mM Tris-HCl (pH 8.0), 250 mM NaCl and 50% glycerol using a sonicator. The supernatant was separated from lysate using centrifugation at 45000xg. The supernatant was then diluted 5-fold using 20 mM Tris-HCl (pH 8.0) and 500 mM NaCl, and 25 mM imidazole was added. IPK1 was purified using NiNTA beads (Thermo Scientific) in a gravity column using 4 mL dry beads per 250 mL of culture. Beads were washed with 20-column volumes of 50 mM KPO_4 (pH 8.0), 800 mM NaCl, 1% Triton X-100, 1.7 mM β-mercaptoethanol. Protein was eluted using 250 mM imidazole in 20 mM Tris-HCl (pH 8.0), 300 mM NaCl buffer and then 2 mM DTT was added to the eluate. Protein concentration was determined by Bradford assay (Thermo Scientific) using BSA as a standard. Protein was stored at 4 ºC and used within 72 h.

Isothermal titration calorimetry (ITC)

Experiments were performed on a MicroCal iTC200 titration calorimeter (GE Healthcare). Wild-type IPK1 was purified and dialyzed into ITC buffer, which contained 50 mM HEPES (pH 7.5), 6 mM $MgCl_2$, 150 mM NaCl, 1 mM TCEP (pH 7.0). After dialysis of protein was complete, dialysis buffer was used to dissolve the ligands, IP and AMPPNP (Jena Bioscience). Titration experiments were performed at 25 ºC with 100 µM IPK1 and 1 mM AMPPNP in the cell and 1-

2 mM of IP in the syringe to ensure a final IP:IPK1 molar ratio of at least 2:1. Titration experiments were performed at least twice for each IP and one set was chosen to represent data. Calorimetric data was analyzed using Origin 7.0 (MicroCal). Data was fitted using a one-site model using Equation (1):

$$Q(i) = \frac{1}{2} nP_t \Delta HV \left\{ 1 + \frac{X_t}{nP_t} + \frac{1}{nKP_t} - \left[\left(1 + \frac{X_t}{nP_t} + \frac{1}{nKP_t} \right)^2 - \frac{4X_t}{nP_t} \right]^{\frac{1}{2}} \right\} \qquad (1)$$

where n is the number of IP binding sites on IPK1, P_t is the total concentration of IPK1, X_t is the total concentration of IP, V is the cell volume, K is the binding constant and ΔH corresponds to the enthalpy change due to IP-IPK1 binding. The heat corresponding to the ith injection only, ΔQ(i), is equal to the difference between Q(i) and Q(i−1) and is given by Equation (2), which is corrected by the injection volume dV_i for the displaced volume:

$$\Delta Q(i) = Q(i) + \frac{dV_i}{V_o} \left[\frac{Q(i) + Q(i-1)}{2} \right] - Q(i-1) \qquad (2)$$

IPK1 activity assay

Inositol phosphates (1,3,4,5,6-IP_5; 1,3,4,5-IP_4; 1,4,5,6-IP_4; 1,3,4,6-IP_4; 3,4,5,6-IP_4) were purchased from Cayman Chemical Company. A source for 1,3,5,6-IP_4 was not located. IPK1 kinase activity was assessed using the Kinase-Glo Max Luminescent Kinase Assay (Promega) as per manufacturer instructions. Kinase reactions were performed in 25 µL volumes in black 96-well plates at 25 ºC. The reaction mixture contained 50 mM HEPES (pH 7.5), 6 mM $MgCl_2$, 50 mM NaCl, and 300 µM ATP. 25 µL of Kinase-Glo reagent was added to stop the reaction, and luminescence was measured after 20 min on a Berthold Orion II Microplate Luminometer. Initially, 80 µM of IP was used and the amount of enzyme was varied to determine conditions in which product formation was linear over 30 min. Subsequently, an array of reactions with varying concentrations of IP (20 µM, 40 µM, 60 µM, 80 µM, 100 µM, 120 µM, 140 µM) stopped at various time points (2 min, 5 min, 10 min, 20 min, 30 min) was performed in triplicate. The rate of product formation versus IP concentration was plotted and fitted to the Michaelis-Menten equation using non-linear regression to determine K_M and V_{MAX}

(GraphPad). The k_{cat} values were calculated using the equation $k_{cat} = V_{MAX}/[E]$, where [E] is the concentration of enzyme in μM.

IPK1 alanine mutants activity assay

Initially, 150 ng of each mutant was tested for kinase activity with 80 μM IP_5 after 30 min. Mutants that exhibited little or no activity were retested using 750 ng of enzyme. Active mutants were further characterized for their kinetic parameters with IP_5 as a substrate using the above-mentioned approach.

Results

5- and 6-phosphates are critical for binding

To determine the role of phosphates at each position of the inositol ring, we measured the effect on binding affinity when using IPs lacking a phosphate group at the 1, 3, 5, or 6 positions. Using ITC, we obtained K_D values for each IP_4 and IP_5 (Table 3.1, Figure S3.1). As expected, IP_5, the native substrate for IPK1, displayed the highest binding affinity with a $K_D = 0.60$ μM. IP_4s exhibited a range of binding affinities. The K_D values of 1,4,5,6-IP_4 and 3,4,5,6-IP_4 were 13-fold higher than that of IP_5, while the K_D values of 1,3,4,6-IP_4 and 1,3,4,5-IP_4 were at least 30-fold higher. These results indicate that different phosphate groups have varying contributions to the binding affinity of IP_5 for IPK1. Comparison of $K_D(IP_4)$:$K_D(IP_5)$ ratios reveal that the 5- and 6-phosphates contribute the most to the binding affinity of the IP, as the absence of either phosphate group dramatically increases the K_D (Figure S3.2).

1- and 3-phosphates are important for substrate recognition

We tested the kinase activity of IPK1 for IP_5 and IP_4s using a luminescent-based assay to determine which phosphates identify an IP as a substrate for IPK1 (Figure 3.1, Table 3.2). Kinase activity of IPK1 was maximal in the presence of IP_5, with a $k_{cat} = 44.02 \pm 3.19$ nmol/min. With 1,3,4,6-IP_4, an IP lacking the 5-phosphate, there was a modest decrease in kinase activity with a $k_{cat} = 27.48 \pm 4.00$ nmol/min. In contrast, IPs lacking 1- and 3-phosphate groups exhibited a substantial 85% decrease in activity compared to IP_5. No activity was detected when 1,3,4,5-IP_4 was used as a substrate, suggesting that the 6-phosphate may also be important for activation. These results indicate that the 1- and 3-phosphates are important for the IP to be recognized as a substrate by IPK1. We also observe that the K_Ds for IPs lacking phosphates vary considerably, while the K_M for each IP remains nearly constant (Table 3.2). This disconnect suggests that the kinetic parameters of ligand binding or catalysis change along with the binding affinity, but we cannot define with the current set of assays how they change.

Alanine mutants identify active site residues critical for IPK1 activity

To identify the contacts between IPK1 and IP that are essential for activity, we mutated to alanine those IPK1 residues that interact with the IP and tested these mutants for activity towards IP_5 (Table 3.3). To compare kinase activity between mutants, we determined k_{cat} values for each mutant. For wild-type IPK1, k_{cat} = 44.02 ± 3.19 nmol/min. Mutation of R130, the only residue that interacts with the 1-phosphate of the IP, resulted in no detectable activity. Mutations of residues K168 and D368, which mediate phosphoryl transfer from ATP to the 2-hydroxyl, also exhibited no activity, as expected. The R45A mutant, which abolishes the contact with the 3-phosphate, displayed a 40% decrease in kinase activity (k_{cat} = 27.16 ± 1.79 nmol/min), while R415A and Y419A mutants, which abolish contacts with the 4-phosphate, both displayed activity equivalent to wild-type IPK1. In contrast, the K411A mutant, which abolishes contacts with both the 3- and 4-phosphates, showed no activity. The R192A mutant displayed a modest decrease in kinase activity (k_{cat} = 22.01 ± 2.05 nmol/min) and H196A had no effect on kinase activity (k_{cat} =34.12 ± 4.33 nmol/min), both of which demonstrate that interactions with the 5-position have modest impact on catalytic activity. The K170A mutant, which abolishes interactions with both the 5- and 6-phosphates, showed no activity. Finally, mutations of residues K200A, N238A, and N239A, which eliminate contacts with the 6-phosphate, displayed reduced activity compared to wild-type IPK1. Figure 3.2 summarizes the effect of alanine mutations in the inositide binding site on IPK1 activity. Here, we observe that the residues that interact with more than one phosphate play important roles in substrate recognition, while most residues that interact with a single phosphate play lesser roles in this process.

Discussion

Roles of different phosphate groups: binding vs. activation

Here, we present a systematic study to identify the relative contributions of the 1-, 3-, 5-, and 6-phosphates to IP_5 binding affinity and recognition as an IPK1 substrate. Initially, we used ITC to determine the binding affinity of IPK1 to IP_5 and to a set of IP_4s, each lacking a single phosphate group. We observed a spectrum of affinities for these differently phosphorylated IP_4 molecules, indicating that phosphates contribute differently to binding. IPs lacking the 5- or the 6-phosphate displayed the lowest binding affinity to IPK1, while IPs lacking the 1- or the 3-phosphate displayed only moderately decreased binding affinity (Table 3.1). The structure of nucleotide-bound IPK1 (Protein Data Bank code: 3UDS) revealed the N-lobe to be unstable compared to the IP-bound state, and in a recent structure of IPK1 engineered to crystallize in the absence of IP (Protein Data Bank code: 4AXC), the N-lobe was too far away from the C-lobe to form a complete inositide binding pocket (Banos-Sanz et al., 2012; Gosein et al., 2012). In both wild-type and mutant structures, the N-lobe fails to assemble into the active conformation. Our ITC binding data, which indicate that the C-lobe binding 5- and 6-phosphates contribute substantially more to binding, are consistent with the C-lobe playing a dominant role in substrate recruitment. This collection of structures and the binding data support the model that substrate recruitment likely occurs though the stable C-lobe, which comprises half of the IP binding site. To complete assembly of the IP binding site, IP must bind to both the N- and C-lobes, thereby coupling binding of the substrate to stabilization of the kinase.

We further investigated the contribution of each phosphate group of the IP to its recognition as a substrate and to activation of IPK1. We determined the K_M and k_{cat} of IPK1 in the presence of IP_5 and our series of IP_4s. These data indicate that k_{cat} for IPK1 is substantially decreased for IPs lacking the 1- or the 3-phosphate compared to IP_5 and 1,3,4,6-IP_4 (Table 3.2). Preliminary studies of IPK1 substrate specificity also revealed the use of 1,3,4,6-IP_4 as a substrate, but not 3,4,5,6-IP_4; however, a kinetic analysis of IPK1 with each IP_4 was not performed (Sweetman et al., 2006). Our observations are consistent with the 1- and 3-phosphates stabilizing the bi-lobed structure of IPK1, thereby promoting its

activation though recruitment of the N-lobe, using a similar mechanism to that reported for protein kinases (Sicheri et al., 1997).

IPK1 was unable to use 1,3,4,5-IP_4 as a substrate, which suggests that the 6-position may play a dual role in both IP binding and activation; abolishing both functions decreased its use as a substrate to levels below the detection limit of our assay. The K_Ds for 1,3,4,5-IP_4 and 1,3,4,6-IP_4 were similar; however, 1,3,4,6-IP_4 could be used as a substrate while 1,3,4,5-IP_4 could not. This indicates that the decreased binding affinity of 1,3,4,5-IP_4 for IPK1 was not by itself the underlying factor for its inability to be used as a substrate (Table 3.1). The 6-phosphate binding site plays a key role in IPK1 activation by preventing clasp formation — a critical step in the IPK1 catalytic cycle — in the absence of IP substrate. Binding of the 6-phosphate to K200 disrupts the interaction between K200 and E255, and this newly freed E255 binds to W129 thereby promoting clasp formation between the L3 loop and the α6 helix (Banos-Sanz et al., 2012). However, the K200A mutant, as well as other mutants that disrupt interaction with the 6-phosphate, K170A, N238A, and N239A, do not show any activity towards 1,3,4,5-IP_4, so intramolecular changes in the 6-phosphate binding site are not essential for IPK1 activation (Figure S3.3). It is possible that 1,3,4,5-IP_4 adopts alternative binding orientations, in which the 2-hydroxyl is not accessible for phosphorylation (Figure S3.4) (Chamberlain et al., 2007; Miller et al., 2005). Further experimentation will be required to ascertain why no activity is displayed towards 1,3,4,5-IP_4.

The critical roles of R130 and 1-phosphate in IPK1 activation

Based on previous crystal structures, we mutated each substrate-binding residue to alanine to determine the critical contacts between IPK1 and the IP. Each mutation abolished an interaction with one or two phosphates (Table 3.3), and we determined the K_M and k_{cat} for each mutant in the presence of IP_5. The impacts of the mutations and the activities of the IP_4s were largely symmetric; abolishing single contacts with a phosphate group through mutation had a similar impact as removing the phosphate from the substrate. A notable difference between the IPK1 mutant and IP_4 data was the asymmetric impact of abolishing the interaction with the 1-phosphate. Given that R130, located on the N-lobe, is the only residue that interacts with the 1-phosphate, we expected that an IP lacking the 1-phosphate would correspond with the activity of this mutant. However, the R130A mutant

displayed no detectable activity while 3,4,5,6-IP_4 could be used as a substrate, albeit with low activity (Tables 3.2, 3.3). Structures of IPK1 in complex with IP show that R130 forms a bond with G254, establishing an interaction between the L3 loop and the α6 helix and promoting clasp formation (Figure S3.5) (Gosein et al., 2012). This interaction, and therefore clasp formation, cannot occur in the R130A mutant, rendering IPK1 inactive. Transient clasp formation can occur in the wild-type IPK1, even in the absence of a 1-phosphate, which allows the use of 3,4,5,6-IP_4 as a substrate with low activity. The 1-phosphate interaction with R130 is conducive to clasp formation thereby rendering IPK1 fully active (Figure S3.5). Thus, the 1-phosphate stabilizes the active conformation of IPK1.

One critical residue at each phosphate-binding site

There are 13 residues that interact with the IP in the IPK1 active site, either directly or indirectly through ordered water molecules, and each of these residues results in a bond to a phosphate group. For each phosphate of the IP, there is a contact residue that plays a critical role, and mutation of that residue abolishes activity. As discussed above, R130 interacts with the 1-phosphate of the substrate and is a primary contact between the IP and the kinase N-lobe. R130 is essential due to its structural role in stabilizing the active state and not exclusively for its role in binding the 1-phosphate, as 3,4,5,6-IP_4 can bind and be recognized as a substrate. An IP lacking the 3-phosphate also displayed low activity; however, the R45A mutation, which disrupts the second contact between the IP and N-lobe, moderately impaired activity (Table 3.3). Thus, it appears that N-lobe interaction with IP is primarily mediated through R130 and the 1-phosphate. Mutation of K411, which interacts with both the 3- and the 4-phosphates, was critical for activity, yet mutations of R415 and Y419 that mediate other interactions with the 4-phosphate did not markedly affect IPK1 activity, nor did R45A, which is the second contact with the 3-phosphate, as described above (Table 3.3). Both the 5- and the 6-phosphates bind to K170, which is critical for activity; however, other 5-phosphate interactions with R192 and H196 and other 6-phosphate interactions with K200, N238, and N239 are dispensable for activity. Wild-type IPK1 displayed activity with IPs lacking the 3- or 5-phosphates, yet mutations of K170 and K411 rendered IPK1 inactive, likely due to the fact that these residues bind more than one phosphate (Tables 3.2, 3.3). Sequence alignments of IPK1 reveal

that R45, R415, and Y419 are the only inositide binding residues that are not conserved among plant, human, rat, and yeast (Gonzalez et al., 2010). Accordingly, R45A, R415A and Y419A mutations retained at least 60% of wild-type activity. The conservation of R130, but not R45, suggests that N-lobe contact with the IP is primarily mediated through the 1-phosphate. In summary, our data indicate that each phosphate has a critical residue in the active site without which the enzyme cannot function, notably R130, K170, and K411 (Table 3.3). Whether K170 and K411 impact binding affinity to the extent that substrate recognition cannot occur, or if these residues play structural roles in shaping the binding site into an active conformation, as R130 does, remains to be determined.

Model of IP-induced stabilization as a mechanism of selectivity of IPs

Our previous crystal structures revealed that IPK1 possesses a stable C-lobe and a destabilized N-lobe in the absence of IP, such that the inositide binding pocket remains partially formed (Gosein et al., 2012). We proposed a model wherein IPK1 links its interactions with IP substrate phosphate groups to stabilization of the N- and C-lobes and kinase activation. The stability of the C-lobe in the absence of IPs suggested that the roles of the 4-, 5-, and 6-phosphates were to mediate initial contact of the IP to IPK1 (Gosein et al., 2012). Our current study reveals that the 5- and 6-phosphates impact binding affinity more than the 1- and 3-phosphates. Our model also proposed that the 1- and 3-phosphates were required for N-lobe stabilization, as they act to bridge the N-lobe with the C-lobe. In our current study, IPK1 displayed substantially lower k_{cat} with 3,4,5,6-IP_4 and 1,4,5,6-IP_4 than with IP_5 or an IP_4 lacking the 5-phosphate. IP-free crystal structures of IPK1 reveal that the destabilization of the N-lobe is centered at R130, which directly binds to the 1-phosphate of the IP substrate (Gosein et al., 2012). The mutation of R130A impaired IPK1 activity, suggesting that the N-lobe is required to be stabilized for IPK1 activation, a key feature of kinase activation (Sicheri et al., 1997). In short, our study reveals specific roles for each of the IP phosphates linking IPK1 substrate specificity to IPK1 stability.

Conclusion

In this report, we demonstrate that the phosphate profile of IP_5 is mechanistically linked to IPK1 activation. We have identified phosphates at positions 1, 3, and 6 as the most important for activation of IPK1, while phosphates at positions 5 and 6 are more important for binding than those at positions 1 and 3. Identification of the roles of the phosphates of the IP supports our proposed model of IPK1 substrate specificity and may provide a basis for selective targeting of IPK1, as similarity among IP substrates continues to hinder development of specific inhibitors for IPKs. Inhibition of IPK1 would prove valuable in the investigation of the roles of higher IPs whose production is dependent on IP_6, the product of IPK1, as well as functional roles of IPK1 in mammals.

Acknowledgements

We thank Dr. Charles A. Brearley (University of East Anglia) for his gift of the AtIPK1-pET28 vector, Dr. Guennadi Kozlov (McGill University) for technical assistance with ITC, Dr. Dan Bernard (McGill University) for access to the luminometer used in enzyme assays, Dr. Hatem Dokainish (McGill University) for helpful discussions, and Anne W. Coventry for thoughtful reading of the manuscript.

This work is supported by a Canadian Institutes of Health Research Operating Grant MOP-93687 awarded to GJM and a CIHR Strategic Training Initiative in Chemical Biology awarded to VG.

Figure 3.1. Kinetic analysis of IPK1 toward IP_5 and IP_4s. IPK1 kinase activity was assessed using a luminescence based assay. The rate of product formation versus IP concentration was plotted and fitted to the Michaelis-Menten equation. Each point represents the mean ± S.D. of triplicate experiments. ●: 1,3,4,5,6-IP_5 ■: 1,3,4,6-IP_4 ◆: 3,4,5,6-IP_4 ▲: 1,4,5,6-IP_4.

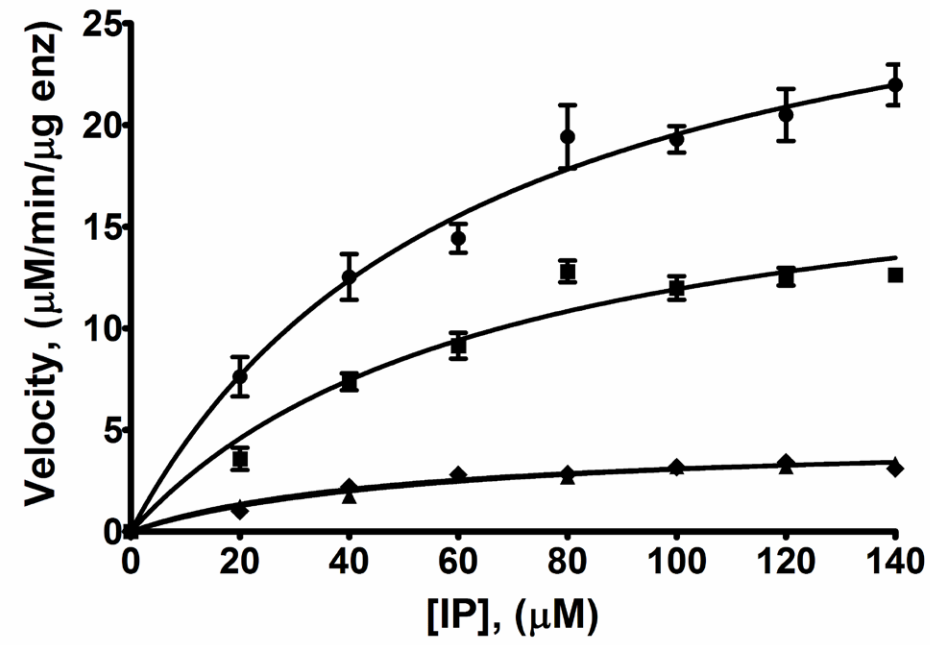
Velocity, (μM/min/μg enz)
25
20
15
10
5
0
0
20
40
60
80
100
120
140
[IP], (μM)

Figure 3.1.

Figure 3.2. Structural representation of kinetic parameters of alanine mutants. IP_5 is shown in yellow, stick form. Side chains of IP binding residues are shown in stick form and colored according to alanine mutant k_{cat}. Maroon indicates no activity. Darker shades of green indicate reduced activity compared to wild-type IPK1. Green indicates equivalent activity to wild-type IPK1. Side chains are grouped according to bound phosphate, overlaid with colored arcs (red: N-lobe; blue: C-lobe).

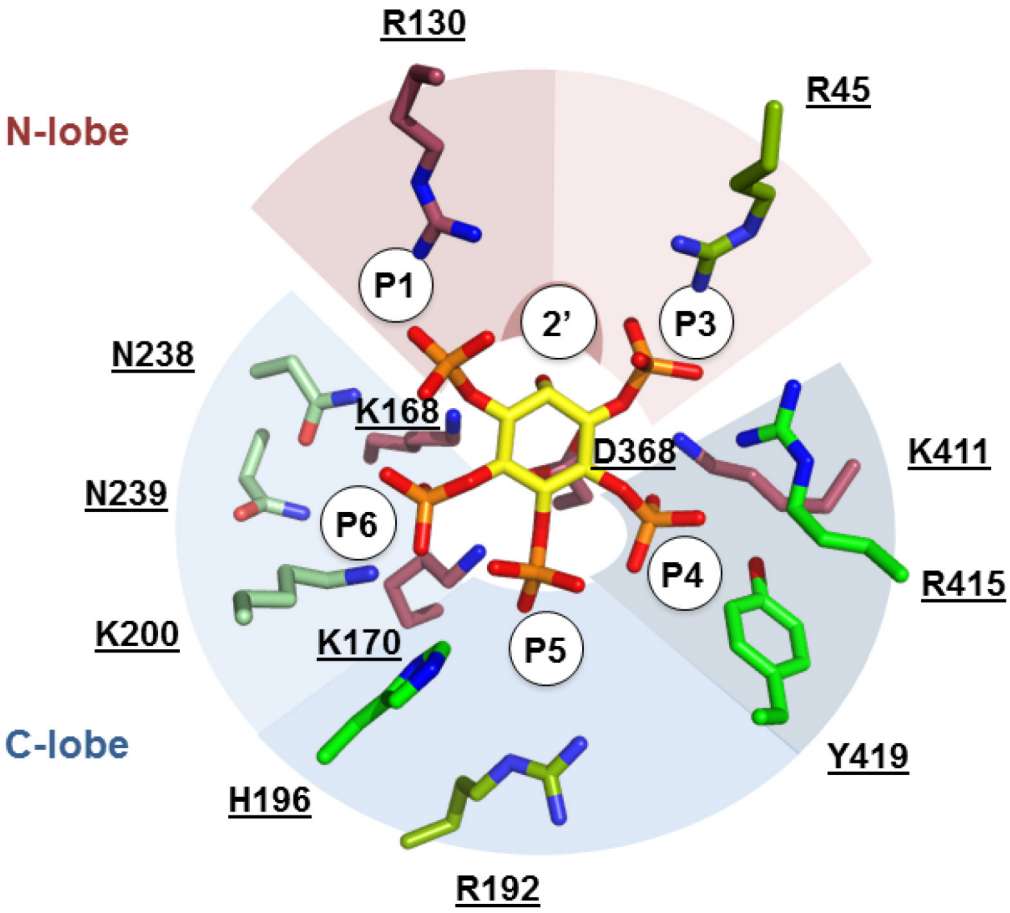
R130
R45
N-lobe
P1
2'
P3
N238
K168
D368
K411
N239
P6
P4
R415
K200
K170
P5
C-lobe
Y419
H196
R192

Figure 3.2.

Figure S3.1. Isotherms for IP_5 and IP_4s. (A) 1,3,4,5,6-IP_5; **(B)** 1,3,4,5-IP_4; **(C)** 1,4,5,6-IP_4; **(D)** 1,3,4,6-IP_4; **(E)** 1,3,4,5-IP_4. ITC was performed using a MicroCal iTC200 titration calorimeter. Titration experiments were performed at 25 ºC with 100 μM IPK1 and 1 mM AMPPNP in the cell and 1-2 mM of IP in the syringe to ensure a final IP:IPK1 molar ratio of at least 2:1. Titration experiments were performed at least twice for each IP and one set was chosen to represent data here. Calorimetric data was analyzed using Origin 7.0. Data was fitted using a one-site model using Equation (1) in main text.

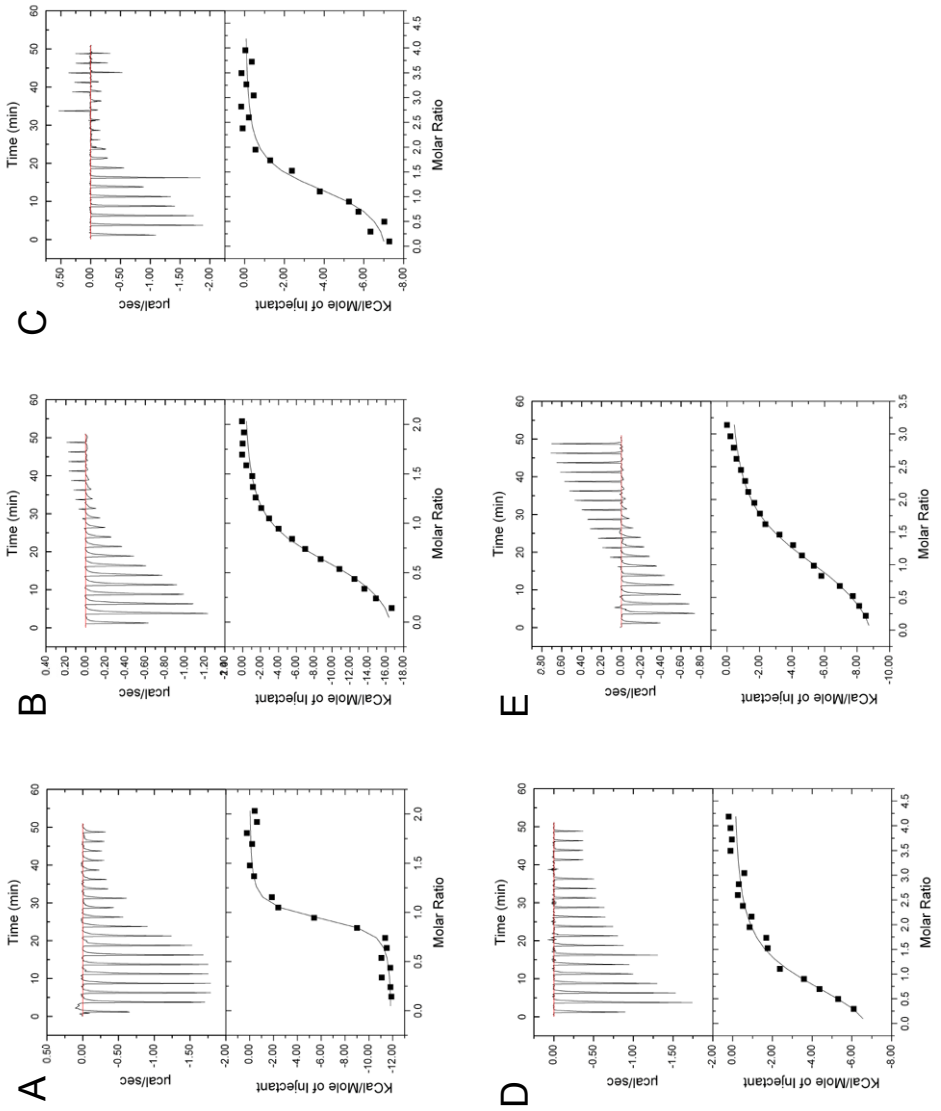

Figure S3.1.

Figure S3.2. Comparison of IPK1 binding affinity for IP_5 and IP_4s. The K_D of each IP was divided by the K_D of IP_5 and plotted. The larger the ratio, the weaker the binding affinity for a given IP.

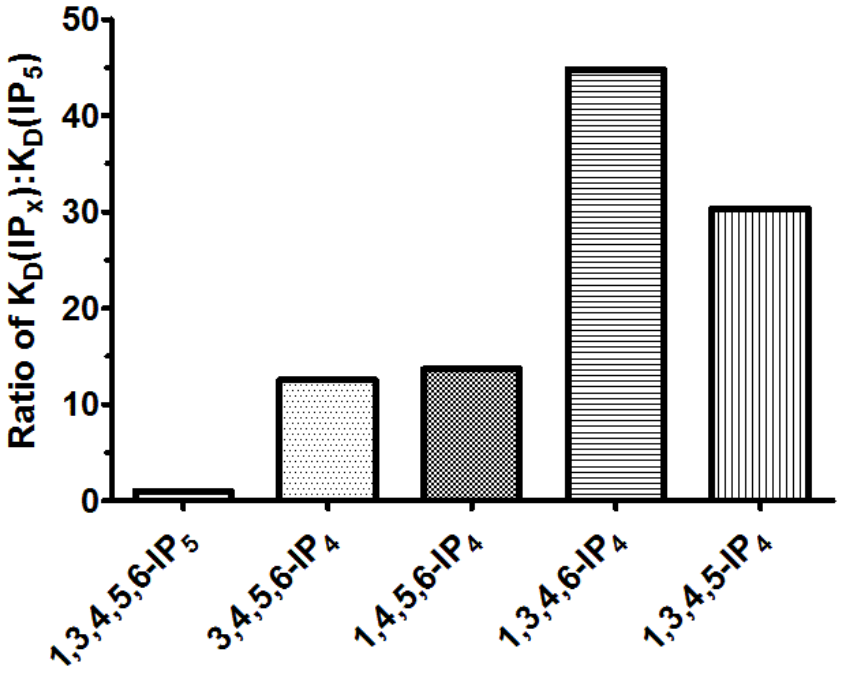
Ratio of $K_D(IP_X):K_D(IP_5)$
50
40
30
20
10
0
1,3,4,5,6-IP5
3,4,5,6-IP4
1,4,5,6-IP4
1,3,4,6-IP4
1,3,4,5-IP4

Figure S3.2.

Figure S3.3. 6-position mutants do not exhibit activity towards 1,3,4,5-IP_4. 150 ng of each IPK1 6-position mutant was tested in the presence of 80 μM 1,3,4,5,6-IP_5 (black bars) or 80 μM 1,3,4,5-IP_4 (grey bars) and 300 μM ATP for 30 min at 25 °C. No activity was detected for any 6-position mutant with 1,3,4,5-IP_4, but K200A, N238A, and N239A, were active with IP_5. Each bar represents the mean ± S.D. of triplicate experiments.

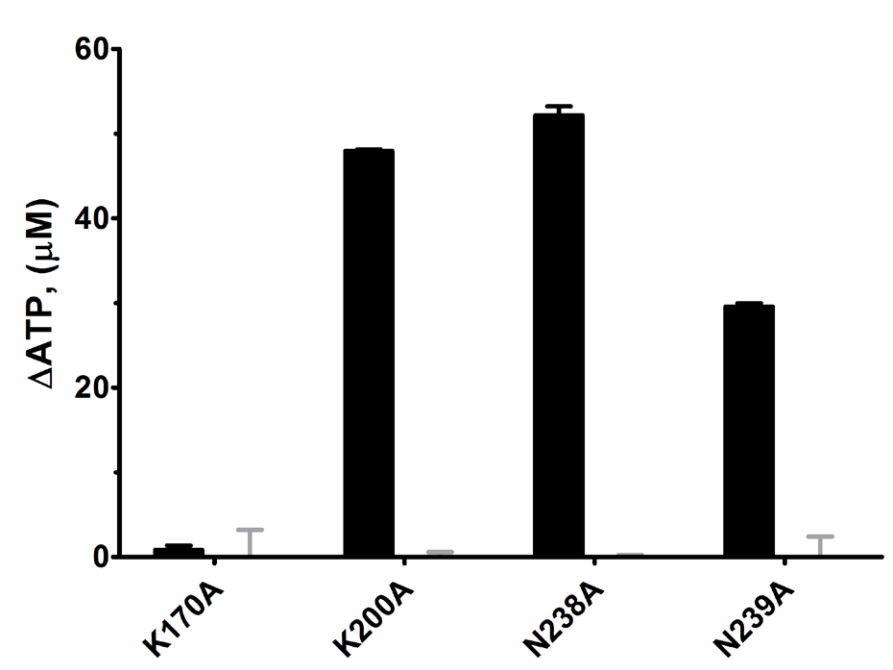

Figure S3.3.

Figure S3.4. Proposed binding orientations of 1,3,4,5-IP_4. (A) Expected orientation; **(B)** Flip around 2'-5' axis of the IP; **(C)** Rotation of IP clockwise of 120°; **(D)** Flip around 2'-5' axis of the IP and a rotation of the IP counterclockwise 120°. 1,3,4,5-IP_4 is shown in cyan, stick form, and IPK1 active site residues that interact with the IP are shown in light grey, stick form. ATP is not shown for clarity. In (A), the 2-hydroxyl is positioned for phosphorylation. Assuming ATP is bound, 1,3,4,5-IP_4 must adopt orientations (B), (C), and (D) to avoid steric hinderance with the γ-phosphate of the ATP, however, in these binding orientations, the hydroxyl group is not optimally positioned for phosphoryl transfer to occur.

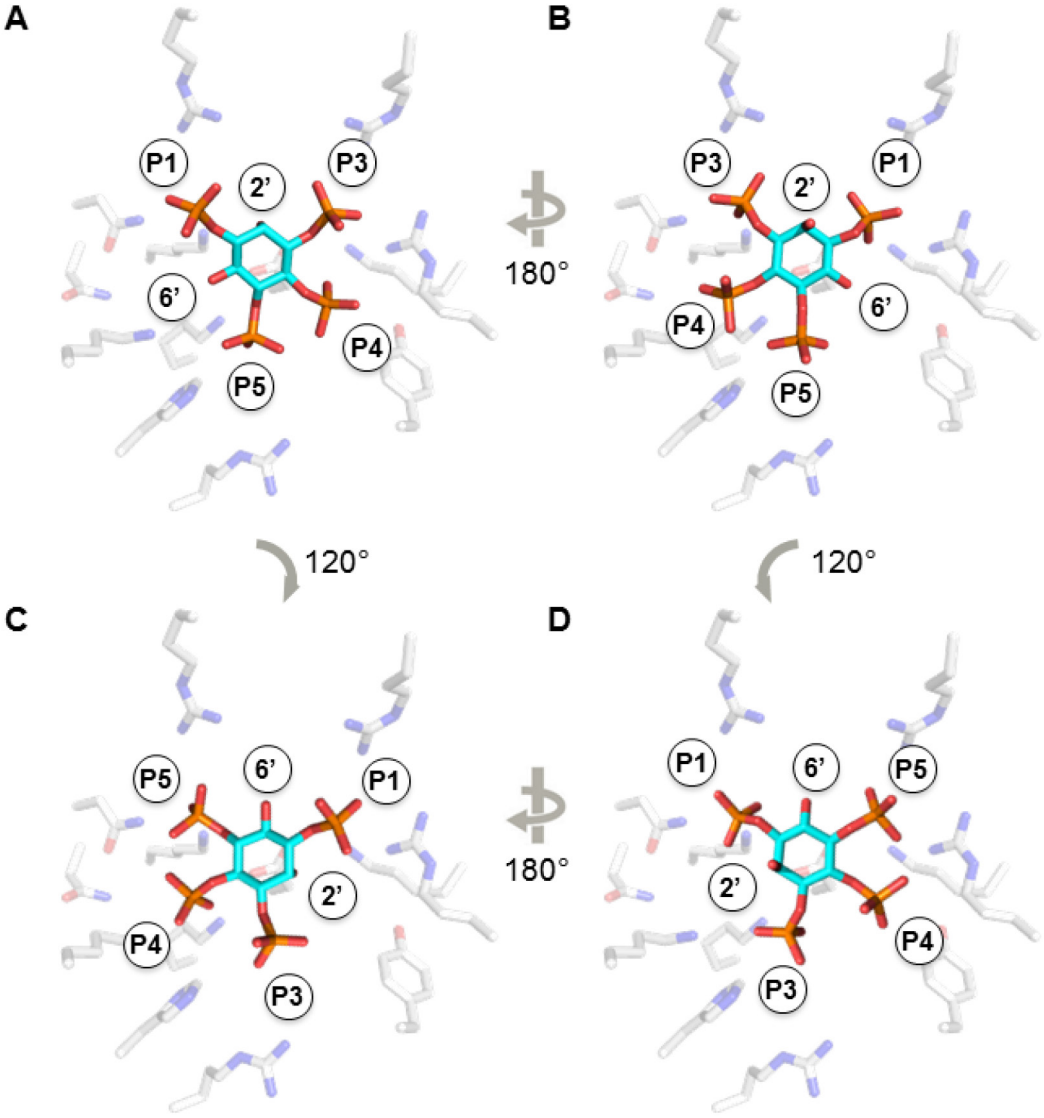

Figure S3.4.

Figure S3.5. Clasp formation between α6 helix and L3 loop. Interactions between R130 (magenta, stick form) and G254 (cyan, stick form) mediate clasp formation between the L3 loop (cyan) and the α6 helix (magenta), of the C-lobe (blue) and of the N-lobe (red), respectively. R130 also forms an interaction with the 1-phosphate of the IP which is conducive to clasp formation. Image was created using PyMol and a product-bound structure of IPK1 (Protein Data Bank code: 3UDZ). ADP (green) and IP_6 (yellow) are shown in stick form. Dashed lines indicate hydrogen bonds.

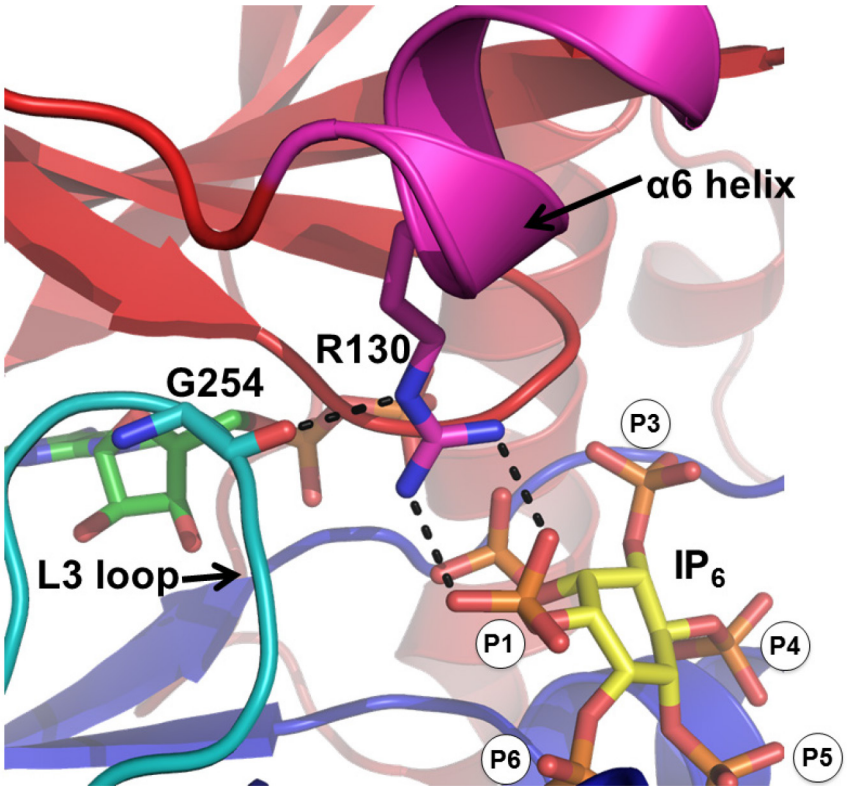

Figure S3.5.

Table 3.1. Binding data of IPK1 toward IP_5 and IP_4s.

IP	N (sites)	K (M^{-1})	K_D (μM)	ΔH (cal/mol)	ΔS (cal/mol/deg)
1,3,4,5,6-IP_5	0.895	1.68E+06	0.60	-11900	-11.4
1,3,4,6-IP_4	0.895	3.72E+04	26.88	-8720	-8.34
1,4,5,6-IP_4	1.14	1.22E+05	8.20	-7551	-2.05
3,4,5,6-IP_4	0.656	1.33E+05	7.52	-18300	-37.9
1,3,4,5-IP_4	1.19	5.49E+04	18.21	-10140	-12.3

Table 3.2. Kinetic parameters of IPK1 toward IP_5 and IP_4s.

IP	K_M (μM)	k_{cat} (min^{-1})
1,3,4,5,6-IP_5	63.05 ± 10.77	44.02 ± 3.19
1,3,4,6-IP_4	66.81 ± 22.37	27.48 ± 4.00
1,4,5,6-IP_4	55.99 ± 13.95	6.60 ± 0.66
3,4,5,6-IP_4	47.54 ± 13.94	6.30 ± 0.68
1,3,4,5-IP_4	nd	nd

Data represents the mean ± S.D. of triplicate experiments. nd: no activity detected.

Table 3.3. Kinetic parameters of IPK1 alanine mutants toward IP_5.

Mutant	K_M (μM)	k_{cat} (min^{-1})	PO_4 interaction
R45A	54.28 ± 9.07	27.16 ± 1.79	3
R130A	nd	nd	1
K168A	nd	nd	2
K170A	nd	nd	5,6
R192A	59.35 ± 13.41	22.01 ± 2.05	5
H196A	43.48 ± 15.62	34.12 ± 4.33	5
K200A	39.79 ± 19.52	16.74 ± 2.77	6
N238A	33.72 ± 7.918	14.74 ± 1.07	6
N239A	83.30 ± 9.53	15.89 ± 0.87	6
D368A	nd	nd	2
K411A	nd	nd	3,4
R415A	62.27 ± 21.89	38.71 ± 5.73	3,4
Y419A	76.86 ± 16.94	41.62 ± 4.25	4

Data represents the mean ± S.D. of triplicate experiments. nd: no activity detected. The last column indicates the IP phosphate that interacts with the mutant side chain, either directly or indirectly, through ordered water molecules.

Table S3.1. List of oligonucleotides used for alanine mutant generation.

R45A	Forward	gattcgtatacagaaggctgcgaggaacgataaagcaatc
	Reverse	gattgctttatcgttcctcgcagccttctgtatacgaatc
R130A	Forward	agcagcgtccgctatgggctgttaatgcagctaatg
	Reverse	cattagctgcattaacagcccatagcggacgctgct
K168A	Forward	gcggtggtgattgcattagtgttgaaatagcgcctaaatgcggatt
	Reverse	aatccgcatttaggcgctatttcaacactaatgcaatcaccaccgc
K170A	Forward	gcattagtgttgaaataaagcctgcatgcggatttcttccaacctcaa
	Reverse	ttgaggttggaagaaatccgcatgcaggctttatttcaacactaatgc
R192A	Forward	catactcaaaacaagcgtaagcgctttcaaaatgcatcaactccta
	Reverse	taggagttgatgcattttgaaagcgcttacgcttgttttgagtatg
H196A	Forward	caagcgtaagccgtttcaaaatggctcaactcctaaagttggaat
	Reverse	attccaactttaggagttgagccattttgaaacggcttacgcttg
K200A	Forward	ccgtttcaaaatgcatcaactcctagcgttggaatatatcgagatatctgaa
	Reverse	ttcagatatctcgatatattccaacgctaggagttgatgcattttgaaacgg
N238A	Forward	aaagctttatattccactcctcaagccaatttccgcgtattcttgaatgg
	Reverse	ccattcaagaatacgcggaaattggcttgaggagtggaatataaagcttt
N239A	Forward	ctataaaagctttatattccactcctcaaaacgctttccgcgtattcttgaat
	Reverse	attcaagaatacgcggaaagcgttttgaggagtggaatataaagcttttatag
D368A	Forward	gatagctgcaactgccaaagcctgtagtattatgatcagttt
	Reverse	aaactgatcataatactacaggctttggcagttgcagctatc
K411A	Forward	gtacatttcattgatctaagcctggcaccacttaagagaatggagtcata
	Reverse	tatgactccattctcttaagtggtgccaggcttagatcaatgaaatgtac
R415A	Forward	atctaagcctgaaaccacttaaggcaatggagtcatactacaaattgg
	Reverse	ccaatttgtagtatgactccattgccttaagtggtttcaggcttagat
Y419A	Forward	ctgaaaccacttaagagaatggagtcagcctacaaattggataagaagataattagc
	Reverse	gctaattatcttcttatccaatttgtaggctgactccattctcttaagtggtttcag

Connecting Text

In Chapter 3, we obtained evidence to support the first half of our two-step model of IP recognition for IPK1. We determined that the phosphate profile of the IP substrate is mechanistically linked to the activation of IPK1, whereby the 5- and 6-phosphates are important for IP binding and the 1- and 3-phosphates are important for activation. The second half of our model stated that the 1-phosphate stabilizes the N-lobe in order to activate IPK1. In Chapter 3, we observed that an alanine mutation of arginine-130, a residue that interacts with the 1-phosphate, impairs IPK1 activity, further suggesting an importance of the interaction between the 1-phosphate and IPK1.

In Chapter 4, we describe experiments to demonstrate a link between IP substrate specificity, IPK1 stability, and subsequent activation. We used our set of IP_4s to infer the role of each phosphate group in two assays that detect IPK1 stability. With this approach, we could determine the role of each phosphate in stabilizing IPK1. Furthermore, we suspected that we could alter the substrate specificity of IPK1 by artificially stabilizing IPK1. We therefore created a series of disulfide mutants and investigated their structure and kinetics using our established assays for activity and stability.

The data from Chapter 4 show that the 1- and 3-phosphates, which engage the N-lobe, contribute the most to IPK1 stability compared to the other phosphates. In addition, our engineered IPK1 disulfide mutants show that N-lobe stability is linked to substrate specificity and is a determinant for IPK1 activation. These findings provide the remaining evidence to fully validate our model of IP-induced stabilization for IPK1.

Chapter 4. Conformational stability of inositol 1,3,4,5,6-pentakisphosphate 2-kinase dictates its substrate selectivity

Varin Gosein and Gregory J. Miller

Journal of Biological Chemistry. 2013. doi: 10.1074/jbc.M113.512731.

Abstract

Inositol 1,3,4,5,6-pentakisphosphate 2-kinase (IPK1) converts IP_5 to IP_6. IPK1 shares structural similarity with protein kinases and is suspected to employ a similar mechanism of activation. Previous studies revealed roles for the 1- and 3-phosphates of IP_5 in IPK1 activation and that the N-lobe of IPK1 is unstable in the absence of IP. Here, we demonstrate the link between IPK1 substrate specificity and the stability of its N-lobe. Limited proteolysis of IPK1 revealed N-lobe stability is dependent on the presence of the 1-phosphate of the substrate, while overall stability of IPK1 was increased in ternary complexes with nucleotide and IPs possessing 1- and 3-phosphates that engage the N-lobe of IPK1. Thus, the 1- and 3-phosphates possess dual roles in both IPK1 activation and stability. To test if kinase stability directly contributed to substrate selectivity of the kinase, we engineered IPK1 mutants with disulfide bonds that artificially stabilized the N-lobe in an IP-independent manner thereby mimicking its substrate-bound state in the absence of IP. IPK1 E82C/S142C exhibited a DTT-sensitive 5-fold increase in k_{cat} for 3,4,5,6-IP_4 compared to wild-type IPK1. The crystal structure of the IPK1 E82C/S142C mutant confirmed the presence of the disulfide bond and revealed a small shift in the N-lobe. Finally, we determined that IPK1 E82C/S142C is substantially more stable than wild-type IPK1 under non-reducing conditions revealing that increased stability of IPK1 E82C/S142C correlates with changes in substrate specificity by allowing IPs lacking the stabilizing 1-phosphate to be used. Taken together, our results show that IPK1 substrate selection is linked to the ability of each potential substrate to stabilize IPK1.

Keywords: IPK1; IP_5; inositol phosphates; differential scanning fluorimetry; substrate recognition; kinase activation

Introduction

Inositol 1,3,4,5,6-pentakisphosphate 2-kinase (IPK1) is an inositol phosphate kinase (IPK) that catalyzes the phosphorylation of inositol 1,3,4,5,6-pentakisphosphate (IP_5) to inositol hexakisphosphate (IP_6) (Sweetman et al., 2006). IP_6 is involved in diverse cellular processes such as mRNA export (Alcazar-Roman et al., 2010), chromatin remodeling (Shen et al., 2003), apoptosis (Agarwal et al., 2009), and development (Sarmah et al., 2005). IPK1 itself has been demonstrated to affect apoptosis, and its expression is markedly elevated in renal samples from patients suffering from diabetic nephropathy, indicating it may play functional roles in disease states (Verbsky and Majerus, 2005; Merchant et al., 2009). Recent crystal structures have revealed that some IPKs possess an N- and C-lobed structure similar to that of protein kinases (PKs), in which both lobes contribute to a conserved ATP binding pocket (Ten Eyck et al., 2008). Both PKs and IPKs require mechanisms to recognize their physiological substrates from among pools of similar molecules. While PKs recognize consensus sequences in their targets, IPKs must recognize their substrates from among more than 30 IPs based on differences in stereochemistry, and numbers and patterns of phosphate groups (Ubersax and Ferrell, 2007; Irvine and Schell, 2001). This mechanism must be able to differentiate physiological substrates from non-substrates that may differ by the presence, absence, or position of a single phosphate. Structures of IP_3K, IPMK, ITPK1, and $PPIP_5K$ all reveal mechanisms that define substrate specificity (Miller and Hurley, 2004; Holmes and Jogl, 2006; Miller et al., 2005; Wang et al., 2012). The first crystal structures of IPK1 revealed how IP_5 is phosphorylated on the 2-hydroxyl of the inositol ring to yield IP_6, but the recognition of all five phosphate groups and the axial hydroxyl group did not offer explanations for how it excludes IPs with fewer than five phosphates from its pool of potential substrates (Gonzalez et al., 2010; Sweetman et al., 2006). For PKs, the stability of the N- and C-lobes is a critical precursor for kinase activation (Knighton et al., 1991; Sicheri et al., 1997; Ozkirimli and Post, 2006) and these IPK1 structures indicated a similar mechanism might be employed for some IPKs. Comparison of IP-bound and free crystal structures of IPK1 suggested stabilization of its N-lobe was triggered by IP binding (Chapter 2) (Gosein et al., 2012); however, this mechanism of IP recognition for IPK1, termed "IP-induced stabilization" has yet to be validated. Recently, we demonstrated the position of the phosphates on IPK1

substrates play different roles in directing IP binding to IPK1 and the recognition of IPs as substrates (Chapter 3) (Gosein and Miller, 2013).

The aim of our current work is to define the contributions of IP phosphates on IPK1 stabilization and define how this relates to enzyme activation. The results presented here demonstrate that the stable conformation of IPK1 is achieved when IP-binding sites in the N-lobe are occupied by the 1- and 3-phosphates of the IP, and that substrate specificity of IPK1 can be manipulated through artificial stabilization of the N-lobe in an IP-independent manner.

Materials and Methods

Ligands

Inositol phosphates (1,3,4,5,6-IP_5; 1,3,4,5-IP_4; 1,4,5,6-IP_4; 1,3,4,6-IP_4; 3,4,5,6-IP_4) were purchased from Cayman Chemical Company (Ann Arbor, MI). Trypsin, ADP, and IP_6 were purchased from Sigma-Aldrich (St. Louis, MO). AMPPNP were purchased from Jena Bioscience (Jena, Germany). ATP was purchased from Fisher (Waltham, MA). All IPs were dissolved in Tris-HCl (pH 8.0) to a stock concentration of 20 mM and stored at -20 °C until use.

Limited Proteolysis

IPK1 was purified as described previously (Gosein et al., 2012). Limited proteolysis of IPK1 was performed in 50 mM Tris-HCl (pH 8.0), 150 mM NaCl, and 2.5 mM DTT. 9 μM of purified IPK1 was incubated with 2 mM $MgCl_2$ and 1 mM of IP (IP_4, IP_5 or IP_6) with and without nucleotides (AMPPNP, ADP) for 20 min at 4 °C. 0.08 μg of trypsin was then added to each reaction, except the undigested control. The reactions were incubated at 20 °C and samples were taken at 2 h, 4 h, 6 h, and 8 h. Samples were analyzed by SDS-PAGE and stained with Coomassie blue and analyzed as described in Gosein et al. 2012 (Gosein et al., 2012).

Densitometry

Densitometry of IPK1 digestion fragments was performed using ImageJ (Schneider et al., 2012). The Analyze Gel module was used as described in the ImageJ manual. The area was measured for the uncut control fragment where no digestion had occurred and for the full-length, and fragments comprising amino acids 52-451, and 130-451 bands in digested conditions. The areas of the digested fragments were plotted as a percentage of the area of the control band.

Differential scanning fluorimetry (DSF)

DSF was performed on a Corbett Life Science Rotor-Gene 6000. All reactions were prepared individually in 0.2 mL PCR tubes at a final volume of 50 μL. The reactions consisted of 9 μM of purified IPK1 in 50 mM HEPES (pH 7.5), 5 mM $MgCl_2$, 50 mM NaCl, and 2.5 mM DTT buffer, incubated with 1 mM of

nucleotide (ADP, AMPPNP) and/or 1 mM IP (IP_4, IP_5 or IP_6) for 5 min on ice. SYPRO Orange (Life Technologies) was then added to 5X under dark conditions. The final DMSO concentration was 0.1%. A temperature melt was carried out between 28-80 °C with 0.15 °C/sec increments and the gain was set to 2. The HRM module was used with an excitation filter of 460 nm and emission filter of 510 nm. Each condition was performed in triplicate. Data was analyzed using the Rotor-Gene software. The first derivative of the raw data was analyzed for peaks, which corresponded to the melting temperature (T_m) of IPK1. DSF was performed similarly using IPK1 E82C/S142C mutant purified in the absence of reducing agents, however, the reactions consisted of IPK1 E82C/S142C incubated with nucleotide and/or IP in the absence or presence of 2.5 mM DTT prior to the DSF run.

Generation of IPK1 disulfide mutants

The structure of IPK1 was processed using "Disulfide by Design" software to identify pairs of residues that could be mutated to cysteines to form disulfide bonds (Dombkowski, 2003). Cysteine mutants of these residues were generated by site-directed mutagenesis using the quick-change method (Stratagene) in two subsequent steps and pairs of oligonucleotides in Table S4.1. A pET28a vector containing wild-type *A. thaliana* IPK1 and a hexahistidine tag was used a template (a generous gift from Dr. C. A. Brearley). All mutations were verified by DNA sequencing.

IPK1 disulfide mutant activity assay

IPK1 kinase activity was measured using the Kinase-Glo Max Luminescent Kinase Assay (Promega) as per manufacturer instructions. Kinase reactions were performed in 25 µL volumes in black 96-well plates at 25 °C and contained 50 mM HEPES (pH 7.5), 6 mM $MgCl_2$, 50 mM NaCl, and 300 µM ATP. 0.1 µM of each IPK1 mutant, purified in the absence of reducing agents, was tested with 80 µM of IP in the presence or absence of 2.5 mM DTT. 25 µL of Kinase-Glo reagent was added to stop the reaction. Luminescence was measured after 20 min on a Berthold Orion II Microplate Luminometer.

IPK1 E82C/S142C kinetic analysis

Initially, 80 μM of IP was used and the amount of IPK1 E82C/S142C enzyme was varied to determine conditions in which product formation was linear over 30 min. Subsequently, an array of reactions with varying concentrations of IP (20 μM, 40 μM, 60 μM, 80 μM, 100 μM, 120 μM, 140 μM) stopped at various time-points (2 min, 5 min, 10 min, 20 min, 30 min) was performed in triplicate. The process was performed for both IP_5 and 3,4,5,6-IP_4, in the absence of reducing agent. The rate of product formation versus IP concentration was plotted and fitted to the Michaelis-Menten equation using non-linear regression to determine K_M and V_{MAX} (GraphPad). Values were reported as mean ± SD. The k_{cat} values were calculated using the equation $k_{cat} = V_{MAX}/[E]$, where [E] is the concentration of enzyme in μM.

Structure determination of IPK1 E82C/S142C mutant

IPK1 E82C/S142C was expressed and purified as described previously for wild-type IPK1, however, DTT and β-mercaptoethanol were omitted in all buffers (Gosein et al., 2012). IPK1 E82C/S142C at 5 mg/mL crystallized with 5 mM ADP/$MgCl_2$, 5 mM IP_6 in 0.08 M MES (pH 6.5), 19.85% PEG 3000, 0.17 M NaCl, 2.35% benzamidine HCl at 20 °C within 6-72 h using the sitting-drop vapour-diffusion method. X-ray diffraction data was collected on a Rigaku MicroMax-007 HF microfocus X-ray generator fitted with Varimax X-ray optics and a Saturn 944+ CCD detector. Crystals were cryoprotected with reservoir solution that included 10% PEG400 and data was collected under cryogenic conditions. Diffraction data was analyzed and processed with HKL2000 software and refined with Phenix and Coot (Otwinowski and Minor, 1997; Adams et al., 2010; Emsley and Cowtan, 2004). Molecular replacement was performed with Protein Data Bank code: 2XAM. All model images were created using PyMol (DeLano Scientific).

Results

Positions of substrate phosphates determines extent of IPK1 stabilization

We used limited proteolysis as a probe for IPK1 stability (Gosein et al., 2012). As reported previously, IPK1 can be cleaved by trypsin at R130 when the N- and C-lobes are not stabilized, but not when the N- and C-lobes have stabilized (Figure 4.1a). To identify phosphate groups of the IP substrate that promote IPK1 stabilization, we performed limited proteolysis of IPK1 in complex with IPs alone or in ternary complexes (AMPPNP+IP_4, AMPPNP+IP_5, or ADP+IP_6). The resulting proteolytic patterns observed on SDS gels were compared (Figure 4.1b). In contrast to IP alone, IPK1 in complex with both nucleotide and IP protected an additional 46 kDa fragment with K52 at its N-terminus, indicating the R130 site was protected under these conditions (Figure 4.1b). To assess the relative stability of IPK1 in the complexes, we performed densitometry to compare the ratios of the stabilized fragments to uncut IPK1 (Figure 4.1c). The amounts of full-length fragment in each of the ternary complexes were similar, indicating that digestion occurred to a similar extent in each of these complexes (Figure 4.1c, green bars). There was little variability in the amount of the R130-S451 band between the different complexes, indicating that C-lobe stability was identical in each of the complexes (Figure 4.1c, blue bars). Finally, the amount of the K52-S451 band varied between each of the ternary complexes, indicating that IPK1 was differentially stabilized specifically at the N-lobe when IPK1 was bound to different IPs (Figure 4.1c, red bars). Protection of the K52 cleavage site is substantially decreased with IPK1 in complex with AMPPNP and 3,4,5,6-IP_4, which demonstrates that the 1-phosphate of the IP is singularly important for N-lobe stabilization.

To further characterize the overall stability of IPK1, we used DSF to measure the melting point of IPK1 in the ligand free state, bound to nucleotide (AMPPNP or ADP), IP (IP_4s, IP_5, or IP_6), or as ternary complexes bound to both nucleotide and IP (Figure 4.2). In the free state, IPK1 exhibited a T_m of 35 °C. When bound to either AMPPNP or ADP, the T_m of IPK1 increased to 38 °C, indicating that nucleotide contributes to the overall stability of IPK1. When bound to IPs only, except 1,4,5,6-IP_4, IPK1 exhibited T_ms of 40 °C, revealing that the stability of IPK1 is impacted more by the binding of IP than nucleotide. Finally, in

the ternary complexes, IPK1 exhibited varying T_ms that were dependent on the phosphorylation pattern of the IP. When also bound to nucleotide, IPK1 displayed markedly lower T_ms in the 3,4,5,6-IP_4 and 1,4,5,6-IP_4 conditions, compared to the 1,3,4,6-IP_4, 1,3,4,5-IP_4, IP_5, and IP_6 conditions. Our results indicate that the 1- and 3-phosphate groups contribute more to the overall stability of IPK1 than other phosphates when IPK1 is in the nucleotide-bound state.

IPK1 disulfide mutants altered specificity

Observing that binding of different IPs led to differential stabilization of IPK1, we hypothesized that IPK1 stabilized in an IP-independent manner would exhibit altered specificity for IP substrates, diminishing the requirement for N-lobe interacting 1- and 3-phosphates that stabilize IPK1. To test this role of IPK1 stabilization, we engineered and tested a series of disulfide bonds to artificially stabilize the N-lobe of IPK1. We created double cysteine mutants of IPK1 at different sites near residues 110-140, the region of the N-lobe that was previously observed to be unstable in the absence of IP (Figure S4.1) (Gosein et al., 2012). We tested the kinase activity of these mutants using its physiological substrate, IP_5, and 3,4,5,6-IP_4, a poor IPK1 substrate (Gosein and Miller, 2013), in reducing and non-reducing conditions (Figure 4.3). Wild-type IPK1 displayed very high activity for IP_5 and very low activity for 3,4,5,6-IP_4 and both activities were unaffected by DTT. Two IPK1 disulfide mutants, IPK1 E82C/S142C and IPK1 G105C/L146C, each displayed activity for IP_5 and 3,4,5,6-IP_4, albeit to different extents (Figure 4.3). The IPK1 E82C/S142C mutant showed moderate activity for IP_5 and greater activity for 3,4,5,6-IP_4 than the wild-type enzyme under non-reducing conditions, and wild-type activity is restored in the presence of DTT (Figure 4.3). IPK1 G105C/L146C also showed a similar pattern to IPK1 E82C/S142C, but the difference between IP_5 activity and 3,4,5,6-IP_4 activity was greater under reducing and non-reducing conditions (Figure 4.3). This demonstrated the mutations themselves, which are remote from the active site, are not responsible for the altered activity and the changes were due primarily to the formation of the disulfide bond.

To further examine the effect of the disulfide bond on IPK1 kinase activity, we performed a kinetic analysis of IPK1 E82C/S142C with IP_5 or 3,4,5,6-IP_4, under non-reducing conditions (Figure 4.4). IPK1 E82C/S142C exhibited

similar K_M and k_{cat} values to that of wild-type IPK1 with IP_5 as a substrate, both possessing k_{cat} values of ~44 nmol/min (Table 4.1). In contrast, IPK1 E82C/S142C displayed a 5-fold increase in kinase activity (k_{cat} = 32.93 nmol/min) with 3,4,5,6-IP_4 as a substrate, compared to wild-type IPK1 (k_{cat} = 6.30 nmol/min) (Table 4.1). The ratio of k_{cat}/K_M for the disulfide mutant and wild-type IPK1 for each IP revealed changes in substrate selectivity due to the presence of the disulfide bond. We observed that wild-type IPK1 had a 5.3:1 preference for IP_5 over 3,4,5,6-IP_4 when comparing IP selectivity. In contrast, IPK1 E82C/S142C displayed a 2.5:1 preference for IP_5 over 3,4,5,6-IP_4 demonstrating that the disulfide bond altered substrate specificity of IPK1.

IPK1 E82C/S142C increases overall stability of IPK1

To explore structural changes associated with the introduction of the disulfide bond, we crystallized the disulfide mutant in presence of ADP and IP_6 under non-reducing conditions to obtain a structure of IPK1 E82C/S142C (Figure 4.5, Table 4.2). Overall, the structure of IPK1 E82C/S142C was very similar to wild-type IPK1 (RMSD = 0.5 Å). The presence of the disulfide bond shifted the N-lobe in the mutant structure when compared to the structure of wild-type IPK1 (Figure 4.5a). Inspection of the electron density indicated the presence of the disulfide bond between C82 and C142 (Figure 4.5b). To confirm the presence of a disulfide bond between these residues, we generated an omit map lacking the side chains at these residues and observed a large unoccupied density in the Fo-Fc map (σ = 3.0) located between both residues, consistent with the presence of a disulfide bond (Figure 4.5c). We performed the same refinement using diffraction data from a wild-type structure of IPK1 (Protein Data Bank code: 3UDZ) and did not observe unoccupied density between the two residues in the Fo-Fc difference map (σ = 3.0), confirming that the density observed is unique to the mutant structure (Figure 4.5d).

To investigate the effect of the disulfide bond on the overall stability of IPK1, we employed DSF to measure the T_m of wild-type IPK1 and IPK1 E82C/S142C. We compared the T_ms of wild-type IPK1 and IPK1 E82C/S142C in the free state, bound to nucleotide (AMPPNP or ADP), IP (3,4,5,6-IP_4, IP_5, or IP_6), or ternary complexes bound to both nucleotide and IP (Figure 4.6). We performed this experiment under reducing conditions (with DTT) and non-reducing

conditions (without DTT) to detect the effect of the disulfide bond. In presence or absence of DTT, wild-type IPK1 exhibited similar T_ms as noted above, with the lowest T_m in the apo condition, a slight 2 °C increase in T_m when bound to nucleotide only, a moderate 5 °C increase in T_m when bound to IP only, and a large 12 °C increase in the ternary complex with IP_5 and IP_6 (Figure 4.6, first and second sets). AMPPNP+3,4,5,6-IP_4 failed to stabilize IPK1 to same extent as AMPPNP+IP_5 and ADP+IP_6 as shown by a 5 °C difference in T_m between the ternary complexes. DTT did not markedly affect any of the T_ms of wild-type IPK1 under any conditions, revealing that the overall stability of wild-type IPK1 is not dependent on disulfide bonds. This is consistent with the structure of wild-type IPK1 that does not have disulfide bonds. In contrast, IPK1 E82C/S142C exhibited an average increase in T_m of 5.6 °C under each condition compared to wild-type IPK1 in absence of DTT, and this increase in T_m is reversible in the presence of DTT, confirming that the disulfide bond is increasing the overall stability of IPK1 (Figure 4.6, third and fourth sets). In our kinetic studies, we observed that IPK1 E82C/S142C exhibited increased selectivity for 3,4,5,6-IP_4 (Table 4.1). Thus, the engineered disulfide bond that was stabilizing the N-lobe of IPK1 in an IP-independent manner conferred specificity to 3,4,5,6-IP_4, a poor substrate that lacks the 1-phosphate that is key for N-lobe stabilization, indicating that the stability of the N-lobe is a determinant for substrate specificity of IPK1.

Discussion

Dual roles of the 1- and 3- phosphates

Here, we investigated the role of the IP phosphates in stabilizing IPK1. We determined that the 1-phosphate is important for localized stability of the N-lobe (Figure 4.1), consistent with the IP-free crystal structure of IPK1 that revealed localized destabilization of the region surrounding R130, which interacts with the 1-phosphate (Gosein et al., 2012). We recently investigated specific roles of phosphate groups in binding and activation of IPK1 and we determined that the 5- and 6-phosphates were important for binding of the IP, while the 1- and 3-phosphates were important for activation of IPK1 (Gosein and Miller, 2013). In our current study, we demonstrated that the overall stability of IPK1 is dependent on the N-lobe binding 1- and 3-phosphates (Figure 4.2). Thus, the dual roles of the N-lobe binding 1- and 3-phosphates in both IPK1 stabilization and IPK1 activation indicates that the stabilization of the N-lobe is an important component of IPK1 activation. We have also demonstrated that the IP, and not the nucleotide, contributes substantially to the stabilization of the N-lobe of the kinase. This is consistent with our earlier observation that the N-lobe is destabilized in the absence of IP and the structures of Gonzales et al., which demonstrated structures bound to IP, but not to nucleotide adopt the stable state (Gosein et al., 2012; Gonzalez et al., 2010).

Substrate specificity is linked to N-lobe stability

Changes in protease accessibility and increased protein stability upon substrate binding suggested that activation of IPK1 may be linked to the ability of the IP substrate to stabilize IPK1 so we hypothesized that artificial stabilization of the N-lobe of IPK1 in an IP-independent manner would alter the substrate specificity of IPK1. We engineered the IPK1 E82C/S142C disulfide mutant by introducing a cysteine in the N-lobe of IPK1 at a site that is unstable in the IP-free crystal structure and a second cysteine at a site that is well-ordered and apparently stable in all IPK1 crystal structures (Figure 4.5) (Gosein et al., 2012; Gonzalez et al., 2010). By covalently linking stable and unstable regions, we endeavored to stabilize some or all of the N-lobe. This increase in stability was reflected in our DSF data with IPK1 E82C/S142C, which shows increased T_ms under non-reducing

conditions (Figure 4.6). This mutant also displays increased selectivity for 3,4,5,6-IP_4 under non-reducing conditions compared to wild-type IPK1 (Table 4.1). Given that 3,4,5,6-IP_4 lacks the ability to stabilize wild-type IPK1 as much as IP_5 in ternary complexes (Figure 4.1), our data collectively shows that substrate specificity is linked to N-lobe stability.

IP-induced stabilization as a model of IP recognition for IPK1

We recently proposed a model for IP recognition wherein interactions with the IP substrate stabilizes the N-lobe and C-lobe to promote kinase activation (Gosein et al., 2012). In this model, the stable C-lobe recognizes the 4-, 5-, and 6-phosphates of the IP, and 1- and 3-phosphates of the IP induces N-lobe stabilization. The key interaction between R130 and the 1-phosphate of the IP stabilizes the N-lobe. Thus, our model possesses a triad of elements that are interconnected for IPK1 activity: 1) substrate specificity, 2) stability, and 3) activation. Our current study provides the necessary evidence for the first time to reconcile all three elements and validate our proposed model. We have linked substrate specificity to kinase stability by demonstrating that IPs possessing the 1-phosphate markedly stabilize the N-lobe as compared to 3,4,5,6-IP_4, which lacks a 1-phosphate, while artificial stabilization of the N-lobe of IPK1 alters substrate specificity. We have also found that the 1- and 3-phosphates of the IP provides increased stability to IPK1, while the 5- and 6-phosphates do not affect the overall stability of IPK1, consistent with an unstable N-lobe and a stable C-lobe in absence of IP. Moreover, previous kinetic studies of IPK1 link substrate specificity to kinase activation (Gosein and Miller, 2013). We contend that IPK1 stability is linked to IPK1 activation because IPK1 stability correlates with the active state in previous crystal structures (Gosein et al., 2012), IPs that display low IPK1 kinase activity (k_{cat}) correlate with a decreased ability to stabilize IPK1 (Gosein and Miller, 2013) and kinase stability has been validated to be a precursor for activation of PKs, for which IPK1 shares similar features (Ubersax and Ferrell, 2007; Gonzalez et al., 2010). In short, our current data provides strong evidence to support our model that IPK1 substrate specificity is coupled to IPK1 stability and subsequent activation (Figure 4.7).

Comparison to PK activation

Conformational changes that stabilize links between PK N- and C-lobes that occur during activation have been well documented (Ubersax and Ferrell, 2007). Stabilization of the kinase structure is promoted by the assembly of a hydrophobic spine spanning the two lobes, one of which consists of the phenylalanine residue from the DFG motif, a hydrophobic residue from the αC helix, and two residues buried in the cores of the N- and C-lobes. This structural spine, called the R-spine assembles only when the DFG and αC helix regulatory motifs sit in their active conformations (Ten Eyck et al., 2008). In IPK1, the αC helix sits at a 46° angle compared to PKA that precludes the αC helix from contributing a hydrophobic residue to the R-spine (Figure 4.8a). Further, the IPK1 DLS motif lacks the large hydrophobic phenylalanine residue, which likely impairs its ability to assemble a stabilizing R-spine (Figure 4.8b,c). These structural differences highlight that IPK1 activation occurs through a different mechanism than found in many PKs. In the proposed model, it is the IP substrate that acts as the bridge between the N-lobe and C-lobe to stabilize the active conformation of the kinase rather than the intrinsic R-spine structure (Figure 4.7). The phosphate profile of the IP dictates the ability of the substrate to stabilize the N-lobe of IPK1 and promote kinase activation. This is consistent with previous suggestions that conformational dynamics may play a role in the catalytic cycle of IPK1 (Gosein et al., 2012; Banos-Sanz et al., 2012). Thus, IPK1 retains important features of PK activation such as N- and C-lobe stabilization, yet distinguishes itself from the PKs. These distinct features could be exploited to selectively inhibit IPK1.

Conclusion

In this report, we demonstrate the missing link between IP substrate specificity and the N-lobe stability of IPK1. Our results conclusively support IP-induced stabilization of IPK1 as a proposed model of IP discrimination. IP substrates are very similar and the elucidation of the unique substrate recognition mechanism of IPK1 among IPKs may provide a basis for selective pharmacological targeting of IPK1. Inhibitors of IPK1 would be useful for ascertaining the functional roles of higher IPs and validation of this IP signaling axis as a therapeutic target.

Acknowledgements

We thank Dr. Charles A. Brearley (University of East Anglia) for his gift of the AtIPK1-pET28 vector, Dr. Dan Bernard (McGill University) for access to both the Rotor-Gene 6000 used for DSF and the luminometer used in enzyme assays, and Anne W. Coventry for thoughtful reading of the manuscript.

This work is supported by a Canadian Institutes of Health Research Operating Grant MOP-93687 awarded to GJM and a CIHR Strategic Training Initiative in Chemical Biology awarded to VG.

Figure 4.1. Localized stability of N-lobe with 1-phosphate IPs. (A) Cartoon representation of product-bound IPK1 depicting overall topology: N-lobe (red), C-lobe (blue), hinge (cyan) with ADP (purple, stick form) and IP_6 (orange, stick form), (Protein Data Bank code: 3UDZ). Dashed lies indicate untraceable regions. **(B)** Limited proteolysis of IPK1. IPK1 (55 kDa) was incubated with trypsin in the presence of nucleotides and/or inositides. Two fragments were protected in multiple conditions: One fragment cleaved at K52 (46 kDa, red arrow) and the other cleaved at R130 (37 kDa, blue arrow). Both residues are shown in yellow in (A) (K52, rectangle; R130, stick form). **(C)** Densitometry of limited proteolysis gel. The ratios of the stabilized fragments to control (uncut) IPK1 were plotted for the full length band (green), the K52 band (red), and R130 band (blue) for each ternary complex.

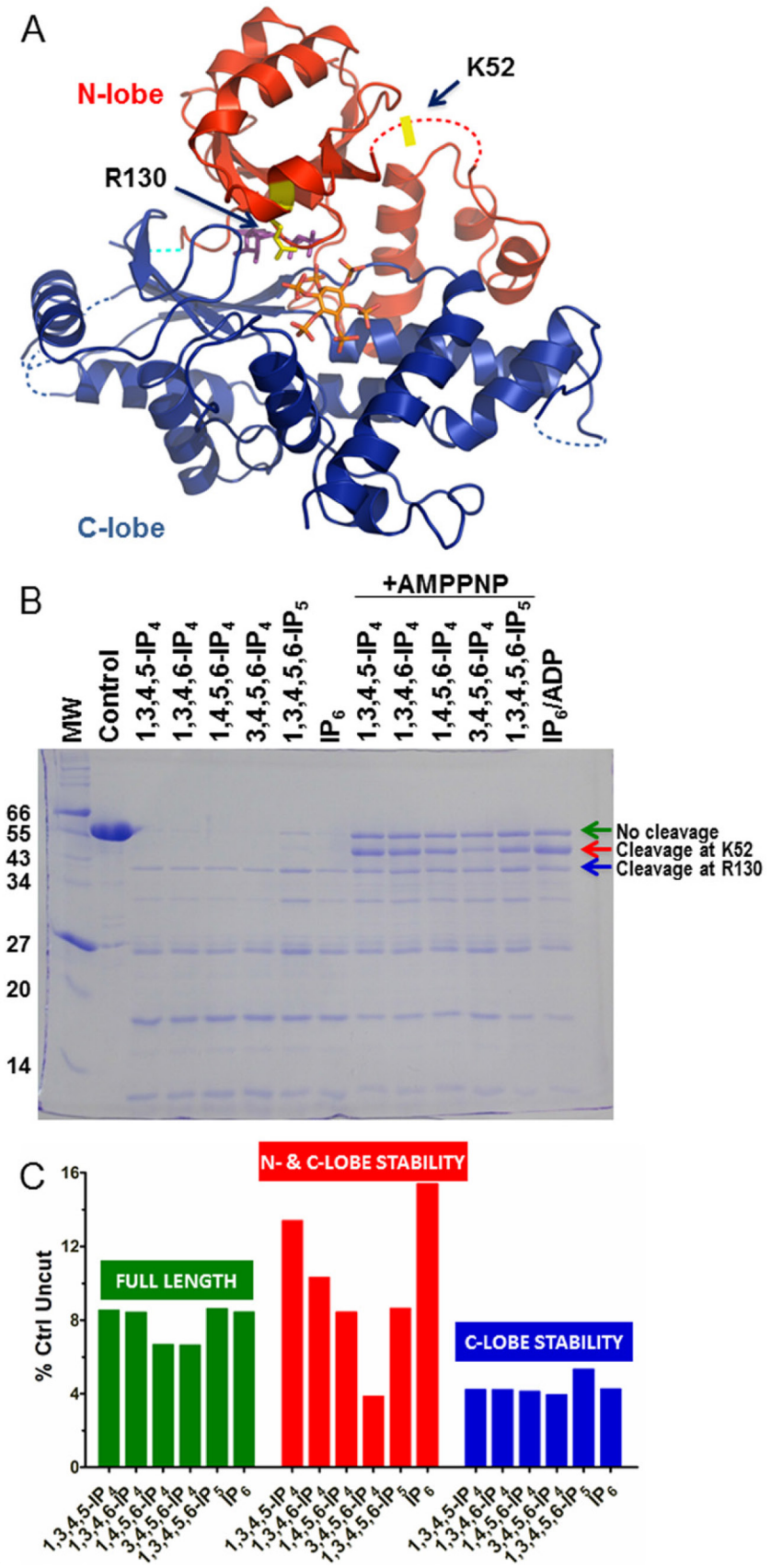
A
N-lobe
K52
R130
C-lobe
B
+AMPPNP
MW
Control
1,3,4,5-IP4
1,3,4,6-IP4
1,4,5,6-IP4
3,4,5,6-IP4
1,3,4,5,6-IP5
IP6
IP6/ADP
66
55
43
34
27
20
14
No cleavage
Cleavage at K52
Cleavage at R130
C
N- & C-LOBE STABILITY
FULL LENGTH
C-LOBE STABILITY
% Ctrl Uncut
16
12
8
4
0

Figure 4.1.

Figure 4.2. N-lobe binding 1- and 3-phosphates increase the overall stability of IPK1. The T_m of IPK1 was measured using DSF to determine the overall stability of IPK1 in complex with different nucleotides and/or inositides as shown. Each point represents the mean ± S.D. of triplicate experiments.

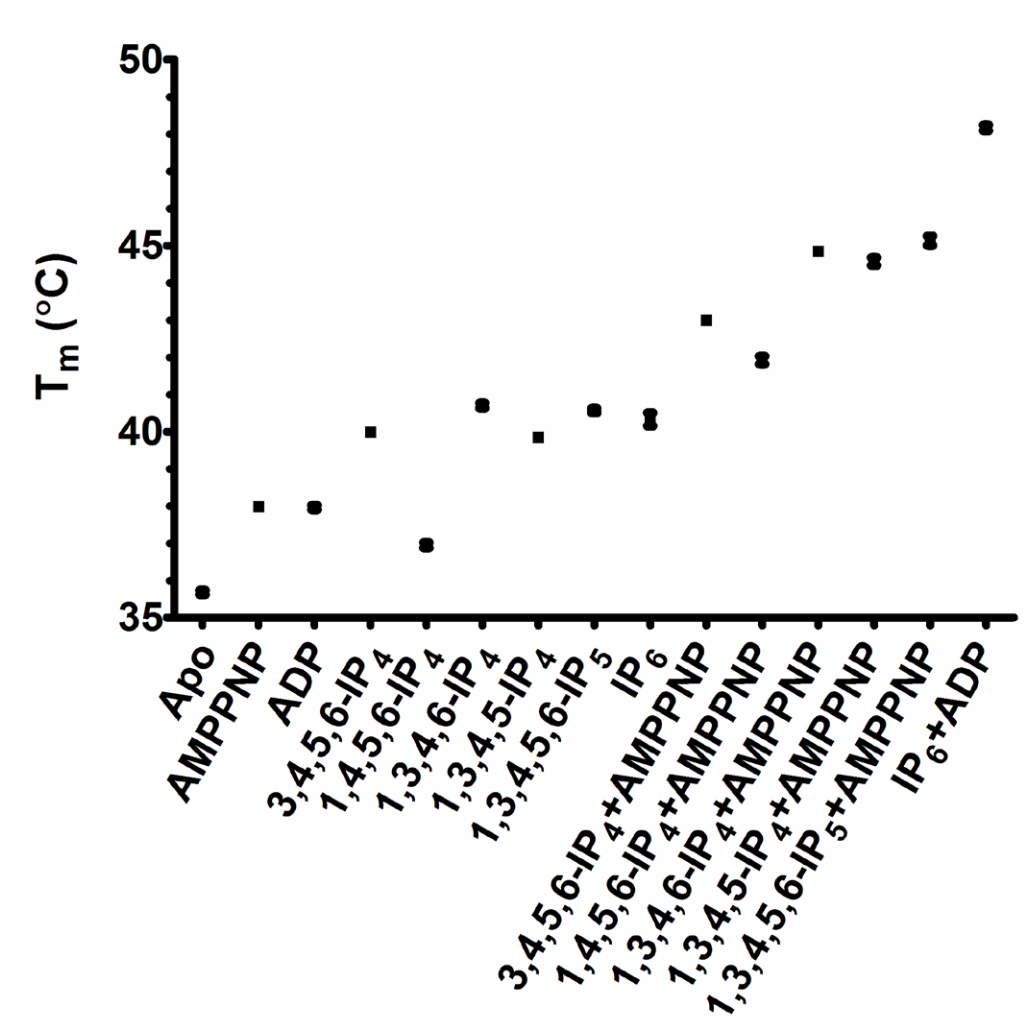
50
45
40
35
T_m (°C)
Apo
AMPPNP
ADP
3,4,5,6-IP_4
1,4,5,6-IP_4
1,3,4,6-IP_4
1,3,4,5-IP_4
1,3,4,5,6-IP_5
IP_6
3,4,5,6-IP_4+AMPPNP
1,4,5,6-IP_4+AMPPNP
1,3,4,6-IP_4+AMPPNP
1,3,4,5-IP_4+AMPPNP
1,3,4,5,6-IP_5+AMPPNP
IP_6+ADP

Figure 4.2.

Figure 4.3. IPK1 E82C/S142C confers specificity to 3,4,5,6-IP_4. Each engineered IPK1 disulfide mutant was tested for its kinase activity with: 1,3,4,5,6-IP_5 in the absence of DTT (black bars); 3,4,5,6-IP_4 in the absence of DTT (dark gray bars); 1,3,4,5,6-IP_5 in the presence of DTT (light gray bars); 3,4,5,6-IP_4 in the presence of DTT (white bars). Each bar represents the mean ± S.D. of triplicate experiments.

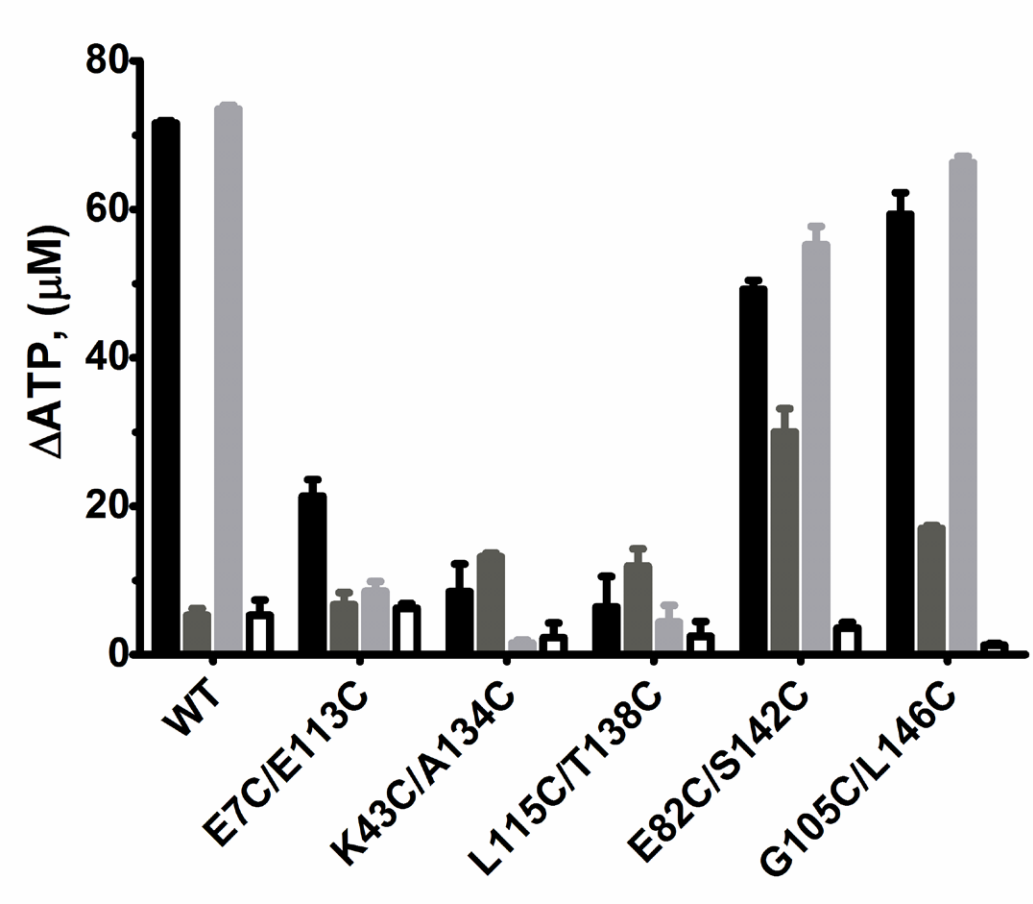
80
60
40
20
0
ΔATP, (μM)
WT
E7C/E113C
K43C/A134C
L115C/T138C
E82C/S142C
G105C/L146C

Figure 4.3.

Figure 4.4. Kinetic analysis of IPK1 E82C/S142C. Kinase activity of IPK1 E82C/S142C towards 1,3,4,5,6-IP_5 or 3,4,5,6-IP_4 was assessed in the absence of DTT by plotting the rate of product formation versus IP concentration fitted to the Michaelis-Menten equation. Each point represents the mean ± S.D. of triplicate experiments.

●: IPK1 E82C/S142C with 1,3,4,5,6-IP_5 ■: IPK1 E82C/S142C with 3,4,5,6-IP_4

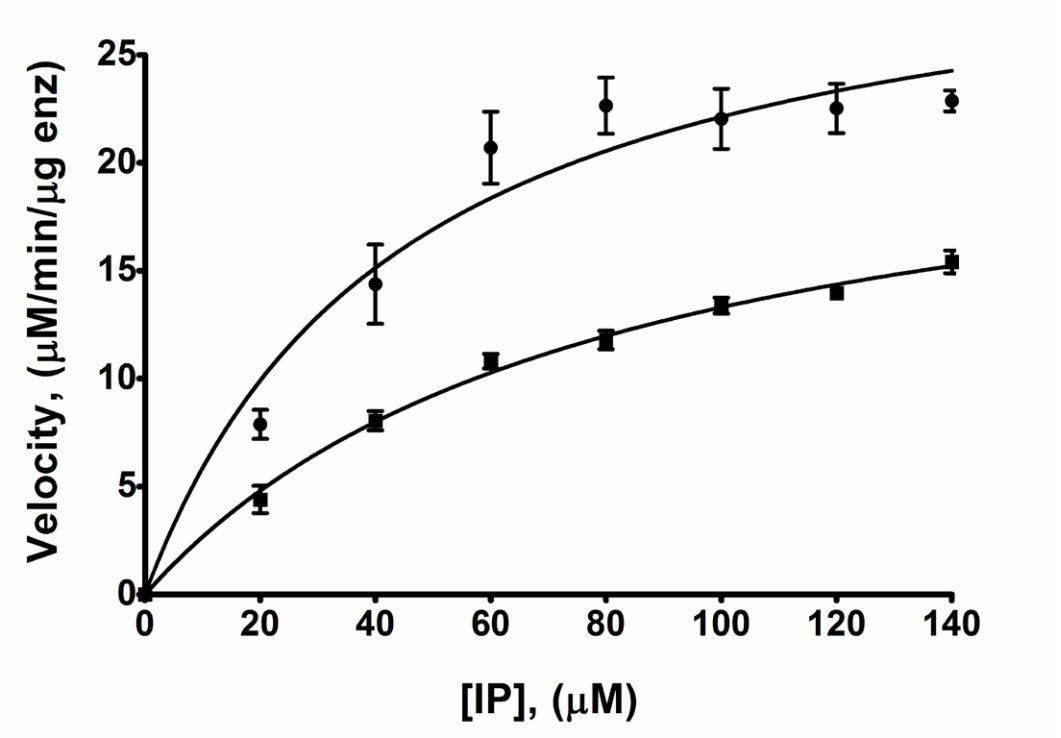
Velocity, (μM/min/μg enz)
25
20
15
10
5
0
0
20
40
60
80
100
120
140
[IP], (μM)

Figure 4.4.

Figure 4.5. Structure of IPK1 E82C/S142C. (A) IPK1 E82C/S142C (Protein Data Bank code: 4LV7) was aligned to wild-type IPK1 (Protein Data Bank code: 3UDZ) using Dali-Lite Server. A small shift of the N-lobe was observed in the structure of IPK1 E82C/S142C (orange) compared to wild-type IPK1 (blue). Black arrows indicate movement of the N-lobe. Alpha helices are displayed in cylindrical form. The disulfide bond between C82 and C142 is displayed in stick form. ADP and IP_6 are shown in orange, stick form. **(B)** Close-up of the disulfide bond between C82 and C142 in structure of IPK1 E82C/S142C. **(C)** Refinement of IPK1 E82C/S142C structure with residues E82 and S142 mutated to glycine. Fo-Fc difference map (green) is shown at $\sigma = 3.0$. **(D)** Refinement of wild-type IPK1 structure with residues E82 and S142 mutated to glycine. Fo-Fc difference map (green) is shown at $\sigma = 3.0$.

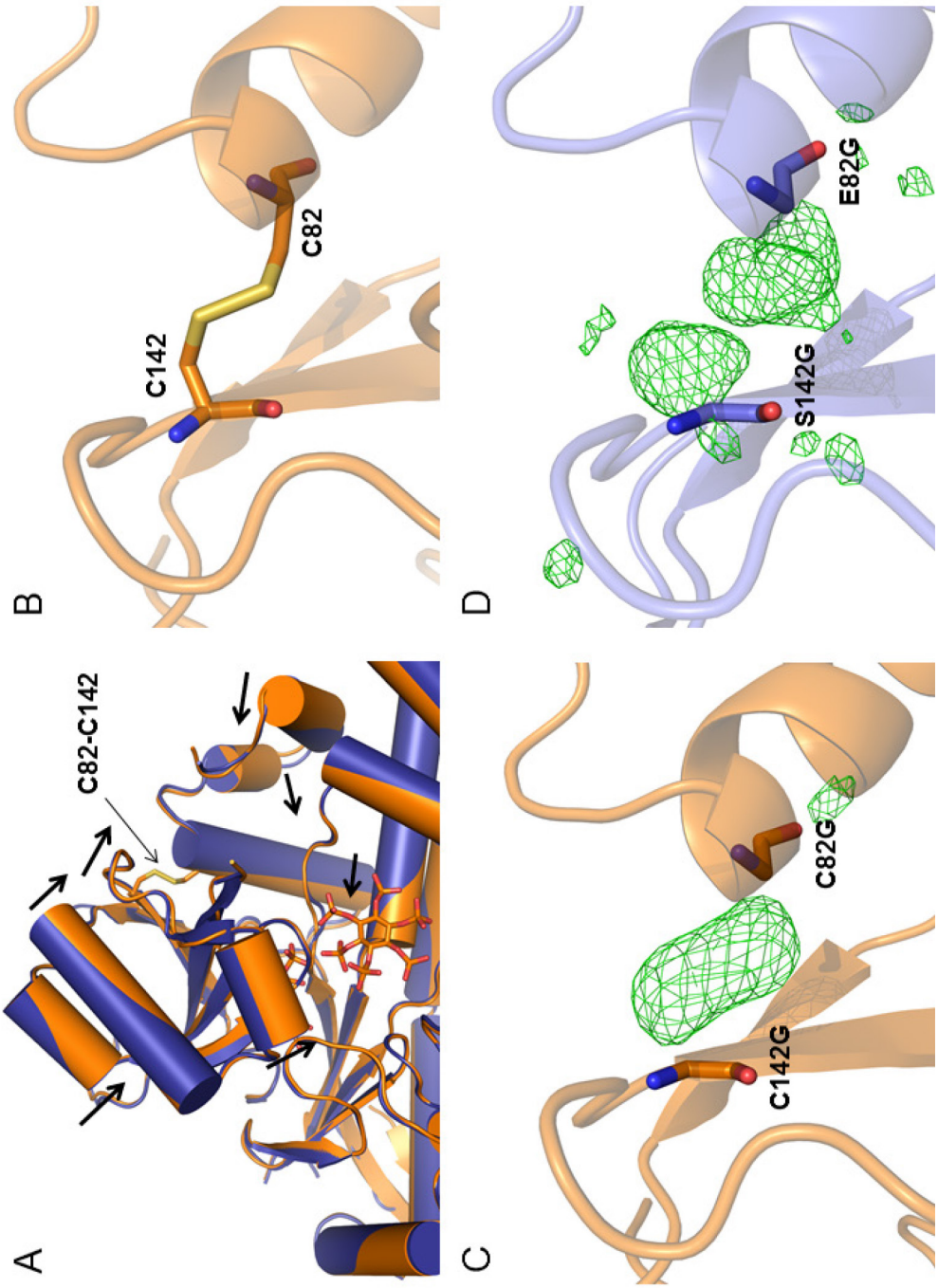

Figure 4.5.

Figure 4.6. C82-C142 disulfide bond increases overall stability of IPK1. DSF was performed with wild-type IPK1 or the disulfide mutant IPK1 E82C/S142C in the presence or absence of DTT in complex with different nucleotides and/or inositides as shown. ■: Wild-type IPK1 in the presence of DTT (first set); ▲: Wild-type IPK1 in the absence of DTT (second set); ◆: IPK1 E82C/S142C in the presence of DTT (third set); ●: IPK1 E82C/S142C in the absence of DTT (fourth set). Each point represents the mean ± S.D. of duplicate experiments. Error bars are shown in grey for clarity.

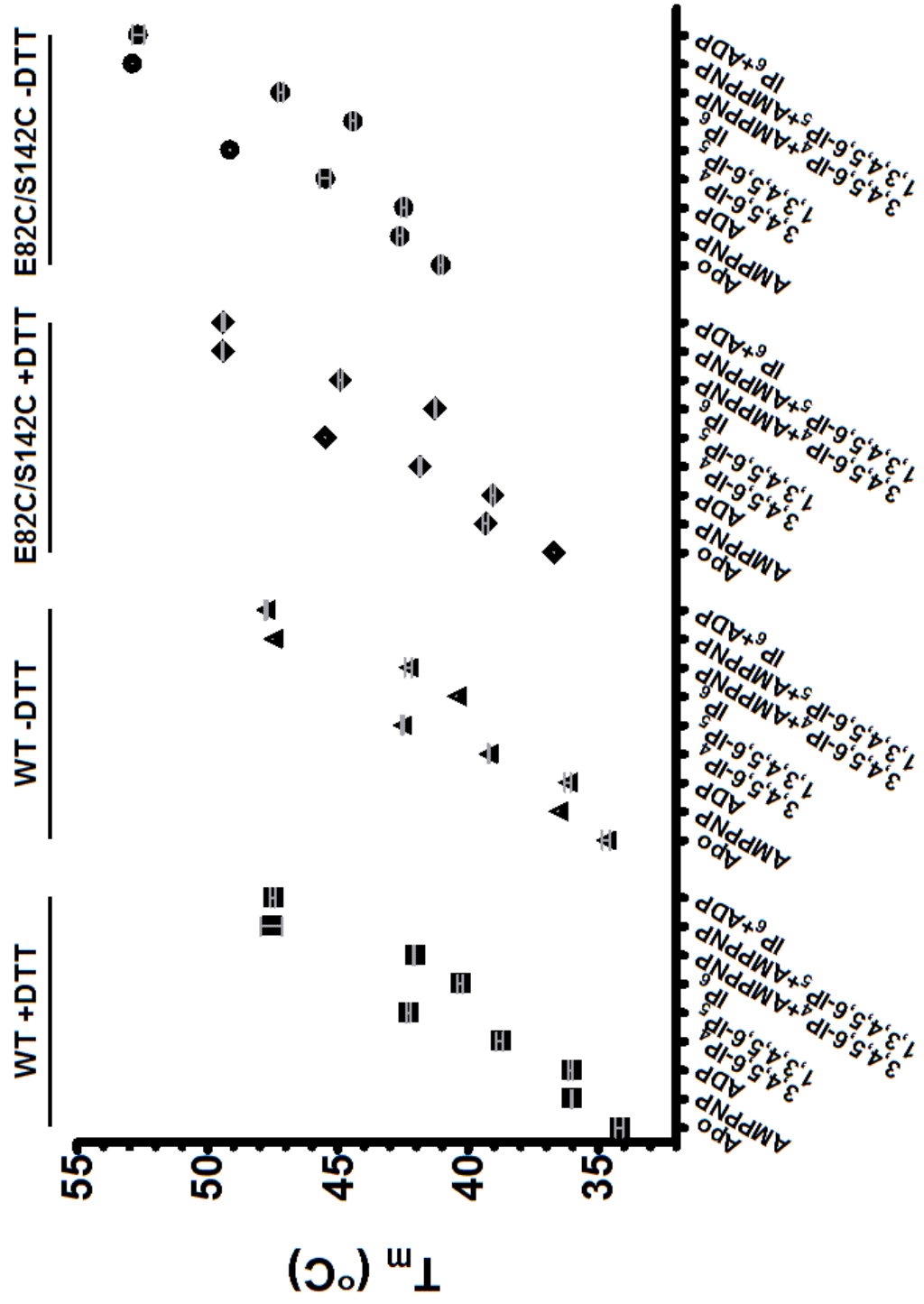
WT +DTT
WT -DTT
E82C/S142C +DTT
E82C/S142C -DTT
T_m (°C)
55
50
45
40
35
Apo
AMPPNP
ADP
3,4,5,6-IP4
1,3,4,5,6-IP5
3,4,5,6-IP4+AMPPNP
1,3,4,5,6-IP5+AMPPNP
IP6+ADP

Figure 4.6.

Figure 4.7. Model of IPK1 activation. 1) In the inactive state, the N-lobe and R130 is labile and the C-lobe is stable. **2)** Upon ATP binding to both the N-lobe and C-lobe, the N-lobe is slightly stabilized. **3)** The IP is initially recognized at the 4-, 5-, and 6-positions by the stable C-lobe. **4)** The 1- and 3-position phosphates of the IP induce N-lobe stabilization and the key interaction between R130 and the 1-phosphate stabilizes the N-lobe resulting in IPK1 activation. **5)** Phosphorylation of the 2-hydroxyl of IP_5 occurs forming IP_6.

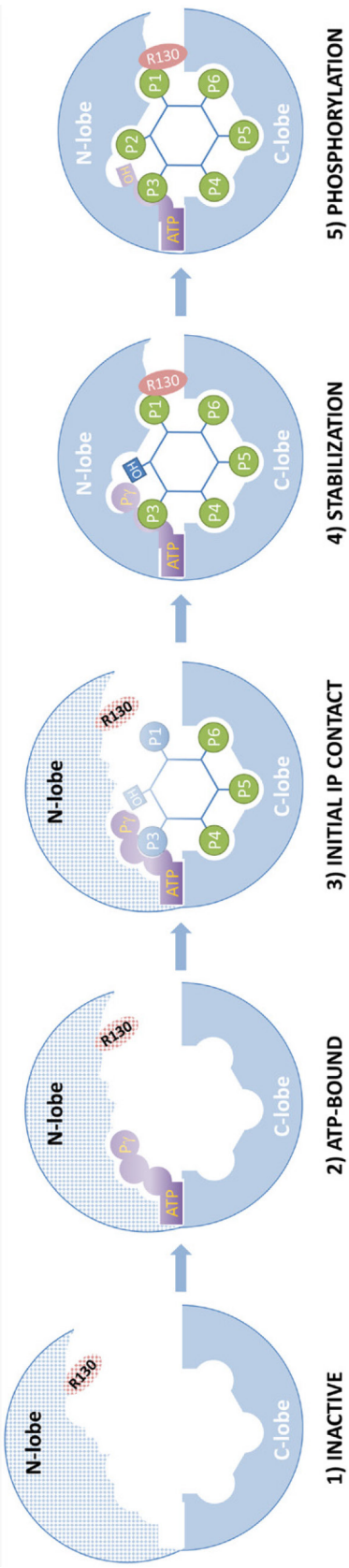
1) INACTIVE
2) ATP-BOUND
3) INITIAL IP CONTACT
4) STABILIZATION
5) PHOSPHORYLATION
N-lobe
C-lobe
R130
ATP
P1
P2
P3
P4
P5
P6
Py
Mg

Figure 4.7.

Figure 4.8. Structural differences between IPK1 and PKA. Overall alignment between IPK1 (Protein Data Bank code: 3UDZ) and PKA (Protein Data Bank code: 1ATP) was performed with DALI-Lite and yielded an RMSD of 4.4 Å. IPK1 is shown in pink. PKA is shown in green. Both are shown in cartoon form. ADP and IP_6 are shown in pink, stick form. ATP is shown in green, stick form. The αC helices of IPK1 and PKA are highlighted in magenta and yellow, respectively. **(A)** The angle between the αC helices of IPK1 and PKA was calculated to be 46° using PyMol. **(B)** In PKA, the αC helix contributes a hydrophobic residue, L106, to the R-spine (shown in blue), a hydrophobic spine that consists of L95, L106, F185, and Y164, and that stabilizes the N-lobe and C-lobe upon activation. **(C)** In IPK1, the αC helix orientation precludes any contribution of the hydrophobic residues located on the αC helix (all shown in stick form). In addition, a L408 from the DLS motif in IPK1 replaces the bulky F185 of the DFG motif of PKA. Thus, there is no assembly of a hydrophobic spine in IPK1.

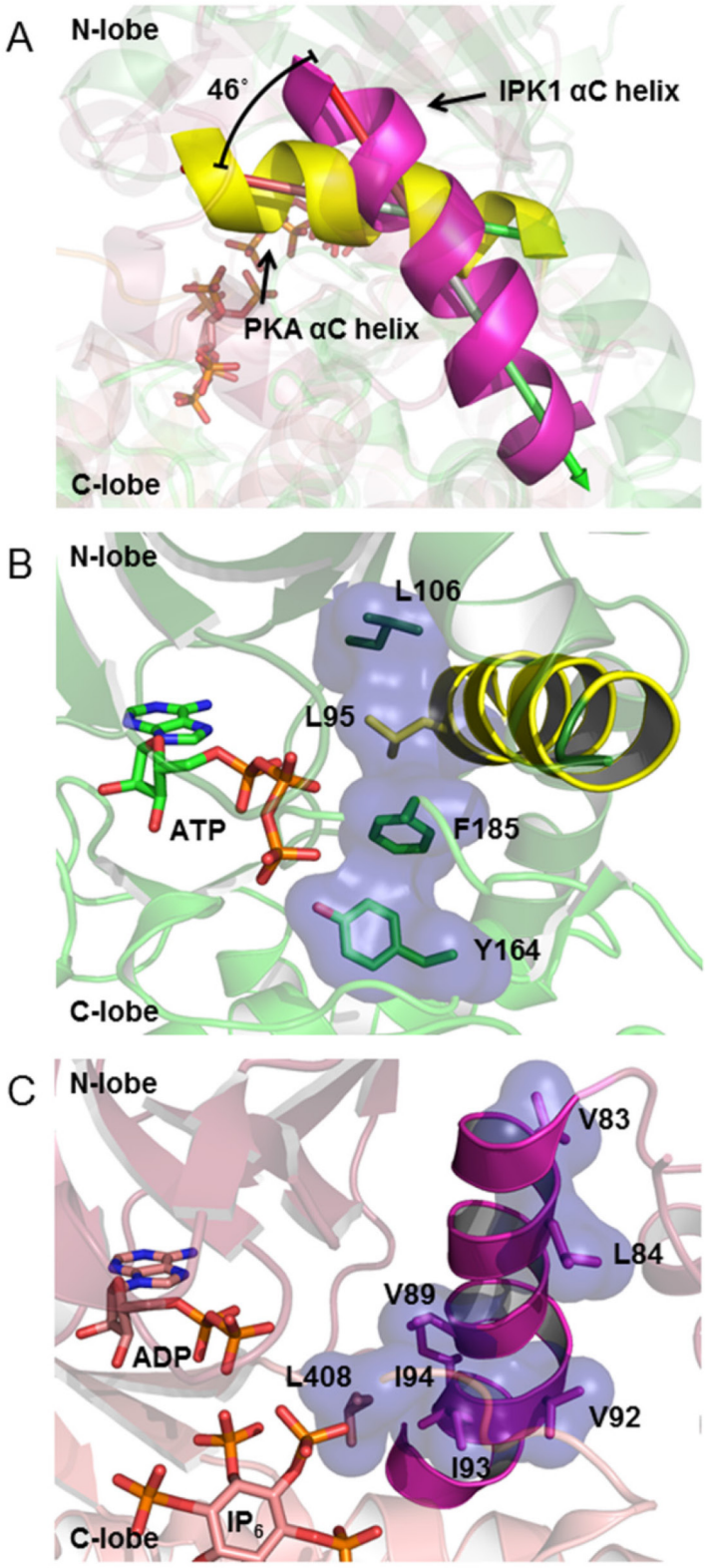
A
N-lobe
46˚
IPK1 αC helix
PKA αC helix
C-lobe
B
N-lobe
L106
L95
ATP
F185
Y164
C-lobe
C
N-lobe
V83
L84
V89
ADP
L408
I94
V92
I93
IP6
C-lobe

Figure 4.8.

Figure S4.1. Location of engineered disulfide bonds. Cartoon representation of product-bound IPK1 using Protein Data Bank code: 3UDZ. The C-lobe is shown in blue and the N-lobe is shown in pink. The region of the N-lobe that is highly unstable in the absence of IP is shown in red. Disulfide bonds were introduced to artificially stabilize this region. Pairs of cysteine mutations were introduced at E7 and E113 (orange); K43 and A134 (yellow); L115 and T138 (cyan); E82 and S142 (green); G105 and L146 (magenta).

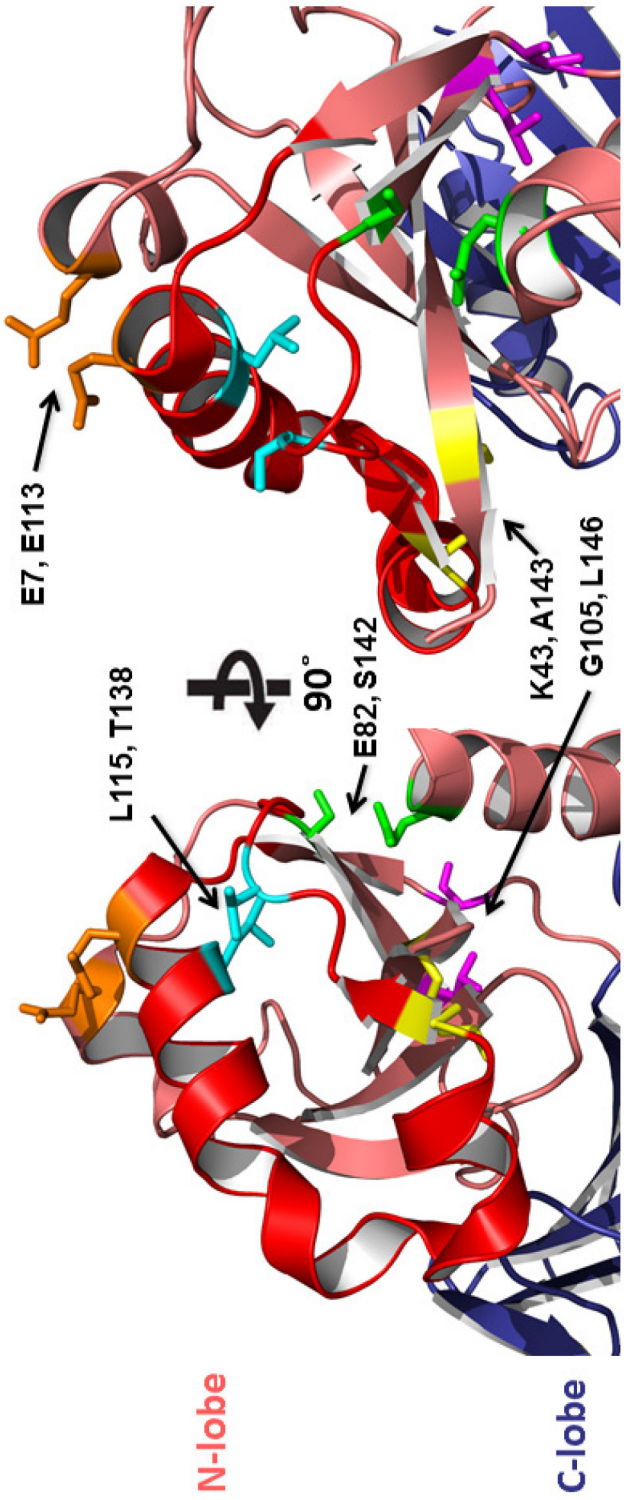

Figure S4.1.

Table 4.1. Kinetic parameters of IPK1 E82C/S142C.

IPK1	IP	K_M (μM)	k_{cat} (min^{-1})	k_{cat}/K_M
Wild-type	3,4,5,6-IP_4	47.54 ± 13.94	6.30 ± 0.68	0.13
Wild-type	1,3,4,5,6-IP_5	63.05 ± 10.77	44.02 ± 3.19	0.70
E82C/S142C	3,4,5,6-IP_4	79.17 ± 8.51	32.93 ± 1.66	0.41
E82C/S142C	1,3,4,5,6-IP_5	44.53 ± 13.43	44.18 ± 4.76	0.99

Wild-type IPK1 data was previously obtained and provided for comparison (Gosein and Miller, 2013). Data represents the mean ± S.D. of triplicate experiments.

Table 4.2. Data collection and refinement statistics for IPK1 E82C/S142C structure.

	IPK1 E82C/S142C (PDB ID: 4LV7)
Data collection[a]	
Space group	P1
Cell dimensions	
a, *b*, *c* (Å)	59.76, 59.35, 82.23
α, β, γ (°)	83.01, 89.91, 63.41
Wavelength (Å)	1.54178
Resolution (Å)	50.00-2.60 (2.69-2.60)
R_{merge}	0.086 (0.254)
I / σI	15.4 (4.2)
Completeness (%)	94.9 (87.5)
Redundancy (%)	3.9 (3.8)
Refinement	
Resolution (Å)	34.55-2.60
No. reflections	28,726
R_{work} / R_{free}	0.2244 / 0.2943
Ramchandran Plot (%)[b]	95/4.6/0.4
No. atoms	6,380
Protein	6,250
Ligand/ion	130
Water	0
B-factors (Å^2)	
Protein	33.01
Ligand/ion	25.54
Water	0
R.m.s. deviations	
Bond lengths (Å)	0.022
Bond angles (°)	1.320

Molecular replacement with PDB ID: 2XAM.

*One single crystal used for data collection.

[a]Values in parentheses are for highest-resolution shell.

[b]Residues in the favored/allowed/disallowed regions, as determined by MolProbity.

Table S4.1. List of oligonucleotides used for disulfide mutant generation.

E7C	Forward	ggatcctaatggagatgattttggagtgcaaagatgcatcagattggatttacag
	Reverse	ctgtaaatccaatctgatgcatctttgcactccaaaatcatctccattaggatcc
E113C	Forward	ggagtacgtgtttctgtgtccaagtgctttcttgagtgtgttgataagaaa
	Reverse	tttcttatcaacacactcaagaaagcacttggacacagaaacacgtactcc
K43C	Forward	tgtggggaaagtgattcgtatacagtgcgctcggaggaacgataa
	Reverse	ttatcgttcctccgagcgcactgtatacgaatcactttccccaca
A134C	Forward	cgctatggcgtgttaatgcatgtaatgttgataccagtcatg
	Reverse	catgactggtatcaacattacatgcattaacacgccatagcg
E82C	Forward	caatgagctgatttcatcaccaaacaagtgcgttcttgaacaaagatatgttcagaatg
	Reverse	cattctgaacatatctttgttcaagaacgcacttgtttggtgatgaaatcagctcattg
S142C	Forward	cagctaatgttgataccagtcatgattgcgctcttatattgaat
	Reverse	attcaatataagagcgcaatcatgactggtatcaacattagctg
G105C	Forward	gtcctaaacatgttgatgcatgcgtacgtgtttctgtgtccaa
	Reverse	ttggacacagaaacacgtacgcatgcatcaacatgtttaggac
L146C	Forward	accagtcatgattccgctcttatatgcaatgatcattcactattctctc
	Reverse	gagagaatagtgaatgatcattgcatataagagcggaatcatgactggt
L115C	Forward	gtacgtgtttctgtgtccaaggagttttgtgagtgtgttgataagaaa
	Reverse	tttcttatcaacacactcacaaaactccttggacacagaaacacgtac
T138C	Forward	cgtgttaatgcagctaatgttgattgcagtcatgattccgctc
	Reverse	gagcggaatcatgactgcaatcaacattagctgcattaacacg

Connecting Text

In previous chapters, we examined the mechanism of how IPK1 discriminates between different IP substrates. We validated a two-step IP recognition model for IPK1 where the IP is initially recognized by its 4-, 5-, and 6-phosphates, and then the 1- and 3-phosphates induce N-lobe stabilization. The key interaction between R130 and the 1-phosphate of the IP stabilizes the N-lobe. The description of this mechanism, and its distinguishing features among IPKs, will prove useful for the rational design of selective inhibitors for IPK1 in the future.

In Chapter 5, we describe experiments to identify novel inhibitors of IPK1. Using our established activity assay for IPK1 kinase activity, we could identify compounds that inhibit IPK1 and determine the nature of their inhibition. We screened polyphenolic compounds that are known to inhibit IPKs, kinase inhibitors that are known to inhibit PKs, and a set of structurally diverse compounds obtained from the NIH.

The data from Chapter 5 show that two compounds, PKRnc and CG, are mixed inhibitors for IPK1 and suggests a possible allosteric binding site on IPK1. Furthermore, IPK1 shows very little sensitivity towards kinase inhibitors. Using these compounds, the structural determinants of IPK1 inhibitor specificity could be determined, which could aid in the development of a selective inhibitor for IPK1 for future studies.

Chapter 5. Identification of small molecule inhibitors of inositol 1,3,4,5,6-pentakisphosphate 2-kinase

Varin Gosein and Gregory J. Miller

Manuscript in preparation.

Abstract

Inositol 1,3,4,5,6-pentakisphosphate 2-kinase (IPK1) catalyses the phosphorylation of IP_5 to IP_6. The precise roles of IPK1 *in vivo* have been largely unexplored, however, *in vitro* studies have revealed a role for IPK1 in apoptosis. Other studies have also implicated IP_6 and higher inositol phosphates in apoptosis, but the underlying mechanisms are unknown. A selective inhibitor of IPK1 that attenuates production of IP_6 would therefore be a useful tool to explore the apoptotic arm of IP signaling and to evaluate its potential as a therapeutic target. To begin the search for an IPK1 inhibitor, we used a three-tiered approach. We screened a library of protein kinase inhibitors to identify IPK1 inhibitors from among those that are known to affect members of the protein kinase superfamily; a set of polyphenolic compounds previously demonstrated to inhibit other IPKs; and a structurally diverse compound set to identify previously unidentified compound classes that may inhibit IPK1. During these initial tests, IPK1 exhibited >70% inhibition to over 40 compounds, each tested at 400 μM. Initially, we identified EGCG as an inhibitor from among the polyphenols (IC_{50} = 303 μM); however, further testing of 6 EGCG analogs identified Catechin Gallate (CG) as more potent than the parent compound (IC_{50} = 78 μM). IPK1 was also sensitive to the protein kinase inhibitors PKRnc (IC_{50} = 78 μM), K-252a (IC_{50} = 1.7 μM), and STS (IC_{50} = 19.4 μM). From this inhibitor profile, IPK1 sensitivity to protein kinase inhibitors appears to be distinct from 300 previously tested kinases. We also determined the mechanism for the IPK1 inhibition by selected inhibitors. PKRnc and CG were non-competitive with respect to IP_5, and mixed-competitive with respect to ATP. Our kinetic studies suggest that IPK1 may possess an allosteric binding site that could be exploited for selective targeting of IPK1.

Keywords: IPK1; polyphenols; kinase inhibitor; PKRnc; structure activity relationship; allosteric binding site

Introduction

Inositol 1,3,4,5,6-pentakisphosphate 2-kinase (IPK1) is an inositol phosphate kinase (IPK) that synthesizes inositol 1,2,3,4,5,6-hexakisphosphate (IP_6) from inositol 1,3,4,5,6-pentakisphosphate (IP_5) (Sweetman et al., 2006). Previous studies have shown that IPK1 null mice are embryonic lethal, revealing an important developmental role for IPK1, but the lethal outcome of these mice prevents further determination of the functional roles of IPK1 *in vivo* using this approach (Verbsky et al., 2005b). *In vitro* studies reveal that knockdown of IPK1 sensitizes cells to TNFα-mediated apoptosis, whereas overexpression of IPK1 protects cells from apoptotic agents (Verbsky and Majerus, 2005; Piccolo et al., 2004). IP_6, the product of IPK1, promotes apoptosis, in both *in vitro* (Morrison et al., 2002; Morrison et al., 2001) and *in vivo* studies (Morrison et al., 2009; Bozsik et al., 2007; Vucenik and Shamsuddin, 2006; Vucenik and Shamsuddin, 2003), but the precise mechanisms underlying the role of IP_6 in apoptosis remain unresolved. IPK1 also regulates the levels of inositol pyrophosphates (PP-IPs), the production of which depends on IP_5 and IP_6 (Menniti et al., 1993; Glennon and Shears, 1993). Production of PP-IPs also induces apoptosis (Agarwal et al., 2009; Nagata et al., 2005), suggesting that there is apoptotic arm of IP signaling that is yet to be explored. Selective chemical inhibition of IPK1 would be a valuable approach to investigate the roles of IPK1 in mammals and the apoptotic arm of IP signaling. Furthermore, an inhibitor for IPK1 could be used to validate higher IP production as a therapeutic target for inducing cell death. The catalytic mechanism of IPK1 possesses similar features to that of protein kinases, which suggests that IPK1 may be sensitive to kinase inhibitors (Banos-Sanz et al., 2012; Gosein et al., 2012). Some IPKs are also sensitive to polyphenols, a natural set of compounds that may have diverse health benefits, but IPK1 sensitivity to polyphenols has not yet been explored (Mayr et al., 2005).

Our current objective was to identify novel inhibitors of IPK1 using a screening approach. Initially, we tested 160 known kinase inhibitors, 6 polyphenolic compounds, and 1200 structurally diverse compounds. We identified multiple compounds that inhibit IPK1 and determined the kinetic properties of a select few. Two compounds, CG and PKRnc, are promising leads for the development of specific inhibitors of IPK1 due to their chemical properties, potential sites for chemical modification, and potency for IPK1 inhibition.

Materials and Methods

Chemical libraries

All polyphenolic compounds, including EGCG analogs, were obtained in powder form (Sigma). The InhibitorSelect 384-Well Protein Kinase Inhibitor Library I, a set of 160 well-characterized ATP-competitive and allosteric protein kinase inhibitors, was obtained from EMD Millipore. The NIH Structural Diversity Set and the Natural Products Set was obtained from the National Cancer Institute. Sulfa analogs were obtained in powder form (Sigma). All compounds were obtained or dissolved at 10 mM in DMSO.

Ligands

IP_5 was purchased from Cayman Chemical Company (Ann Arbor, MI). ATP was purchased from Fisher (Waltham, MA). All ligands were dissolved in Tris-HCl (pH 8.0) to a stock concentration of 20 mM and stored at -20 °C.

IPK1 expression and purification

Purified *A. thaliana* IPK1 was obtained using a previously described protocol in (Gosein et al., 2012). Protein concentration was determined by Bradford Assay using BSA as a standard. Protein was stored at 4 °C and all experiments were performed within 96 h.

Initial screening

IPK1 kinase activity was assessed using the Kinase-Glo Max Luminescent Kinase Assay (Promega) as per manufacturer instructions. Kinase reactions were performed in 25 µL volumes in black 96-well plates at 25 °C. The final reaction mixture consisted of 50 mM HEPES (pH 7.5), 6 mM $MgCl_2$, 50 mM NaCl, 50 µM IP_5 and 50 µM ATP. 1 µL of each inhibitor was added directly to each well, resulting in a final concentration of 400 µM of inhibitor and 4% DMSO. 0.1 µM of IPK1 was subsequently added directly to each well. IPK1 does not exhibit reduced activity in DMSO under 10%. The plates were incubated for 5 min and then ATP was added to initiate the reaction. After 30 min, 25 µL of Kinase-Glo reagent was added to stop the reaction. Luminescence was measured after 20 min on a Berthold Orion II Microplate Luminometer. Wells containing ATP, 4% DMSO, IPK1, but

no IP_5, were used as positive controls and the resulting values were considered to be equivalent to the signal that would result from 100% IPK1 inhibition. Wells containing ATP, 4% DMSO, IPK1, and IP_5, were used as negative control and the resulting values were considered to be 0% inhibition. All compounds that inhibited IPK1 were retested for luminescence, by omitting ATP in the well. This protocol was used to test the kinase inhibitor screen, the NIH inhibitor screen, and polyphenolic screen as well as sets of sulfa analogs, and EGCG analogs.

IC_{50} determination

Kinase reactions, as described above, were performed in 25 µL containing 50 mM HEPES (pH 7.5), 6 mM $MgCl_2$, 50 mM NaCl, 50 µM IP_5 and 50 µM ATP. Inhibitor was added in concentrations ranging from 12.5 µM to 1000 µM for EGCG analogs, 12.5 µM to 400 µM for PKRnc, 0.78 µM to 150 µM for staurosporine (STS), and 0.19 µM to 25 µM for K-252a. The highest and lowest values of ATP depletion were considered to be 0% and 100% inhibition, respectively. The log(concentration of inhibitor) versus response was plotted and fitted to a variable slope equation using non-linear regression to determine the IC_{50} (GraphPad). Experiments were performed in triplicate and are reported as mean ± SD.

IPK1 kinase activity

Kinase activity was assessed using a previously described protocol in (Gosein and Miller, 2013). Kinase reaction conditions were as described above. To obtain kinetic parameters for IPK1 and its substrate, IP_5, reaction mixtures contained 50 mM HEPES (pH 7.5), 6 mM $MgCl_2$, 50 mM NaCl, and 300 µM ATP in the presence of DMSO or inhibitor ([EGCG] = 80 µM, [CG] = 20 µM, [PKRnc] = 20 µM, or [K-252a] = 1 µM). 25 µL of Kinase-Glo reagent was added to stop the reaction, and luminescence was measured after 20 min. Initially, 80 µM of IP_5 was used and the amount of enzyme was varied to determine conditions in which product formation was linear over 30 min to accurately determine the initial velocity of the reaction. Subsequently, reactions were performed using the enzyme concentration determined and with varying concentrations of IP_5 (20 µM, 40 µM, 60 µM, 80 µM, 100 µM, 120 µM, 140 µM). These reactions were stopped at various time points (0 min, 15 min, and 30 min) and were performed in triplicate.

The rate of product formation was plotted against IP_5 concentration and the data was fit using the Michaelis-Menten equation using non-linear regression to determine K_M and V_{MAX} for IP_5 (GraphPad). Values are reported as mean ± SD. To obtain kinetic parameters for ATP, reaction mixtures contained 50 mM HEPES (pH 7.5), 6 mM $MgCl_2$, 50 mM NaCl, and 80 μM of IP_5 in the presence of DMSO or inhibitor. Reactions were performed using the enzyme concentration determined and with varying concentrations of ATP (25 μM, 50 μM, 75 μM, 100 μM, 200 μM, 300 μM, 400 μM) stopped at various time points (0 min, 15 min, and 30 min) and were performed in triplicate. A plot of the rate of product formation versus ATP concentration was used to determine K_M and V_{MAX} for ATP (GraphPad). The type of enzyme inhibition for each inhibitor with respect to IP_5 and ATP was determined by comparing the K_M and V_{MAX} for IPK1 in the presence or absence of inhibitor.

Results

Initial screening yields multiple hits

To identify an inhibitor for IPK1, we first screened known protein kinase inhibitors (Figure 5.1). Only 3 compounds out of 160 were identified as potent (>70%) inhibitors of IPK1: STS, K-252a, and PKRnc (Figure S5.1, Table S5.1). Both STS and K-252a are well-established ATP competitive inhibitors for many kinases; however, PKRnc is much more specific, and only inhibits a few kinases (Anastassiadis et al., 2011). The identification of STS and K-252a as IPK1 inhibitors is consistent with their known promiscuity. However, IPK1's lack of sensitivity to the 157 other potent inhibitors that target multiple families of kinases indicates that the nucleotide binding site of IPK1 is indeed unusual among kinases.

Second, we screened a set of polyphenolic compounds, which are known inhibitors of other IPKs, including IP_3K and IPMK, to identify a possible inhibitor of IPK1 (Mayr et al., 2005). These polyphenolic compounds consisted of myricetin, quercetin, EGCG, curcumin, ellagic acid, and chlorogenic acid (Figure 5.2). In contrast to the reported sensitivity of other IPKs to these inhibitors, IPK1 is only sensitive to EGCG (Mayr et al., 2005).

Third, we screened a set of 1200 structurally diverse compounds. The top 79 compounds, as determined by % inhibition of IPK1, were retested for their ability to inhibit IPK1 (Figure 5.3). There were no obvious structural patterns for those compounds that inhibited IPK1, however, the structure of 48_C6 resembled that of sulfonamides, for which analogs are readily available (Figure S5.2). The compound 48_C6 was not commercially available for further study.

EGCG analogs reveal structure-activity relationships (SARs)

The availability of analogs for EGCG and sulfa drugs enabled further testing of these compounds to identify compounds with improved potency and to establish SARs. We tested inhibition of IPK1 with C, EC, GC, CG, EGC, ECG, and EGCG (Figure S5.3). The compounds C, EC, GC, and EGC, exhibited less than 50% inhibition compared to DMSO, while ECG, CG, and EGCG provided near 100% inhibition at 400 μM, revealing that the presence of a second gallate group in the chemical structure of the inhibitor improves IPK1 inhibition (Figure 5.4a, Figure S5.3). We also tested our set of sulfonamides, but these analogs did

not inhibit IPK1 (Figure 5.4b), which may be attributable to differences in the structures of these sulfonamides and compound 48_C6.

CG, PKRnc, STS, and K-252a are potent inhibitors of IPK1

To accurately assess the potency of the EGCG analogs and kinase inhibitors STS, K-252a, and PKRnc, we determined the IC_{50} values of each of these compounds. Among the EGCG analogs, CG is the most potent, displaying an IC_{50} = 78 μM (Figure 5.5a), which compares favorably with EGCG (IC_{50} = 303 μM). ECG displayed an IC_{50} = 191 μM, suggesting that the stereochemistries of the bonds between arm 1 and arm 2 and the core of the compound is a determinant of inhibitor potency (Figure S5.3). Amongst the kinase inhibitors, K-252a displayed the highest potency at IC_{50} = 1.7 μM, followed by STS at IC_{50} = 19.4 μM, consistent with these two inhibitors being highly potent kinase inhibitors (Figure 5.5b). The final inhibitor, PKRnc, exhibited a much lower potency with an IC_{50} = 78 μM, but was still comparable to the CG analog.

CG and PKRnc are mixed inhibitors

To identify the binding sites for CG and PKRnc, we determined the nature of their inhibition with respect to ATP and IP_5. We also tested K-252a, a known ATP competitive inhibitor, which exhibited the highest potency towards IPK1, and EGCG, our initial polyphenolic hit. We first determined that IPK1 possesses a K_M = 88.71 ± 22.95 μM and V_{MAX} = 26.51 ± 3.39 μM/min/μg for IP_5, in the absence of inhibitor, which is consistent with previously reported values for wild-type IPK1 (Gosein and Miller, 2013) (Figure 5.6a, Table S5.2). In the presence of each inhibitor, the K_M for IP_5 remained unchanged, however, the V_{MAX} for IP_5 decreased, indicating that each inhibitor is non-competitive towards IP_5 and none of the inhibitors bound to the IP_5 binding site (Figure 5.6b,c). We then determined that IPK1 possesses a K_M = 68.98 ± 7.95 μM and V_{MAX} = 25.42 ± 0.94 μM/min/μg for ATP (Figure 5.7a, Table S5.2). As expected, K-252a is highly competitive for ATP, increasing the K_M almost 3-fold while the V_{MAX} was unaffected (Figure 5.7b,c). Thus, K-252a inhibits IPK1 by binding to the ATP binding site of IPK1. There was also a slight increase in K_M for ATP with PKRnc, but the V_{MAX} decreased, revealing that PKRnc exhibits a mixed type of inhibition. This mode indicates that PKRnc and ATP may be bound to IPK1 at the same time, but PKRnc

is non-competitive for IP_5, suggesting that there is an allosteric binding site on IPK1. In the presence of PKRnc, there was a large decrease in V_{MAX} compared to a small increase in K_M suggesting that PKRnc acts more like an allosteric inhibitor rather than a competitive inhibitor to ATP. CG, like PKRnc, also displayed a mixed type of inhibition with respect to ATP. In contrast, EGCG displayed a decrease in both K_M and V_{MAX}, indicative of uncompetitive inhibition towards ATP, which also suggests that an alternative binding site may be present, such that EGCG, ATP, and IP_5 may bind simultaneously.

Discussion

PKRnc, CG, and K-252a as IPK1 inhibitors

Here, we screened kinase inhibitors, polyphenolic compounds, and structurally diverse natural compounds to identify inhibitors for IPK1. We have identified over 40 compounds that can inhibit the kinase activity of IPK1 by >70% (Figures 5.1-5.3). These include the polyphenol EGCG and the kinase inhibitors PKRnc, STS and K-252a. By testing EGCG analogs, CG and ECG were determined to have increased potency compared to the parent compound (Figures 5.4, 5.5). Finally, we performed kinetic characterization of PKRnc, K-252a, EGCG, and CG to determine their types of inhibition with respect to ATP and IP_5 (Figures 5.6, 5.7). In our study, we used plant IPK1, which shares 60% sequence similiarity with human IPK1, and all secondary structural elements are conserved (Gonzalez et al., 2010). Moreover, active site residues that bind ATP and IP are 95% identical between the plant and human form, suggesting that the identified compounds would also affect the human form.

IPK1 is sensitive to the polyphenol EGCG

Previously, IPKs have been reported to be sensitive to polyphenolic compounds, but our study is the first to characterize IPK1 sensitivity to these compounds. We observed that IPK1 is sensitive only to EGCG from among the IPK inhibitors (Figure 5.2). In contrast, IP_3K and IPMK, showed varied sensitivity to different polyphenols we and others have tested (Mayr et al., 2005). IP_3K was inhibited by EGCG, quercetin, myricetin, hypericin, and THF, while IPMK was inhibited by ellagic acid, chlorogenic acid, ATA, and rose bengal (Mayr et al., 2005). Inhibitor selectivity between IP_3K and IPMK was reflected in differences within structurally related regions of the C-lobe of each IPK (Mayr et al., 2005). One residue in the ATP binding site on the C-lobe was critical for IP_3K inhibition by THF, while a basic region inserted on the C-lobe of IPMK mediated sensitivity only towards acidic polyphenols (Mayr et al., 2005). We suspect that the sensitivity of IPK1 to EGCG alone from among this set of compounds is determined by its distinct C-lobe, which forms a large IP binding site, and a portion of the nucleotide-binding site, which is a feature that is not shared with other IPKs (Gonzalez et al., 2010). IPK1 also possesses a highly basic IP binding

pocket to promote interaction with the five acidic phosphate groups of the IP, however, ellagic acid and chlorogenic acid did not inhibit IPK1 (Figure 5.2). This indicates that IPK1 inhibitor sensitivity towards polyphenols is not solely dependent on electrostatic interactions, as observed with IPMK (Mayr et al., 2005). In our study, we observed an increase in IC_{50} between EGCG, ECG, and CG, likely determined by their stereochemistry and functional groups (Figure 5.5a). EGCG is a potent inhibitor for human topoisomerase II and prolyl-endopeptidases (Kim et al., 2001); however, no specific target of CG, our most potent polyphenol inhibitor for IPK1, is known. Inhibition of IPK1 and other IPKs by numerous polyphenols indicates that the antiproliferative effects of polyphenols *in vitro* and *in vivo* may be elicited through an IP signaling axis that is mediating cell death (Agarwal et al., 2009; Piccolo et al., 2004; Mayr et al., 2005).

IPK1 kinase inhibitor sensitivity is unique among 300 kinases

We screened a protein kinase inhibitor library, consisting of 160 potent, reversible ATP-competitive and allosteric inhibitors, for their ability to inhibit IPK1 (Figure 5.1). These inhibitors were previously tested for their activity against 300 kinases, representing 10 different kinome trees (Anastassiadis et al., 2011). Previous reports have suggested that the mechanisms of IPK1 activation may be similar to that of protein kinases (Banos-Sanz et al., 2012; Gosein et al., 2012). IPK1 showed high sensitivity to only three inhibitors: STS, K-252a, and PKRnc. Of these three inhibitors, STS and K-252a, well known promiscuous kinase inhibitors, possess Gini scores of 0.20 and 0.29, the lowest two scores among all kinase inhibitors in the set, while masitinib, a highly selective tyrosine kinase inhibitor, has a Gini score of 0.81 (Anastassiadis et al., 2011). Our third hit, PKRnc, is reported to have a Gini score of 0.60, which is moderately positioned among all inhibitors in the set (Anastassiadis et al., 2011). PKR, known as Protein Kinase RNA-activated, is activated by viral dsRNA and subsequently phosphorylates the translation initiation factor EIF2A to inhibit cellular mRNA translation and thus viral protein synthesis (Meurs et al., 1993). PKRnc was used as a negative control for studies that employed the PKR inhibitor (Jammi et al., 2003). Our results show that PKRnc inhibited IPK1, but the structurally related analog, PKR inhibitor, did not (Table S5.1, L14). PKR inhibitor has an IC_{50} = 210 nM for PKR, while PKRnc has an IC_{50} >100 μM for PKR and an IC_{50} = 78 μM for

IPK1. Thus, selectivity for IPK1 is opposite to that of PKR for these two compounds, likely due to chemical group differences between these two analogs (Figure S5.1c,d) (Anastassiadis et al., 2011).

We suspected that the kinase subfamily sensitive to PKRnc would reveal the subfamily closest to IPK1. PKRnc inhibits 12 kinases from different kinase subfamilies with >70% inhibition (Anastassiadis et al., 2011). Of those 12 kinases, only 2 kinases, BRAF and RAF1, are sensitive to PKRnc, but resistant to PKR inhibitor, like IPK1; however, both BRAF and RAF1 are resistant to STS and K-252a, unlike IPK1, indicating that IPK1 displays a unique profile of sensitivity to this set of kinase inhibitors (Anastassiadis et al., 2011).

Inhibitor competition to ATP and IP_5

The similarity of the ATP binding site among IPKs suggests that the IP binding site may be the best target to develop selective inhibitors for an IPK, however, the similarity among IP substrates may limit the specificity of an inhibitor for any specific IP binding site. Thus, an inhibitor that competes with both ATP and the IP substrate, or that uses an allosteric mechanism, may provide increased selectivity for a specific IPK. EGCG, CG, PKRnc, and K-252a were non-competitive to IP_5 (Figure 5.6) but showed varied competition to ATP (Figure 5.7). Many other hits remain uncharacterized and may be competitive for IP_5, but many of these hits are commercially unavailable, or their chemical structures are not amenable for crystallographic studies (Figure 5.3). Our competition data shows that K-252a is a potent ATP competitive inhibitor of IPK1 (Figure 5.7). We contend that this result validates our experimental approach for assessing the type of competition for IPK1 inhibitors, as K-252a is well established as an ATP competitive inhibitor for many kinases (Kase et al., 1987). Although K-252a, and its analog, STS, displayed the lowest IC_{50} values among the compounds we tested, their promiscuity among kinases precludes their use as a selective inhibitors for IPK1 (Anastassiadis et al., 2011). Our competition data also shows that EGCG is uncompetitive with ATP, however, EGCG competition with ATP varies considerably among kinases (Ranjith-Kumar et al., 2010; Lewis et al., 2008; Kim et al., 2001). Both CG and PKRnc exhibited mixed competition with respect to ATP, and with the observed mechanisms for EGCG inhibition, suggests that there is one or more alternative binding sites on IPK1 that may be targeted to modulate

IPK1 activity. This combination of non-competitive inhibition towards IP and mixed inhibition towards ATP was previously reported for polyphenolic compounds tested against IP_3K (Mayr et al., 2005). IP_3K possesses a CaM-binding domain that controls its IPK activity and may be involved in inhibitor binding; however, no allosteric site on IPK1 has been identified. A very recent study has identified a tripeptide on the surface of human IPK1 that mediates interaction with the nucleolar protein UBF, however, mutations of these residues or UBF binding did not compromise IPK1 kinase activity, so it is unlikely this tripeptide forms part of an allosteric site (Brehm et al., 2013). Further characterization will be required to determine the structural basis of inhibition by CG or PKRnc. Ligands with an uncompetitive or mixed type of inhibition towards ATP are considered to be advantageous for the development of highly selective inhibitors whereas pure competitors of ATP, an extensively used substrate within the cell, tend to act against numerous targets (Karni et al., 2003).

Conclusion

In this report, we identify CG and PKRnc as novel inhibitors of IPK1. Both inhibitors are non-competitive with IP_5 and show mixed competition with ATP, which suggests a possible allosteric binding site on IPK1. Furthermore, IPK1 is sensitive to very few kinase inhibitors, revealing dissimilarity between IPK1 and protein kinases. Identification of compounds that inhibit IPK1 enables us to explore the structural basis of inhibitor sensitivity of IPK1 for the development of selective inhibitors of IPK1.

Acknowledgements

We thank Dr. Charles A. Brearley (University of East Anglia) for his gift of the AtIPK1-pET28 vector and Dr. Dan Bernard (McGill University) for access to the luminometer used in enzyme assays. We thank the NIH for their gift of the Structural Diversity Set and the Natural Products Set.

This work is supported by a Canadian Institutes of Health Research Operating Grant MOP-93687 awarded to GJM and a CIHR Strategic Training Initiative in Chemical Biology awarded to VG.

Figure 5.1. Kinase inhibitor screen. 160 known kinase inhibitors were tested for IPK1 inhibition. K-252a, PKRnc, and staurosporine were identified as inhibitors of IPK1, displaying >70% inhibition of IPK1 at 400 μM, compared to a positive control without IP_5 substrate.

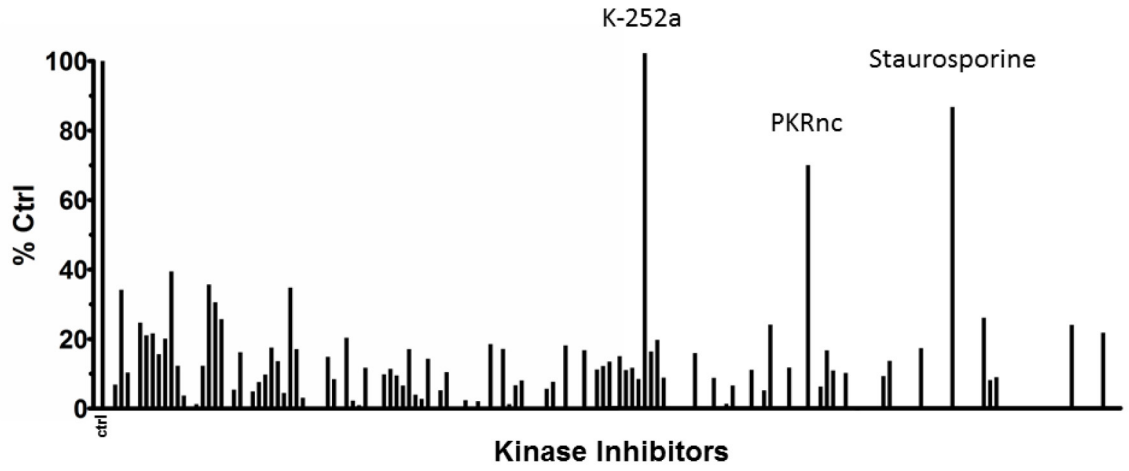
K-252a
Staurosporine
PKRnc
100
80
60
40
20
0
% Ctrl
ctrl
Kinase Inhibitors

Figure 5.1.

Figure 5.2. Polyphenolic inhibition of IPK1. Myricetin, quercetin, EGCG, curcumin, ellagic acid, and chlorogenic acid were tested for IPK1 inhibition. EGCG was identified as a polyphenolic inhibitor of IPK1 compared to a positive control without IP_5 substrate. Data represents the mean ± S.D. of triplicate experiments.

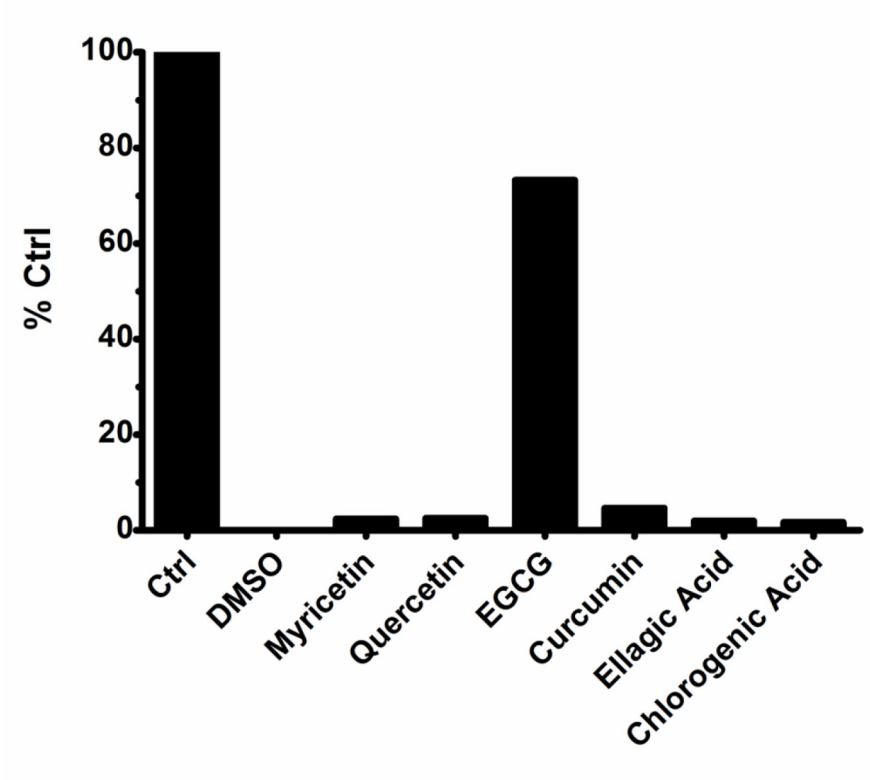
100
80
60
40
20
0
% Ctrl
Ctrl
DMSO
Myricetin
Quercetin
EGCG
Curcumin
Ellagic Acid
Chlorogenic Acid

Figure 5.2.

Figure 5.3. NIH library rescreen. The top 79 compounds out of the 1200 compounds from the NIH library originally tested were rescreened for IPK1 inhibition and compared to a positive control without IP_5 substrate. 16 compounds showed 100% inhibition at 400 μM.

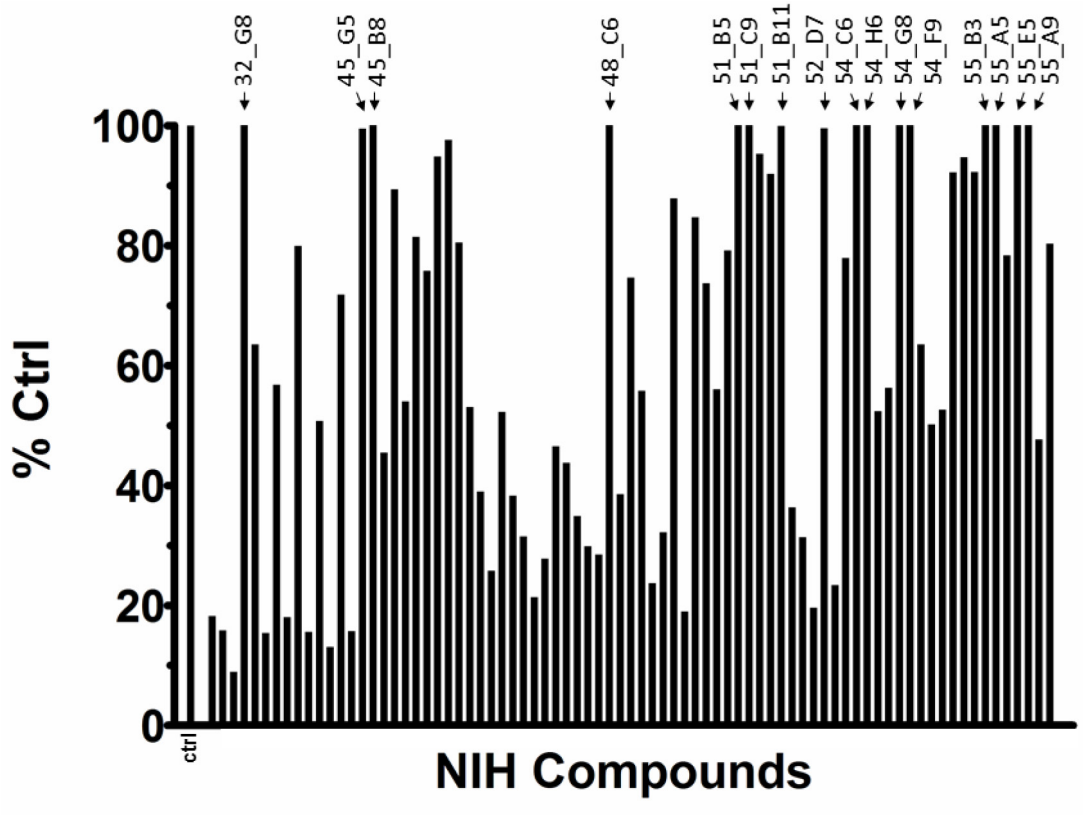
32_G8
45_G5
45_B8
48_C6
51_B5
51_C9
51_B11
52_D7
54_C6
54_H6
54_G8
54_F9
55_B3
55_A5
55_E5
55_A9
100
80
60
40
20
0
% Ctrl
ctrl
NIH Compounds

Figure 5.3.

Figure 5.4. Structure-activity relationships of EGCG analogs. (A) EGCG analogs were tested for their inhibition of IPK1. The analogs possessing a second gallate group were more potent. **(B)** Sulfa analogs were tested for IPK1 inhibition, but no analog was potent. Data represents the mean ± S.D. of triplicate experiments.

A

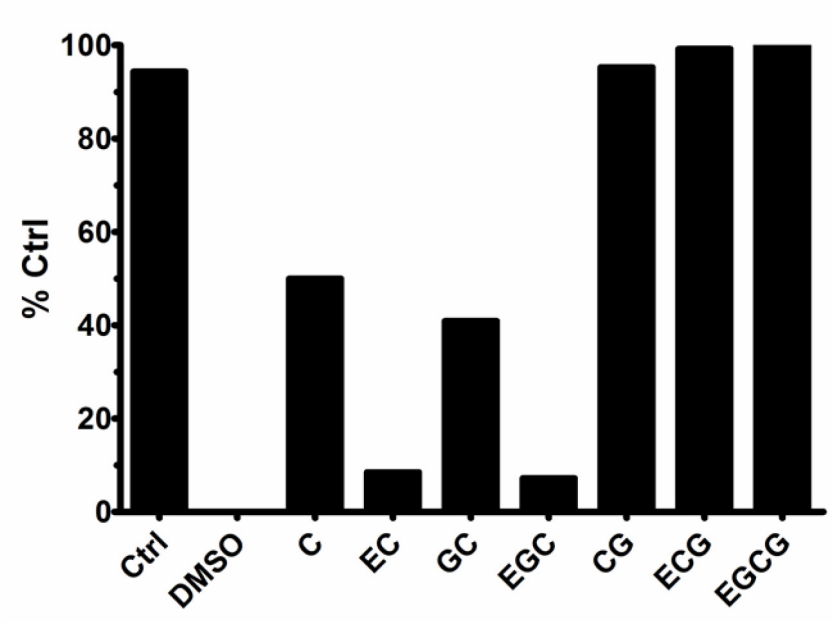
100
80
60
40
20
0
% Ctrl
Ctrl
DMSO
C
EC
GC
EGC
CG
ECG
EGCG

B

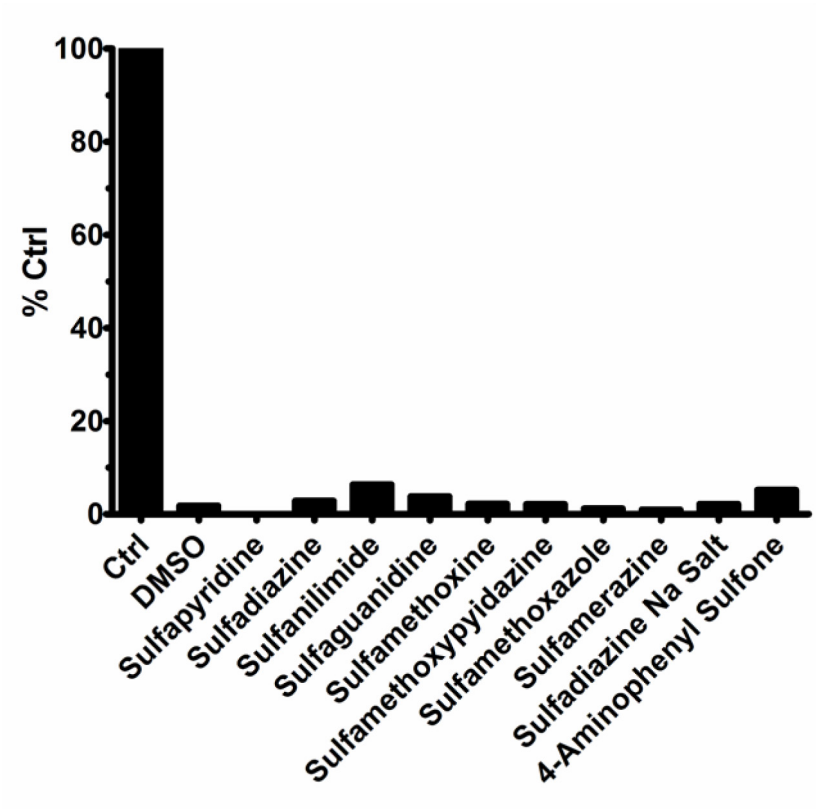
100
80
60
40
20
0
% Ctrl
Ctrl
DMSO
Sulfapyridine
Sulfadiazine
Sulfanilimide
Sulfaguanidine
Sulfamethoxine
Sulfamethoxypyridazine
Sulfamethoxazole
Sulfamerazine
Sulfadiazine Na Salt
4-Aminophenyl Sulfone

Figure 5.4.

Figure 5.5. Potency of EGCG analogs and kinase inhibitors.

(A) EGCG analogs.

●: C (IC_{50} = 308 μM)

■: EC (IC_{50} = 288 μM)

▲: GC (IC_{50} = 284 μM)

⬣: CG (IC_{50} = 78 μM)

★: EGC (IC_{50} > 1000 μM)

▼: ECG (IC_{50} = 191 μM)

◆: EGCG (IC_{50} = 303 μM).

(B) Kinase inhibitors.

●: PKRnc (IC_{50} = 78.3 μM)

■: STS (IC_{50} = 19.4 μM)

▲: K-252a (IC_{50} = 1.7 μM).

Each point represents the mean ± S.D. of triplicate experiments.

A

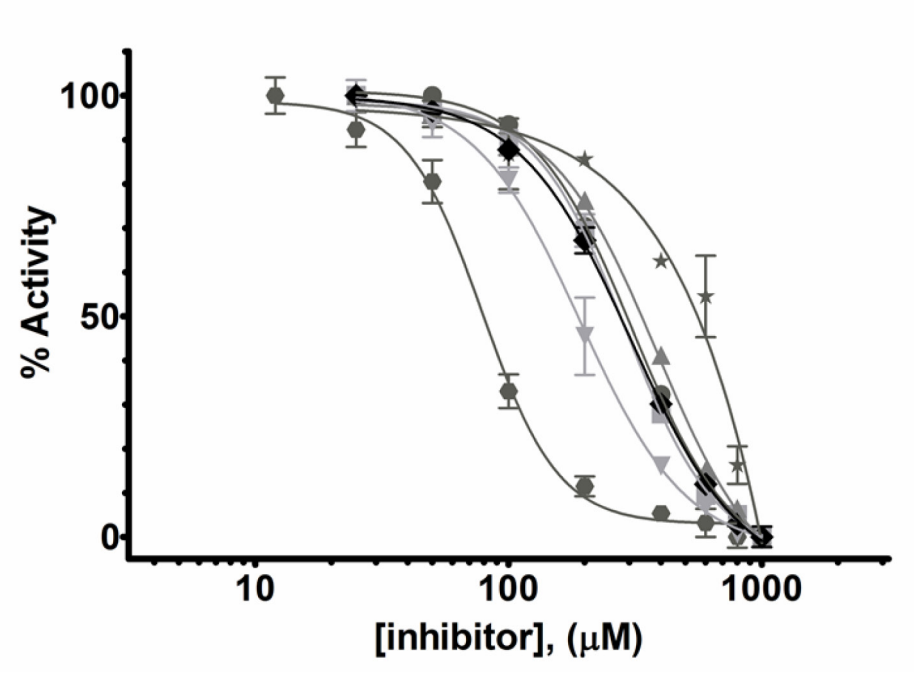
100
50
0
% Activity
10
100
1000
[inhibitor], (μM)

B

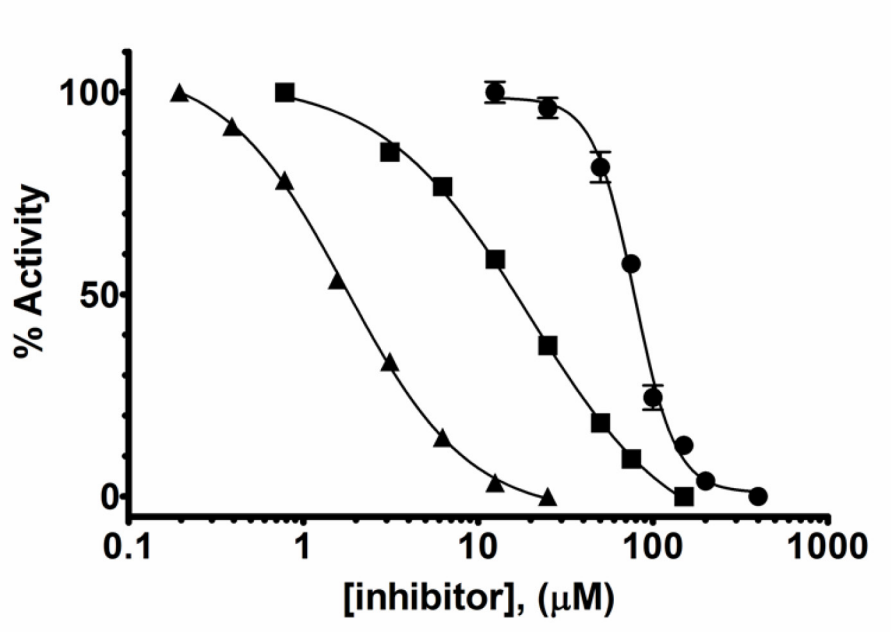
100
50
0
% Activity
0.1
1
10
100
1000
[inhibitor], (μM)

Figure 5.5.

Figure 5.6. Inhibitor competition with IP_5. (A) IPK1 kinase activity in the presence of inhibitor was assessed by plotting the rate of product formation versus IP_5 concentration fitted to the Michaelis-Menten equation. Each point represents the mean ± S.D. of triplicate experiments. ●: DMSO ■: EGCG ▲: CG ▼: PKRnc ◆: K-252a. **(B)** Comparison of K_M values for each inhibitor compared to DMSO. **(C)** Comparison of V_{MAX} values for each inhibitor compared to DMSO.

A

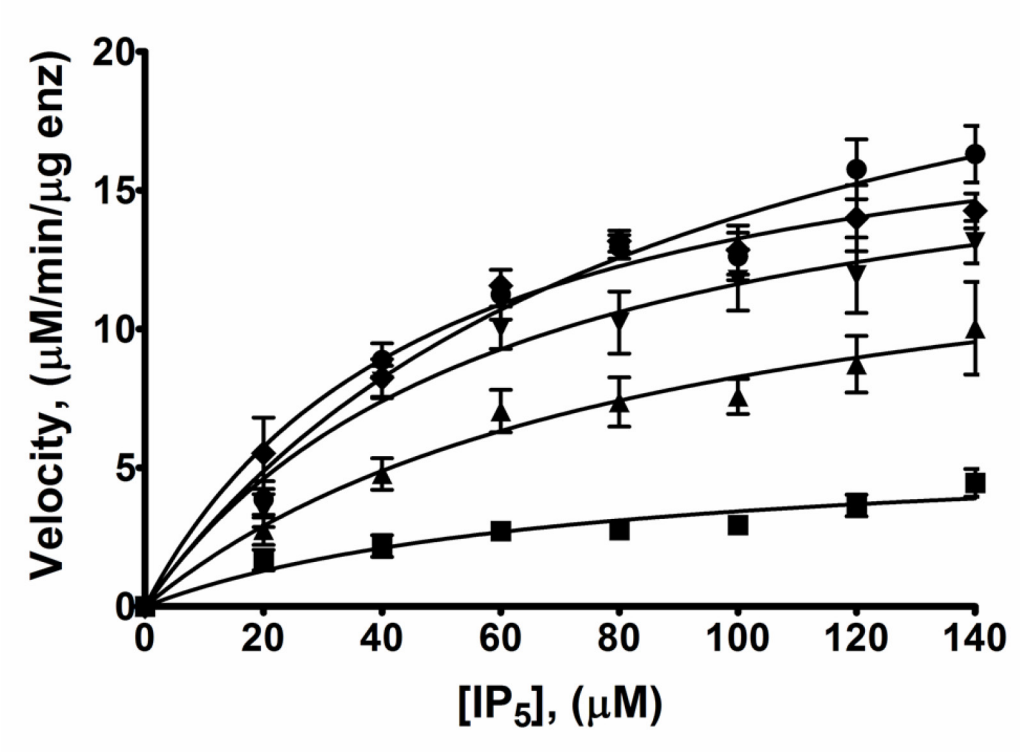

B

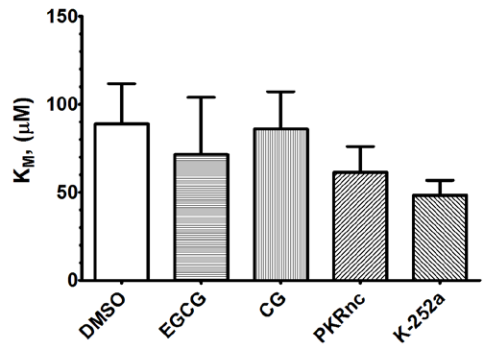

C

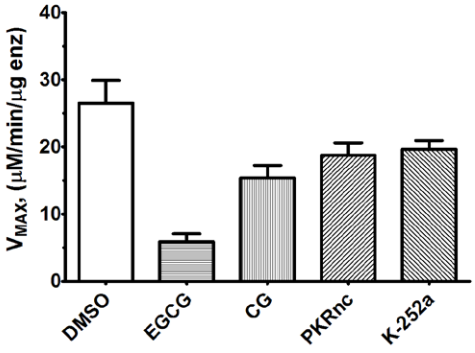

Figure 5.6.

Figure 5.7. Inhibitor competition with ATP. (A) IPK1 kinase activity in the presence of inhibitor was assessed by plotting the rate of product formation versus ATP concentration fitted to the Michaelis-Menten equation. Each point represents the mean ± S.D. of triplicate experiments. ●: DMSO ■: EGCG ▲: CG ▼: PKRnc ◆: K-252a. **(B)** Comparison of K_M values for each inhibitor compared to DMSO. **(C)** Comparison of V_{MAX} values for each inhibitor compared to DMSO.

A

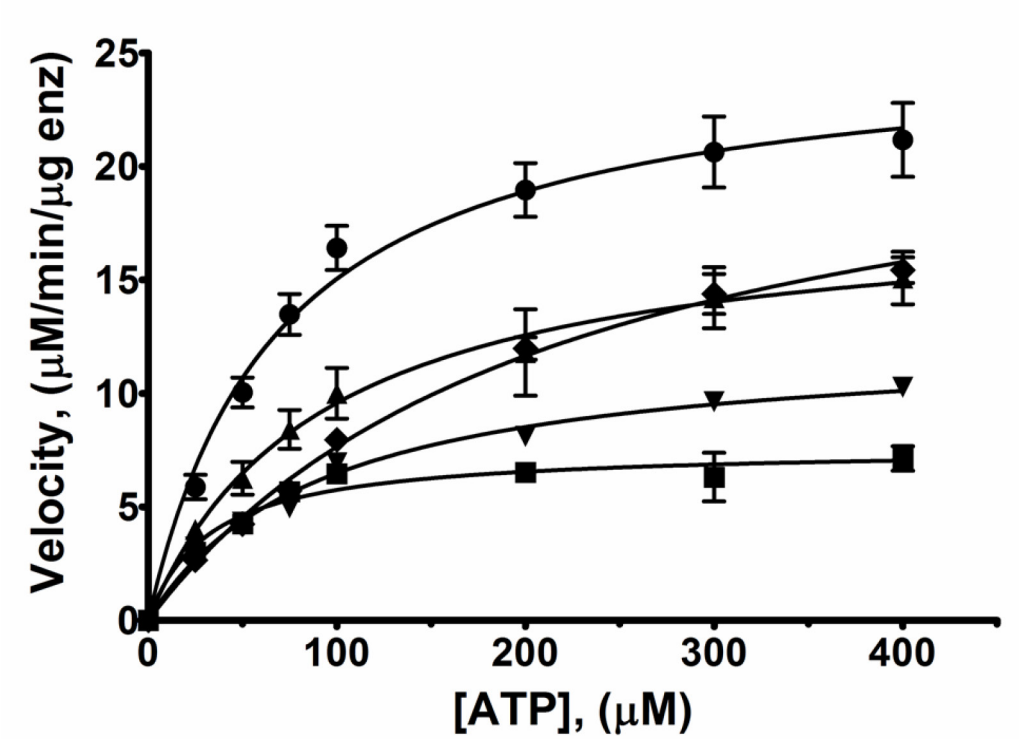

B

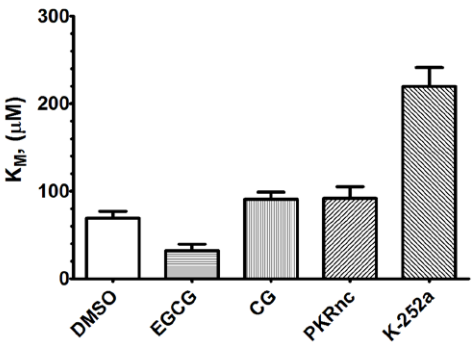

C

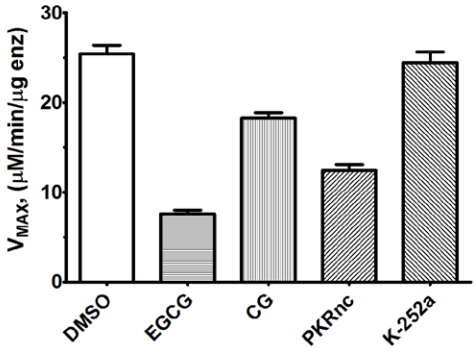

Figure 5.7.

Figure S5.1. Structures of kinase inhibitors that inhibit IPK1. (A) STS; **(B)** K-252a; **(C)** PKRnc. **(D)** The structure of PKR inhibitor is shown for structural comparison with PKRnc.

A

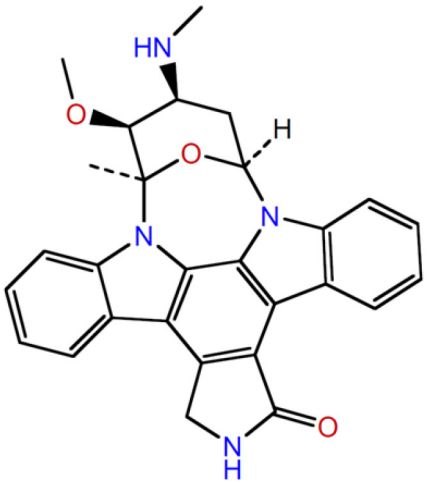

B

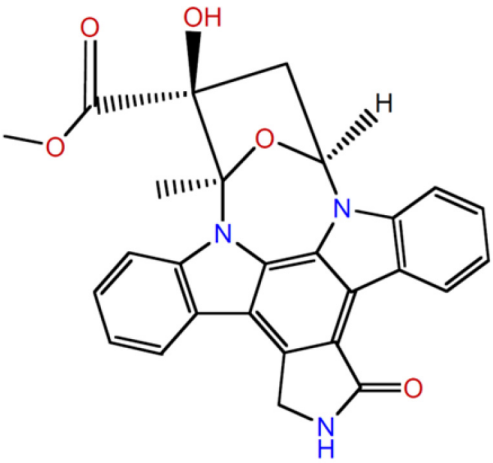

C

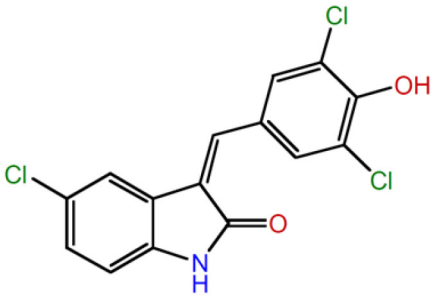

D

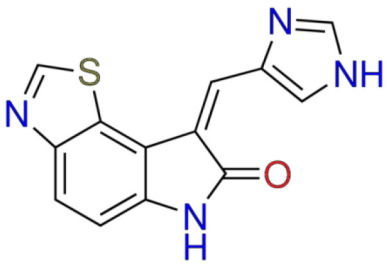

Figure S5.1.

Figure S5.2. Structures of top 16 compounds from NIH screen that inhibit IPK1. (A) 32_G8; **(B)** 45_G5; **(C)** 45_B8; **(D)** 48_C6; **(E)** 51_B5; **(F)** 51_C9; **(G)** 51_B11; **(H)** 52_D7; **(I)** 54_C6; **(J)** 54_H6; **(K)** 54_G8; **(L)** 54_F9; **(M)** 55_B3; **(N)** 55_A5; **(O)** 55_E5; **(P)** 55_A9.

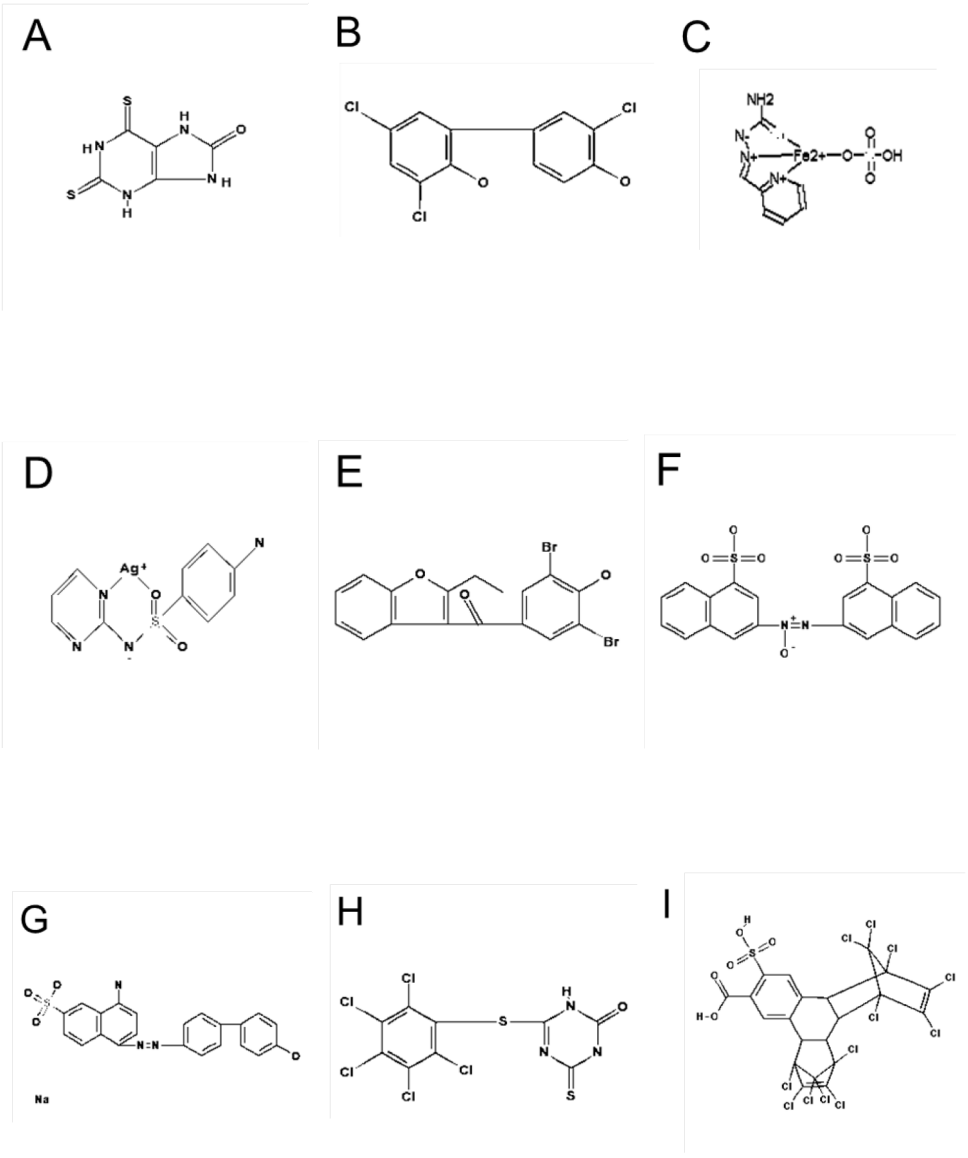

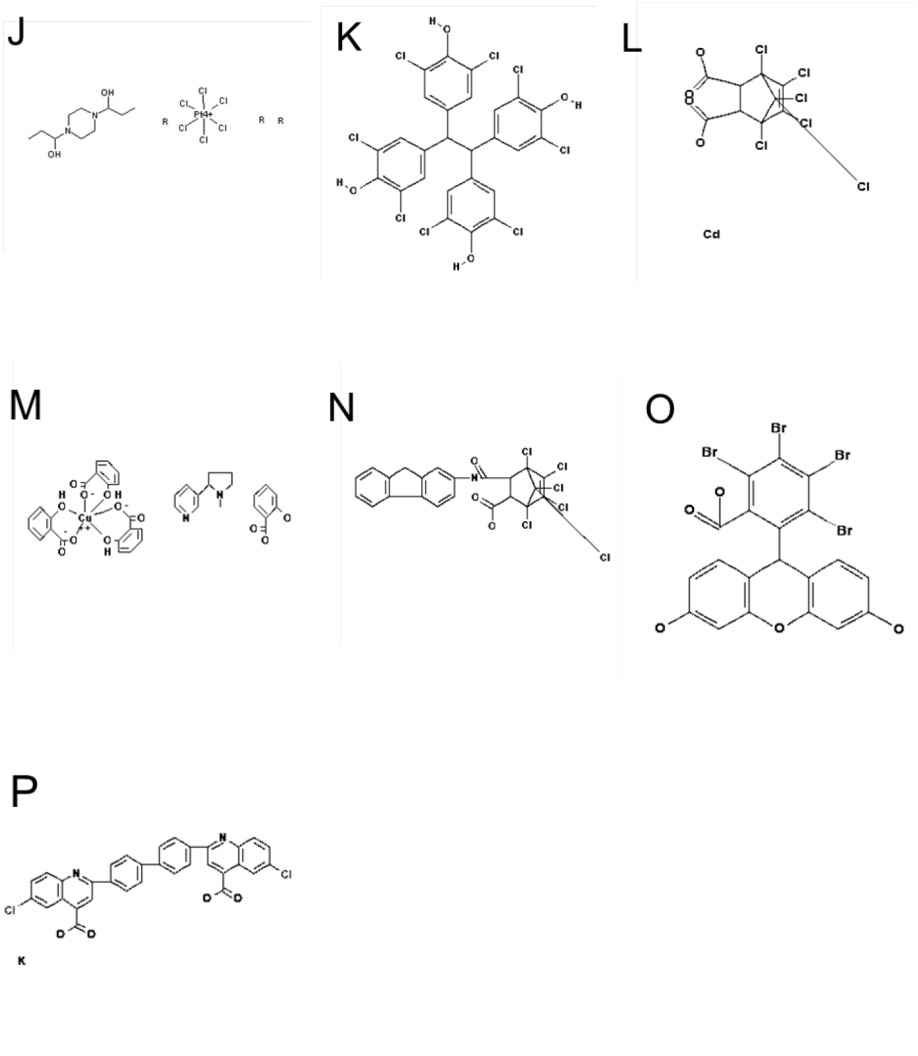

Figure S5.2.

Figure S5.3. Structures of EGCG analogs. EGCG is composed of a core and two arms.

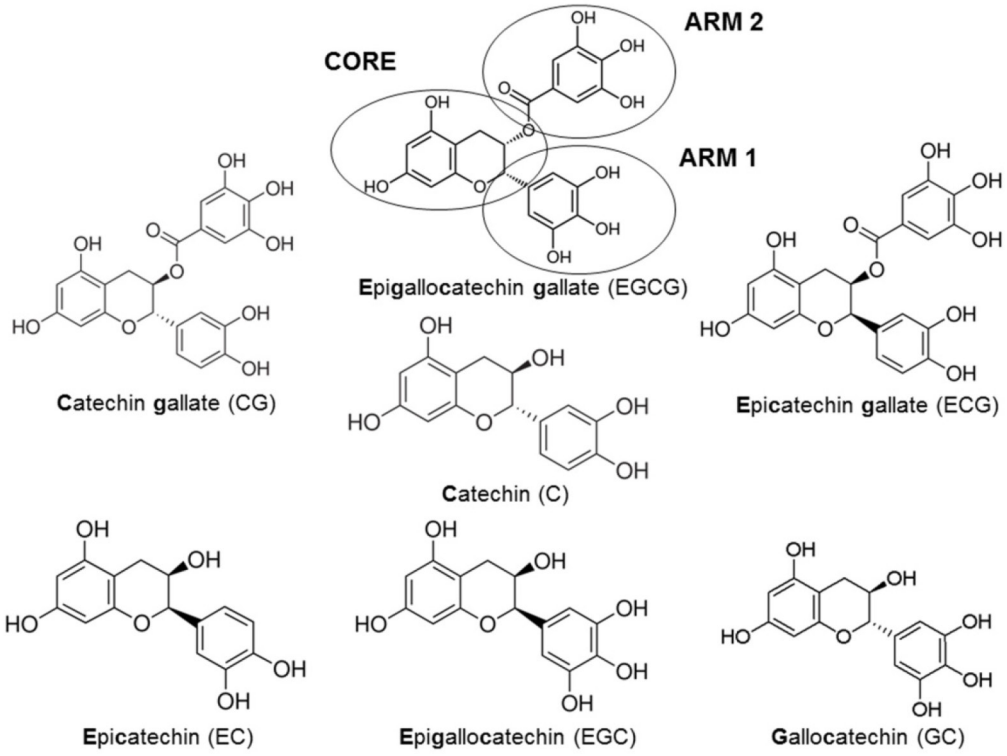

Figure S5.3.

Table S5.1. Kinase inhibitor screen normalized data. Each value represents the percentage of ATP remaining in the reaction compared to a positive control with no IP_5 substrate. **(J9)** K-252a; **(L15)** PKRnc; and **(N18)** STS were identified as inhibitors of IPK1.

B3 6.85	D3 16.22	F3 11.71	H3 18.50	J3 -12.34	L3 6.45	N3 -13.71	P3 25.49
B4 34.15	D4 -1.97	F4 -6.45	H4 -0.74	J4 -3.39	L4 -14.99	N4 -12.42	P4 7.92
B5 10.33	D5 4.88	F5 -1.25	H5 17.13	J5 14.67	L5 0.58	N5 -13.62	P5 8.71
B6 -12.50	D6 7.60	F6 9.79	H6 1.27	J6 10.73	L6 10.83	N6 -2.30	P6 -1.33
B7 24.68	D7 9.77	F7 11.41	H7 6.66	J7 11.38	L7 -3.11	N7 9.04	P7 -4.59
B8 21.03	D8 17.51	F8 9.50	H8 8.07	J8 8.25	L8 5.04	N8 13.35	P8 -14.38
B9 21.61	D9 13.59	F9 6.57	H9 -2.31	**J9 100.17**	L9 23.54	N9 -4.53	P9 -10.12
B10 15.64	D10 4.45	F10 17.06	H10 -4.09	J10 15.96	L10 -8.55	N10 -8.15	P10 -15.71
B11 20.09	D11 34.75	F11 3.99	H11 -3.22	J11 19.30	L11 -7.83	N11 -19.49	P11 -16.73
B12 39.42	D12 17.09	F12 2.75	H12 5.68	J12 8.61	L12 11.47	N12 -7.26	P12 -20.72
B13 12.31	D13 3.08	F13 14.28	H13 7.64	J13 -3.07	L13 -20.30	N13 16.89	P13 -18.37
B14 3.73	D14 -10.56	F14 0.05	H14 -6.31	J14 -6.40	L14 -5.81	N14 -8.59	P14 -24.75
B15 -6.90	D15 -5.14	F15 5.24	H15 18.13	J15 -9.05	**L15 70.54**	N15 -13.01	P15 -20.09
B16 1.28	D16 -1.62	F16 10.45	H16 -7.22	J16 -10.72	L16 -8.86	N16 -13.27	P16 -1.82
B17 12.28	D17 14.88	F17 -3.65	H17 0.12	J17 15.55	L17 6.12	N17 -5.96	P17 23.52
B18 35.63	D18 8.42	F18 -3.56	H18 16.77	J18 -3.73	L18 16.26	**N18 84.92**	P18 -15.76
B19 30.54	D19 -1.68	F19 2.39	H19 -1.69	J19 -4.57	L19 10.64	N19 -6.57	P19 -15.97
B20 25.67	D20 20.37	F20 -10.61	H20 11.17	J20 8.54	L20 -3.45	N20 -5.94	P20 -11.46
B21 -0.80	D21 2.27	F21 2.10	H21 12.22	J21 -4.03	L21 9.94	N21 -13.40	P21 -19.45
B22 5.41	D22 0.96	F22 -7.47	H22 13.49	J22 1.23	L22 -0.04	N22 -19.95	P22 21.26

Table S5.2. Kinetic parameters of IPK1 toward IP_5 and ATP in the presence of inhibitors.

Inhibitor	IP_5		ATP	
	K_M (μM)	V_{MAX} (μM/min/μg enz)	K_M (μM)	V_{MAX} (μM/min/μg enz)
DMSO	88.71 ± 22.95	26.51 ± 3.39	68.98 ± 7.95	25.42 ± 0.95
EGCG	71.52 ± 32.45	5.88 ± 1.20	32.39 ± 7.18	7.61 ± 0.40
CG	85.97 ± 21.20	15.40 ± 1.85	90.72 ± 8.12	18.26 ± 0.59
PKRnc	61.36 ± 14.62	18.76 ± 1.87	91.74 ± 13.54	12.43 ± 0.66
K-252a	48.33 ± 8.51	19.67 ± 1.29	219.70 ± 21.41	24.46 ± 1.18

Data represents the mean ± S.D. of triplicate experiments.

Chapter 6. General Discussion

6.1 General Summary

IP signaling has attracted interest for its suspected roles in different diseases, however, the precise mechanisms of action of IPs remain poorly understood. Control of IP production at different stages of the IP metabolic pathway could be used as an approach to determine the functional roles of each IP. Inositol 1,3,4,5,6-pentakisphosphate 2-kinase (IPK1) phosphorylates IP_5 to IP_6 and is a key enzyme in the production of higher IPs. IP_5 and IP_6 have been implicated in cell death signaling pathways, both *in vitro* and *in vivo*, but their signaling roles are not well-defined.

The overall goal of this thesis was the structural and biochemical characterization of IPK1 with the aims of:

a) Identifying conformational states of IPK1,
b) Defining the roles of phosphate recognition in IP binding and IPK1 activation,
c) Describing the conformational changes and kinase activation of IPK1, and
d) Identifying novel small molecule inhibitors of IPK1.

In Chapter 2, we described the IP-free crystal structure of IPK1, which revealed that the N-lobe of IPK1 is unstable in the absence of IP. This result led us to postulate a new mechanism for IP recognition by IPK1: the IP is initially recognized by the C-lobe of IPK1 through the 4-, 5-, and 6-phosphates, and then N-lobe stabilization is induced by the 1- and 3-phosphates. The interaction between R130 and the 1-phosphate is critical to stabilize the N-lobe for subsequent kinase activation. In Chapter 3, we tested the first half of our hypothesis by investigating the roles of each IP phosphate in IPK1 binding and activation. We showed that the 5- and 6-phosphates were more important than other phosphates for binding, while the 1- and 3-phosphates were most important for IPK1 activation. In Chapter 4, we further validated our hypothesis by describing the link between IPK1 substrate specificity and IPK1 activation. We demonstrated that IPs lacking the 1- or 3-phosphates were unable to stabilize IPK1 to the same extent as IP_5, and that artificial stabilization of the N-lobe altered IPK1 substrate specificity.

In Chapter 5, we identified and characterized small molecule inhibitors of IPK1. We demonstrated that IPK1 was especially sensitive to PKRnc and CG and our evidence indicates IPK1 may possess an allosteric binding site.

In this chapter, we will discuss the relevance of our approaches in the study of the IPK family of kinases and the implications of our findings in context of the field of IP signaling.

6.2 Experimental approaches for IPK characterization

6.2.1 Kinase activity

Assessing kinase activity has been instrumental in determining the substrate specificity for each IPK and simple, rapid, and sensitive platforms for measuring kinase activity are key for development of specific inhibitors for each IPK. Previous characterization of IPK kinase activity has mainly been determined using radiolabeled IPs to track the progression of the kinase reaction. This process involves commercially acquiring IPs that are [^{3}H]-labeled or [^{32}P]-labeled or by synthesizing radiolabeled IPs *in vitro* using purified enzymes (Wilson and Majerus, 1996; Wilson et al., 2001; Choi et al., 2007; Gokhale et al., 2011; Otto et al., 2007). [γ^{32}P]-ATP can also be used as a substrate in kinase reactions, which allows the labeled phosphate to be tracked from ATP to IP (Chamberlain et al., 2007; Gonzalez et al., 2010). The IP products can then be measured by reverse-phase high performance liquid chromatography (HPLC) and the kinetic parameters determined. Alternatively, production of [^{32}P]-labeled IPs can be analyzed by thin-layer chromatography (TLC) using polyethyleneimine-cellulose sheets combined with phosphorimaging (Otto et al., 2007; Endo-Streeter et al., 2012). Both HPLC and TLC approaches require expensive lab equipment, the use of radiation, or are time consuming, thereby limiting their use for high-throughput screening of inhibitors for IPKs. An optical assay coupling ADP formation to NADH consumption via pyruvate kinase and lactate dehydrogenase reactions has also been employed to measure kinase activity of IPKs (Mayr et al., 2005), but this assay requires numerous components in the reaction mix, large reaction volumes, and its accuracy is limited due to optical measurements.

In our work, we used a luminescence-based ATP-depletion kinase assay that quantifies the amount of ATP present in solution following a kinase reaction. There are several advantages to our method to measure kinase activity over previous methods: i) there is no use of radiation, ii) it consists of only one reagent aside from the enzyme and its substrates, which is added to stop the kinase reaction and detect ATP, and iii) a plate reader is the only equipment required to measure ATP. Our approach is reproducible as we obtained comparable K_M and k_{cat} values for wild-type IPK1 by independent measurements in Chapters 3, 4, and 5. In addition, the sensitivity of our assay is in the μM range, which is suitable for measuring kinase activities of other IPKs, whose K_M values also fall within the μM range (Otto et al., 2007). This assay has revealed a clearer picture of the IP selectivity of IPK1. Initial characterization of IPK1 using TLC indicated that IPK1 could not recognize 3,4,5,6-IP_4 as a substrate (Sweetman et al., 2006). In Chapter 3, we were able to detect very low, but measureable IPK1 activity when 3,4,5,6-IP_4 was used as a substrate using our luminescence-based assay, which demonstrates the value of the sensitivity of our assay over other methods. Moreover, in Chapter 5, we used our assay to identify the type of competition for inhibitors of IPK1. Using the same reaction conditions with other IP substrates, other IPKs could easily be screened to assess the specificity of these inhibitors for IPK1.

One shortfall of our assay is the inability to distinguish IP products formed during a kinase reaction. For example, ITPK1 produces both 1,3,4,5-IP_4 and 1,3,4,6-IP_4 from 1,3,4-IP_3 (Balla et al., 1987; Shears et al., 1987; Stephens et al., 1988); however, since only levels of ATP are measured, we can only assess the overall activity of ITPK1, and not the individual activity of ITPK1 towards 1,3,4,5-IP_4 or 1,3,4,6-IP_4 production. This is not an issue with IPK1, however, as IPK1 is able to phosphorylate only the unique axial 2-hydroxyl group, so the identity of the product was not in question. Nevertheless, an inhibitor for any IPK could be characterized using this assay if all kinase activity was inhibited.

6.2.2 Protein stability

In Chapter 4, we used differential scanning fluorimetry (DSF), a type of thermal shift assay, to measure the stability of IPK1 bound to different nucleotides and inositides. To our knowledge, DSF has not been previously used to

characterize any IPK. This approach could be applied to other IPKs that undergo conformational changes during kinase activation. For example, $PPIP_5K$ undergoes substantial conformational changes to accommodate highly phosphorylated IPs as shown by crystal structures of $PPIP_5K$; however, it is unclear from these structures why $PPIP_5K$ displays a preference for 5-PP-IP_5 over IP_6 (Wang et al., 2012). The authors suspected that conformational dynamics may play a role in substrate preference for $PPIP_5K$, as we have shown with IPK1, in Chapter 4 (Wang et al., 2012). DSF could also be used as an alternative to ITC to characterize the binding affinity of ligands, such as IPs or inhibitors, by titrating the concentration of ligand and measuring the T_m (Lea and Simeonov, 2012; Soon et al., 2012). For example, the binding affinity for the inhibitors of IPK1 in Chapter 5 could be measured using DSF. Moreover, the stability of IPK1 in the presence of newly synthesized analogs of inhibitors could be used to develop SARs, since the activity of IPK1 is linked to its overall stability, as we have shown in Chapter 4.

6.3 Roles of the 4- and 6-position phosphates

In Chapter 3, we determined that the 1- and 3-phosphates of the IP substrate were more important for IPK1 activation and the 5- and 6-phosphates of the IP substrate were more important for IP binding. We were unable to investigate the role of the 4-phosphate in IP binding and IPK1 activation as we could not locate a source for 1,3,5,6-IP_4, which lacks the 4-phosphate. Kinase activity of IPK1 alanine mutants revealed that K411A, was sufficient to render IPK1 inactive, while mutations of other 4-phosphate interacting residues, R415 and Y419, impaired kinase activity. We predict that the role of the 4-phosphate is similar to the 5-phosphate, whereby a single mutation in one of the residues that interacts with the 5-phosphate, K170A, also rendered IPK1 inactive. Whether K170 and K411 impact binding affinity to an extent that substrate recognition cannot occur remains to be determined. This would be resolved by performing ITC or DSF with each of the alanine mutants K170A and K411A to determine K_D values with IP_5. Comparison of the K_Ds with wild-type IPK1 would confirm that the lack of substrate recognition for these mutants is attributed to decreased binding affinity.

In Chapter 3, we also observed that 1,3,4,5-IP_4 was not recognized as a substrate by IPK1, suggesting that the 6-phosphate is also important for IPK1

activation. The binding affinity of both 1,3,4,5-IP_4 and 1,3,4,6-IP_4 were similar, but only 1,3,4,6-IP_4 was used as a substrate, so decreased binding affinity did not contribute to the lack of substrate recognition of 1,3,4,6-IP_4. Furthermore, 6-position alanine mutants indicated that intramolecular changes in the 6-phosphate binding site were not essential for IPK1 activation. We postulated that 1,3,4,5-IP_4 may adopt alternative binding orientations, in which the 2-hydroxyl is not accessible for phosphorylation. Alternative binding orientations for IP substrates have been observed for other IPKs (Chamberlain et al., 2007; Miller et al., 2005); however, we have not obtained conclusive evidence to support or refute alternative binding orientations for 1,3,4,5-IP_4 from our studies. Binding isotherms of 1,3,4,5-IP_4 fitted only to a one-site model, which is consistent with the crystal structure of IPK1 that reveals a single IP binding site; however, this model cannot discern between multiple binding orientations that possess varied or comparable binding affinities. We hypothesized that 1,3,4,5-IP_4 may be adopting one or more of three alternative orientations, in which the IP is flipped about the 2'-5' axis, such that the axial 2-hydroxyl is pointing away from the γ-phosphate. We suspected that a quadruple mutant for all 6-phosphate binding residues, IPK1 K170A/K200A/N238A/N239A, would cause the IP to flip back and reorient the 2-hydroxyl towards the γ-phosphate, but no kinase activity was detected with 1,3,4,5-IP_4. Thus, one or both of the two remaining alternative orientations may be preferred. We also focused our efforts on co-crystallization of IPK1 with AMPPNP and 1,3,4,5-IP_4, but these efforts were not successful. We also attempted to soak nucleotide-bound crystals of IPK1 with 1,3,4,5-IP_4, which resulted in partially damaged crystals that produced no diffraction, which was not entirely surprising given the conformational changes we have demonstrated to occur during the transition between IP-free and IP-bound states. Finally, we soaked 1,3,4,5-IP_4 into IPK1 crystals that were grown in complex with ADP and IP_6. Comparison of the electron density between data sets obtained from soaked and unsoaked crystals revealed a loss of density where the 2-phosphate of IP_6 is found, suggesting that soaking of 1,3,4,5-IP_4 was successful; however, occupancies for the five other phosphate binding sites were inconsistent with the predicted set of alternative orientations. Further investigation will be required to ascertain why 1,3,4,5-IP_4 is not recognized as a substrate, but can still bind IPK1.

6.4 Comparison of IP recognition mechanisms of IPKs

In Chapters 2, 3, and 4, we describe and test a hypothesis that IPK1 employs a mechanism of IP-induced stabilization whereby the phosphate profile of IP_5 facilitates IP binding through the 4-, 5-, and 6-phosphates and promotes IPK1 stabilization through the 1- and 3-phosphates. The inositide binding site of IPK1 does not present any steric occlusions to IP phosphate groups or hydroxyl groups as seen in the tightly shaped inositide binding site of IP_3K (Gonzalez et al., 2004; Miller and Hurley, 2004), or the less restrictive inositide binding pocket of IPMK (Holmes and Jogl, 2006; Endo-Streeter et al., 2012). These steric occlusions confer single substrate specificity for IP_3K and enable 6/3/5-kinase activities of IPMK for different IP substrates (Shears, 2004; Endo-Streeter et al., 2012). Like IPK1, ITPK1 does not discriminate between IP substrates based on steric exclusions of phosphate groups or hydroxyl groups of IPs. In ITPK1, hydroxyl groups have no direct contact with ITPK1 side chains, allowing phosphate groups to occupy these positions, so substrate selectivity for ITPK1 is dictated by affinity of phosphate groups, which allows ITPK1 to recognize multiple IP substrates (Miller et al., 2005). However, IPK1 is highly specific for IP_5, so if specificity were dictated solely by phosphate affinity, the large, unhindered inositide-binding site of IPK1 would not be sufficient for discrimination of IPs. A hybrid shape-affinity mechanism of IP recognition has been described for $PPIP_5K$ (Wang et al., 2012). In $PPIP_5K$, the inositide-binding site is precisely shaped to accommodate six or more phosphates of the IP substrate and steric occlusion prevents reorientation of the IP substrate. Moreover, each phosphate group is highly coordinated by multiple $PPIP_5K$ side chains that when mutated, reduce $PPIP_5K$ activity by 90% (Wang et al., 2012). In Chapter 3, we determined that only three side chains of IPK1, R130, K170, and K411 are critical for IP substrate recognition, so the hybrid shape-affinity model is not appropriate for IPK1.

The model of IP-induced stabilization for IP recognition for IPK1 reconciles IPK1's unshaped inositide binding site, capable of binding any monophosphorylated IP and redundant interactions with IP phosphates. The transition of IPK1 from an unstable, IP-free state to a stable, IP-bound state provides a third element of IP discrimination based on enzyme stability. Thus, the unique combination of shape, affinity, and stability, allows IPK1 to be highly

selective for IP_5, over IP_4s and IP_3s, which can undoubtedly fit into the active site of IPK1. Figures 6.1 and 6.2 provide a diagrammatical summary of known IP recognition mechanisms employed by IPKs, depicting i) the topology of each IPK, ii) the relative size and shape of the IP binding site, and iii) orientation of IP substrates to achieve specific kinase activities.

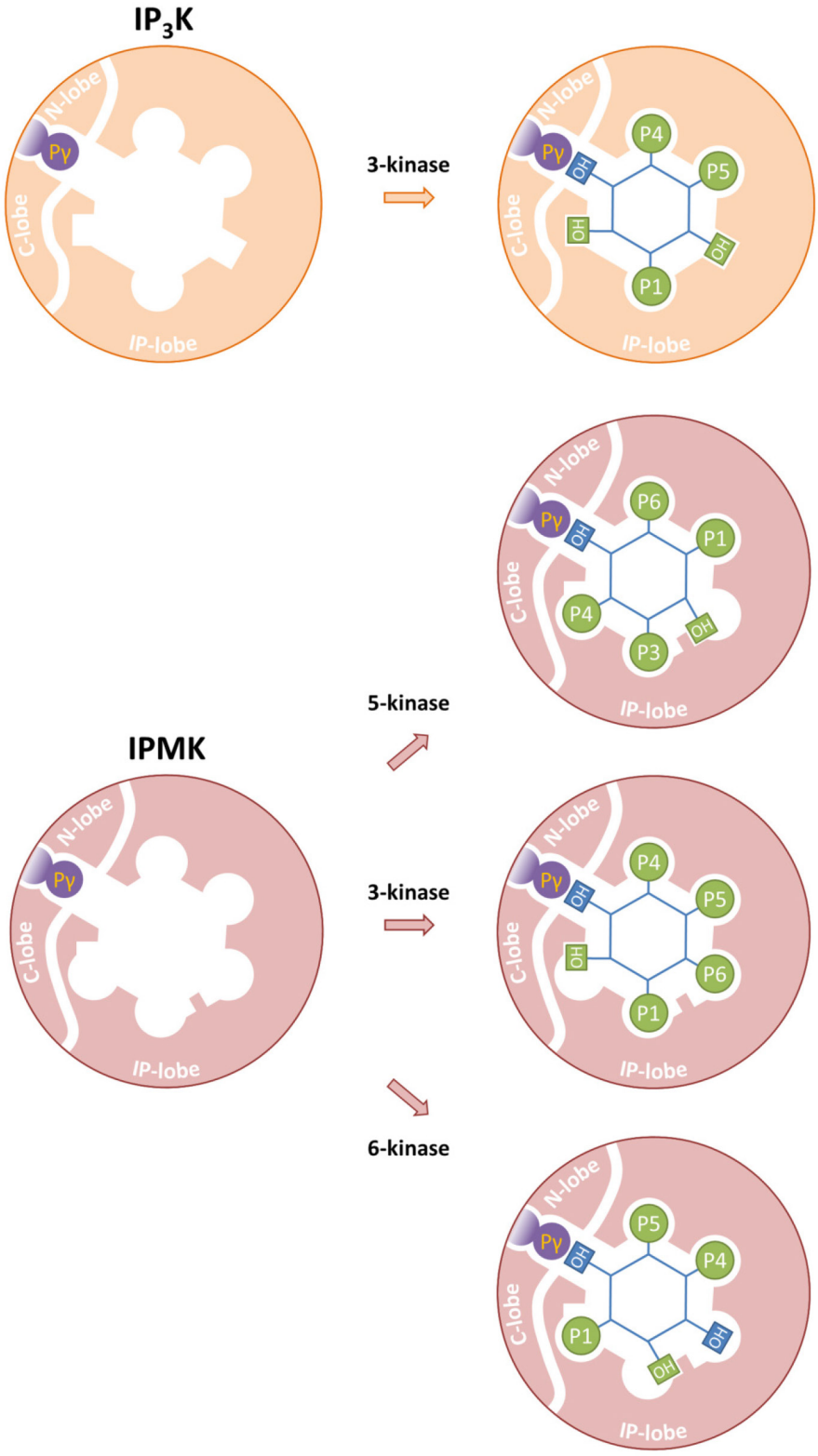

Figure 6.1. IP recognition mechanisms for IP_3K and IPMK. Phosphate and hydroxyl groups that directly interact with the IPK are shown in green, as described in the text.

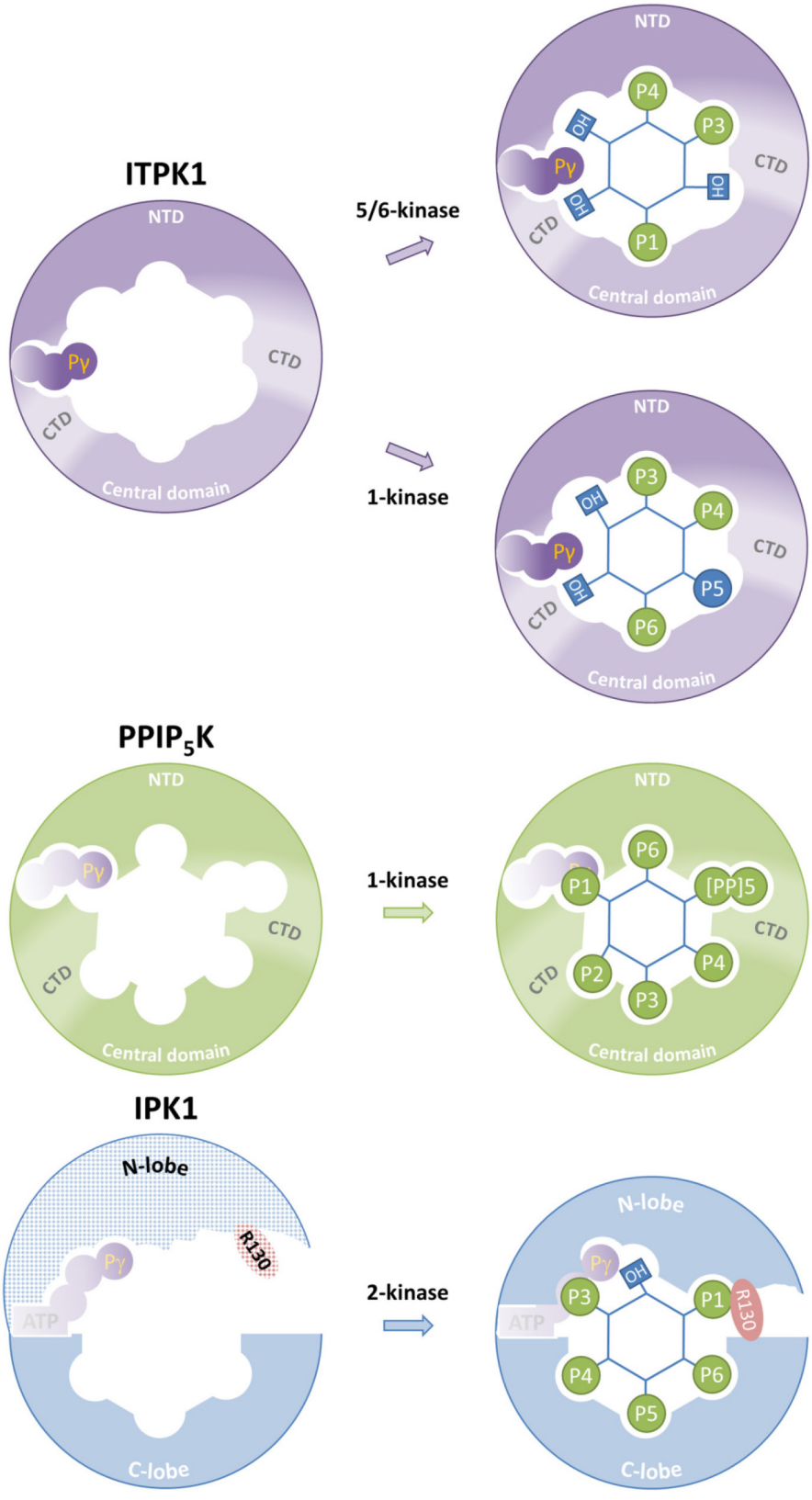

Figure 6.2. IP recognition mechanisms for ITPK1, $PPIP_5K$, and IPK1.

6.5 Considerations for IPK inhibition

The model of IP-induced stabilization of IPK1 adds to our overall knowledge of the IP recognition mechanisms for IPKs and provides a basis for selectively targeting each member of the IPK family. IP substrates of IPKs are very similar, sometimes differing by only one phosphate group, so other features of IPKs need to be considered for selectively targeting IPKs. IPK recognition mechanisms reveal that there are a number of unique characteristics for each IPK that can be exploited. These include the size and shape of the active site, the angle between the nucleotide γ-phosphate and the IP, IPK affinity for different phosphate groups, and allosteric modulation (Table 6.1). For example, an inhibitor occupying the tightly shaped inositide binding site of IP_3K, could still occupy the inositide binding sites of other IPKs, whose IP substrates possess more than three phosphates, like IPMK or IPK1; however, an inhibitor designed for both the nucleotide and inositide binding sites, and that mimics the angle between the nucleotide and inositide, would increase selectivity for IP_3K. In contrast, an inhibitor designed to occupy the unrestricted 6-position in IPMK, would selectivity target IPMK over IP_3K (Endo-Streeter et al., 2012). ITPK1 recognizes its IP substrates based on phosphate affinity, so an inhibitor that blocks high affinity interactions with ITPK1 at the 1-, 3-, and 4-phosphate positions would be favorable for ITPK1 inhibition. In $PPIP_5K$, the active site is shaped to accommodate highly phosphorylated IPs and the angle between ATP and 5-PP-IP_5 is unique among IPKs, both features that could be exploited to selectively inhibit $PPIP_5K$ (Wang et al., 2012). The crystal structure of IP_6K has not yet been solved, but inhibition of IP_6K2 by HSP90 has been demonstrated, which could eventually be used for the design of peptidomimetics to selectively inhibit IP_6K (Chakraborty et al., 2008; Shames and Minna, 2008). In Chapters 3 and 4, we demonstrated that IP substrates are recognized by IPK1, based on their ability to stabilize IPK1, and that N-lobe stability is a precursor for IPK1 activation. Therefore, an inhibitor that occupies the active site of IPK1, without forming interactions with N-lobe residues R45 and R130, would prevent N-lobe stabilization and selectively inhibit IPK1. Moreover, in Chapter 5, we showed that PKRnc and CG were non-competitive with respect to IP_5, and mixed-competitive with respect to ATP, indicating the presence of an allosteric binding site on IPK1. Further characterization of this

allosteric site, either through co-crystallization with PKRnc and CG or docking studies, could also be useful to develop selective inhibitors of IPK1. Taken together, features of IPKs can be used for the rational design of small molecule inhibitors that are selective for a specific IPK.

The possibility that an IPK inhibitor can bind to other proteins that bind the same IP substrates as the target IPK should be considered with inhibition of any IPK. IPs can bind to different proteins, via PH domains or other sites, to modulate their activity or promote protein-protein interactions (Cozier et al., 2000; Millard et al., 2013; Komander et al., 2004; Theibert et al., 1991; Chadwick et al., 1992; Jackson et al., 2011). Careful design of each IPK inhibitor should ensure that other proteins that bind IP substrates are not sensitive to the inhibitor. This can be accomplished by exploiting the IP recognition mechanisms of IPKs, as described above. A pull-down experiment using beads coated with inhibitor and cellular extracts, combined with mass spectrometry, could identify other proteins that may interact with an IPK inhibitor.

IPK	Main Substrate	Kinase activity	Phosphate interactions	Hydroxyl interactions	IP binding site shape	Pγ-IP orientation	IP recognition mechanism	Allosteric modulation	Target for inhibition
IP_3K	1,4,5-IP_3	3	1, 4, 5	2, 3, 6	Fitted	Planar (180°)	Shape complementarity	Stimulation by CaM	Shape/angle
IP_6K	IP_6	5	?	?	?	?	?	Inhibition by HSP90	HSP90 binding site
IPMK	1,3,4,6-IP_4	5/6/3	1, 3, 4, 6	2, 5	Fitted	Planar (180°)	Shape complementarity	No	6-phosphate binding pocket
ITPK1	1,3,4-IP_3	5/6/1	1, 3, 4	none	Loose	Planar (180°)	Phosphate affinity	No	1-, 3-, 4-phosphtate binding pockets
$PPIP_5K$	5-PP-IP_5	1	1, 2, 3, 4, 5, 6	n/a	Fitted	Perpendicular (90°)	Hybrid shape-affinity	?	Shape/angle
IPK1	IP_5	2	1, 3, 4, 5, 6	2	Loose	Angled (45°)	IP-induced stabilization	Yes	a) Allosteric site b) Disrupt N-lobe stabilization

Table 6.1. IPK substrate recognition characteristics. “?” indicates unknown.

6.6 Inhibitor selectivity of IPK1

In Chapter 5, we identified CG and PKRnc, as leads for the development of an inhibitor for IPK1; however, very little information is known about the specificity of these compounds. To date, no specific targets have been identified for CG, but its parent compound, EGCG, is an inhibitor of human topoisomerase II and prolyl-endopeptidases (Kim et al., 2001), and IP_3K also exhibits sensitivity towards EGCG in the nM range (Mayr et al., 2005). As such, CG should be tested with all other IPKs and PKs from different subfamilies to ensure selectivity for IPK1. Moreover, PKRnc has been demonstrated to inhibit 300 different PKs to varying extents; only 12 kinases, from varying subfamilies, exhibited >70% inhibition with PKRnc (Anastassiadis et al., 2011), but IPKs have yet to be tested for their sensitivity towards PKRnc.

In our studies, we showed that EGCG analogs composed of catechin and gallate, which have two chemical "arms" were more potent than analogs composed of only catechin with its one "arm;" however, we did not test any chemical modifications of CG, or enhance specificity for IPK1. Analogs of PKRnc should be tested as well. In our kinase inhibitor library, there are 10 other compounds that possess a 2-oxindole scaffold like PKRnc, but only PKRnc inhibited IPK1, indicating that the 3-position carbon could be modified to improve inhibitor specificity for IPK1.

Our competition studies in Chapter 5 suggested that alternative binding sites for inhibitors may be present on IPK1. Characterizing the binding sites of inhibitors could be used to improve inhibitor specificity by tailoring the inhibitor for the binding site. Structures of four different proteins in complex with EGCG have been deposited in the Protein Data Bank (2KDH, 3NGS, 3OOB, 4AWM), which indicate that EGCG, and likely CG, binding occurs primarily on hydrophobic regions, but these proteins do not possess any structural similarity to IPK1 that could be used to predict the binding site of either EGCG or CG on IPK1. Molecular docking studies could be used to identify alternative binding sites on IPK1 and dock the structures of CG or PKRnc to IPK1. Introducing mutations in combination with our activity assays or binding assays would then validate these results. Alternatively, ^{15}N HSQC studies (NMR) could be performed to determine the interactions between IPK1 and inhibitor. Ultimately, co-crystallization of IPK1

with inhibitors would be most useful to determine the binding sites of CG and PKRnc on IPK1. We showed that CG and PKRnc are non-competitive with respect to IP_5, and mixed-competitive with respect to ATP, therefore, crystallization trials should be carried out with IPK1 in the presence of Mg^{2+}, IP_5, AMPPNP, and inhibitor.

6.7 Exploring the role of IPK1 and higher IPs

Previous studies have revealed a role for IPK1 in cell death. IPK1 overexpression protects cells from TNFα-mediated and Fas-induced apoptosis (Verbsky and Majerus, 2005), while knockdown of IPK1 sensitizes cells to the chemotherapeutic agents cisplatin and etoposide (Piccolo et al., 2004). Moreover, both IP_5 and IP_6 promote cell death *in vitro* and *in vivo*, which seem to contradict conclusions from IPK1 overexpression and knockdown studies (Piccolo et al., 2004; Maffucci et al., 2005; Vucenik and Shamsuddin, 2003; Shi et al., 2006). These inconsistencies into the role of IPK1 in cell death may arise due to overexpression and knockdown studies of IPK1 that do not discriminate between catalytic and non-catalytic roles of IPK1 (Brehm et al., 2013). Moreover, treatment of cells with non-physiological concentrations of IP_5 or IP_6 can disrupt IP levels in different compartments within the cell due to IP diffusion through cellular membranes (Miller et al., 2004). It is hypothesized that the intracellular localization of IPK1 is necessary for maintenance of localized and specific IP profiles which contributes to its cellular functions (Brehm et al., 2007). Therefore, a chemical inhibitor of IPK1 would be useful to modulate local levels of IP_5 and IP_6 and elucidate the specific roles of IPK1.

Current studies suggest that IP_5 and IP_6 may be eliciting their pro-apoptotic mechanism of action through the PI3K/PDK1/Akt pathway (Komander et al., 2004; Gu et al., 2010) and/or the Fas death receptor pathway (Verbsky and Majerus, 2005), both of which are extrinsic pathways for apoptotic signaling (Taylor et al., 2008). Therefore, changes in these pathways during induction of apoptosis could be determined in the presence or absence of IPK1 inhibitor to further characterize the role of IPK1 in cell death. IPK1 may also possess a role in the activation of the intrinsic apoptosis pathway that is activated upon DNA damage (Taylor et al., 2008), since IPK1 is localized in the nucleus (Brehm et al.,

2007) and chemotherapeutic agents used to induce apoptosis in previous studies function in the nucleus (Piccolo et al., 2004).

IPK1 also possesses a developmental role as IPK1 null mice display embryonic lethality (Verbsky et al., 2005b), but the underyling mechanisms are unknown. Accumulation of IP_5 was also observed upon stimulation of the Wnt/β-catenin pathway, which regulates embryonic development (Gao and Wang, 2007; Kim et al., 2013), suggesting a link between IPK1 and Wnt signaling. Inhibition of IPK1 during embryonic development would help to clarify the role of IPK1 in this process.

Finally, the diverse functions of PP-IPs could be further investigated through inhibition of IPK1, since a substantial amount of the PP-IPs are produced from IP_6 (Glennon and Shears, 1993; Menniti et al., 1993). Protein pyrophosphorylation by PP-IPs is also a poorly characterized mechanism, which could be better understood through attenuation of levels of PP-IPs (Saiardi et al., 2004).

6.8 Proposed reclassification of IPKs

IPKs are currently organized into three subfamilies according to their sequence similarity and structural homology (see section 1.8). Our structural and biochemical studies of IPK1 now indicate that IPK1 is more similar to inositol polyphosphate kinases than previously thought, and that IPK1 shares many features with PKs. IPK1 possesses an N-lobe, with an α+β fold, and a C-lobe connected by a hinge, and a glycine rich loop and aspartic acid residue coordinating the nucleotide and its phosphates like PKs (Madhusudan et al., 1994). Moreover, stabilization of the N- and C-lobes of IPK1 are a precursor to IPK1 activation, as observed with PKs (Ozkirimli and Post, 2006; Ubersax and Ferrell, 2007). Finally, IPK1 showed high sensitivity to both STS and K-252a, well known promiscuous PK inhibitors (Anastassiadis et al., 2011). We therefore propose that IPKs be classified into two subfamilies: the PK-like subfamily, consisting of IP_3K, IPMK, IP_6K, and IPK1 and the ATP-grasp fold subfamily, consisting of ITPK1 and $PPIP_5K$ (Figure 6.3) to accurately reflect the structural homology among IPKs.

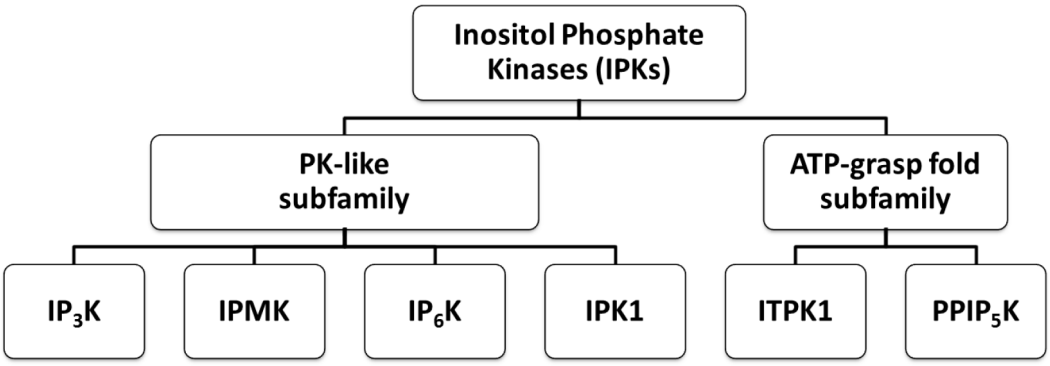

Figure 6.3. Proposed reclassification of IPKs.

Conclusions

The cellular events mediated by IP signaling are poorly understood, largely due to the lack of tools to attenuate production of specific IPs to discover their functional importance. The work presented in this thesis builds a foundation for the study of individual IPKs and the IPs that they produce using selective inhibition of IPKs as an approach. We focused on the structural and biochemical characterization of IPK1, a critical enzyme involved in the production of higher IPs that are implicated in cell death. In Chapter 2, we hypothesized that IPK1 employs a mechanism of IP-induced stabilization to select IP_5 as its substrate. In Chapters 3 and 4, we validated our proposed mechanism by determining the role of each phosphate of the IP substrate on binding affinity and IPK1 activation, and describing the conformational dynamics of IPK1 activation. These studies allowed us to compare the mechanisms of IP recognition for members of the IPK family, which provide considerations for the selective inhibition of each IPK. In Chapter 5, we identified PKRnc and Catechin Gallate as novel small molecule inhibitors of IPK1, which operate through an as yet undefined allosteric mechanism. Taken together, our studies provide a basis for the development of selective inhibitors for IPK1 to investigate the roles of higher IPs that modulate apoptotic signaling pathways. Ultimately, uncovering the role of IPs in different cellular processes may lead to novel treatments for diseases whose underlying mechanisms are mediated by IP signaling.

References

Adams, PD, Afonine, PV, Bunkoczi, G, Chen, VB, Davis, IW, Echols, N, Headd, JJ, Hung, LW, Kapral, GJ, Grosse-Kunstleve, RW, McCoy, AJ, Moriarty, NW, Oeffner, R, Read, RJ, Richardson, DC, Richardson, JS, Terwilliger, TC, Zwart, PH (2010) PHENIX: a comprehensive Python-based system for macromolecular structure solution. Acta Crystallogr D Biol Crystallogr. 66:213-221.

Agarwal, C, Dhanalakshmi, S, Singh, RP, Agarwal, R (2003) Inositol hexaphosphate inhibits constitutive activation of NF- kappa B in androgen-independent human prostate carcinoma DU145 cells. Anticancer Res. 23:3855-3861.

Agarwal, R, Mumtaz, H, Ali, N (2009) Role of inositol polyphosphates in programmed cell death. Mol Cell Biochem. 328:155-165.

Agranoff, B (1978) Textbook errors: Cyclitol confusion. Trends in Biochemical Sciences. 3:N283-N285.

Albert, C, Safrany, ST, Bembenek, ME, Reddy, KM, Reddy, K, Falck, J, Brocker, M, Shears, SB, Mayr, GW (1997) Biological variability in the structures of diphosphoinositol polyphosphates in Dictyostelium discoideum and mammalian cells. Biochem J. 327:553-560.

Alcazar-Roman, AR, Tran, EJ, Guo, S, Wente, SR (2006) Inositol hexakisphosphate and Gle1 activate the DEAD-box protein Dbp5 for nuclear mRNA export. Nat Cell Biol. 8:711-716.

Alcazar-Roman, AR, Bolger, TA, Wente, SR (2010) Control of mRNA export and translation termination by inositol hexakisphosphate requires specific interaction with Gle1. J Biol Chem. 285:16683-16692.

Anastassiadis, T, Deacon, SW, Devarajan, K, Ma, H, Peterson, JR (2011) Comprehensive assay of kinase catalytic activity reveals features of kinase inhibitor selectivity. Nat Biotechnol. 29:1039-1045.

Anraku, K, Inoue, T, Sugimoto, K, Kudo, K, Okamoto, Y, Morii, T, Mori, Y, Otsuka, M (2011) Design and synthesis of biotinylated inositol 1,3,4,5-tetrakisphosphate targeting Grp1 pleckstrin homology domain. Bioorg Med Chem. 19:6833-6841.

Artymiuk, PJ, Poirrette, AR, Rice, DW, Willett, P (1996) Biotin carboxylase comes into the fold. Nat Struct Biol. 3:128-132.

Azevedo, C, Burton, A, Ruiz-Mateos, E, Marsh, M, Saiardi, A (2009) Inositol pyrophosphate mediated pyrophosphorylation of AP3B1 regulates HIV-1 Gag release. Proc Natl Acad Sci U S A. 106:21161-21166.

Balla, T, Guillemette, G, Baukal, AJ, Catt, KJ (1987) Formation of inositol 1,3,4,6-tetrakisphosphate during angiotensin II action in bovine adrenal glomerulosa cells. Biochem Biophys Res Commun. 148:199-205.

Banos-Sanz, JI, Sanz-Aparicio, J, Whitfield, H, Hamilton, C, Brearley, CA, Gonzalez, B (2012) Conformational changes in inositol 1,3,4,5,6-pentakisphosphate 2-kinase upon substrate binding: role of N-terminal lobe and enantiomeric substrate preference. J Biol Chem. 287:29237-29249.

Barker, CJ, Illies, C, Gaboardi, GC, Berggren, PO (2009) Inositol pyrophosphates: structure, enzymology and function. Cell Mol Life Sci. 66:3851-3871.

Batty, IH, Downes, CP (1994) The inhibition of phosphoinositide synthesis and muscarinic-receptor-mediated phospholipase C activity by Li+ as secondary, selective, consequences of inositol depletion in 1321N1 cells. Biochem J. 297:529-537.

Batty, IH, Currie, RA, Downes, CP (1998) Evidence for a model of integrated inositol phospholipid pools implies an essential role for lipid transport in the maintenance of receptor-mediated phospholipase C activity in 1321N1 cells. Biochem J. 330:1069-1077.

Batty, IR, Nahorski, SR, Irvine, RF (1985) Rapid formation of inositol 1,3,4,5-tetrakisphosphate following muscarinic receptor stimulation of rat cerebral cortical slices. Biochem J. 232:211-215.

Bennett, M, Onnebo, SM, Azevedo, C, Saiardi, A (2006) Inositol pyrophosphates: metabolism and signaling. Cell Mol Life Sci. 63:552-564.

Berridge, MJ (1993) Inositol trisphosphate and calcium signalling. Nature. 361:315-325.

Bezprozvanny, I, Hayden, MR (2004) Deranged neuronal calcium signaling and Huntington disease. Biochem Biophys Res Commun. 322:1310-1317.

Bhandari, R, Saiardi, A, Ahmadibeni, Y, Snowman, AM, Resnick, AC, Kristiansen, TZ, Molina, H, Pandey, A, Werner, JK, Jr., Juluri, KR, Xu, Y, Prestwich, GD, Parang, K, Snyder, SH (2007) Protein pyrophosphorylation by inositol pyrophosphates is a posttranslational event. Proc Natl Acad Sci U S A. 104:15305-15310.

Bhandari, R, Juluri, KR, Resnick, AC, Snyder, SH (2008) Gene deletion of inositol hexakisphosphate kinase 1 reveals inositol pyrophosphate regulation of insulin secretion, growth, and spermiogenesis. Proc Natl Acad Sci U S A. 105:2349-2353.

Bird, GS, Obie, JF, Putney, JW, Jr. (1992) Sustained Ca2+ signaling in mouse lacrimal acinar cells due to photolysis of "caged" glycerophosphoryl-myo-inositol 4,5-bisphosphate. J Biol Chem. 267:17722-17725.

Bird, GS, Putney, JW, Jr. (1996) Effect of inositol 1,3,4,5-tetrakisphosphate on inositol trisphosphate-activated Ca2+ signaling in mouse lacrimal acinar cells. J Biol Chem. 271:6766-6770.

Boynton, AL, Dean, NM, Hill, TD (1990) Inositol 1,3,4,5-tetrakisphosphate and regulation of intracellular calcium. Biochem Pharmacol. 40:1933-1939.

Bozsik, A, Kokeny, S, Olah, E (2007) Molecular mechanisms for the antitumor activity of inositol hexakisphosphate (IP6). Cancer Genomics Proteomics. 4:43-51.

Brehm, MA, Schenk, TM, Zhou, X, Fanick, W, Lin, H, Windhorst, S, Nalaskowski, MM, Kobras, M, Shears, SB, Mayr, GW (2007) Intracellular localization of human Ins(1,3,4,5,6)P5 2-kinase. Biochem J. 408:335-345.

Brehm, MA, Wundenberg, T, Williams, J, Mayr, GW, Shears, SB (2013) A non-catalytic role for inositol 1,3,4,5,6-pentakisphosphate 2-kinase in the synthesis of ribosomal RNA. J Cell Sci. 126:437-444.

Brough, D, Bhatti, F, Irvine, RF (2005) Mobility of proteins associated with the plasma membrane by interaction with inositol lipids. J Cell Sci. 118:3019-3025.

Caffrey, JJ, Darden, T, Wenk, MR, Shears, SB (2001) Expanding coincident signaling by PTEN through its inositol 1,3,4,5,6-pentakisphosphate 3-phosphatase activity. FEBS Lett. 499:6-10.

Carew, MA, Yang, X, Schultz, C, Shears, SB (2000) myo-inositol 3,4,5,6-tetrakisphosphate inhibits an apical calcium-activated chloride conductance in polarized monolayers of a cystic fibrosis cell line. J Biol Chem. 275:26906-26913.

Chadwick, CC, Timerman, AP, Saito, A, Mayrleitner, M, Schindler, H, Fleischer, S (1992) Structural and functional characterization of an inositol polyphosphate receptor from cerebellum. J Biol Chem. 267:3473-3481.

Chakraborty, A, Koldobskiy, MA, Sixt, KM, Juluri, KR, Mustafa, AK, Snowman, AM, van Rossum, DB, Patterson, RL, Snyder, SH (2008) HSP90 regulates cell survival via inositol hexakisphosphate kinase-2. Proc Natl Acad Sci U S A. 105:1134-1139.

Chamberlain, PP, Qian, X, Stiles, AR, Cho, J, Jones, DH, Lesley, SA, Grabau, EA, Shears, SB, Spraggon, G (2007) Integration of inositol phosphate signaling pathways via human ITPK1. J Biol Chem. 282:28117-28125.

Chang, SC, Miller, AL, Feng, Y, Wente, SR, Majerus, PW (2002) The human homolog of the rat inositol phosphate multikinase is an inositol 1,3,4,6-tetrakisphosphate 5-kinase. J Biol Chem. 277:43836-43843.

Chang, SC, Majerus, PW (2006) Inositol polyphosphate multikinase regulates inositol 1,4,5,6-tetrakisphosphate. Biochem Biophys Res Commun. 339:209-216.

Cheek, S, Ginalski, K, Zhang, H, Grishin, NV (2005) A comprehensive update of the sequence and structure classification of kinases. BMC Struct Biol. 5:6.

Cheung, JC, Salerno, B, Hanakahi, LA (2008) Evidence for an inositol hexakisphosphate-dependent role for Ku in mammalian nonhomologous end joining that is independent of its role in the DNA-dependent protein kinase. Nucleic Acids Res. 36:5713-5726.

Choi, JH, Williams, J, Cho, J, Falck, JR, Shears, SB (2007) Purification, sequencing, and molecular identification of a mammalian PP-InsP5 kinase that is activated when cells are exposed to hyperosmotic stress. J Biol Chem. 282:30763-30775.

Coates, ML (1975) Hemoglobin function in the vertebrates: an evolutionary model. J Mol Evol. 6:285-307.

Communi, D, Vanweyenberg, V, Erneux, C (1995) Molecular study and regulation of D-myo-inositol 1,4,5-trisphosphate 3-kinase. Cell Signal. 7:643-650.

Connolly, TM, Bansal, VS, Bross, TE, Irvine, RF, Majerus, PW (1987) The metabolism of tris- and tetraphosphates of inositol by 5-phosphomonoesterase and 3-kinase enzymes. J Biol Chem. 262:2146-2149.

Cozier, GE, Lockyer, PJ, Reynolds, JS, Kupzig, S, Bottomley, JR, Millard, TH, Banting, G, Cullen, PJ (2000) GAP1IP4BP contains a novel group I pleckstrin homology domain that directs constitutive plasma membrane association. J Biol Chem. 275:28261-28268.

Crossley, I, Swann, K, Chambers, E, Whitaker, M (1988) Activation of sea urchin eggs by inositol phosphates is independent of external calcium. Biochem J. 252:257-262.

Cullen, PJ, Hsuan, JJ, Truong, O, Letcher, AJ, Jackson, TR, Dawson, AP, Irvine, RF (1995) Identification of a specific Ins(1,3,4,5)P4-binding protein as a member of the GAP1 family. Nature. 376:527-530.

Currie, RA, Walker, KS, Gray, A, Deak, M, Casamayor, A, Downes, CP, Cohen, P, Alessi, DR, Lucocq, J (1999) Role of phosphatidylinositol 3,4,5-trisphosphate in regulating the activity and localization of 3-phosphoinositide-dependent protein kinase-1. Biochem J. 337 (Pt 3):575-583.

Dewaste, V, Moreau, C, De Smedt, F, Bex, F, De Smedt, H, Wuytack, F, Missiaen, L, Erneux, C (2003) The three isoenzymes of human inositol-1,4,5-trisphosphate 3-kinase show specific intracellular localization but

comparable Ca2+ responses on transfection in COS-7 cells. Biochem J. 374:41-49.

Di Cristofano, A, Pandolfi, PP (2000) The multiple roles of PTEN in tumor suppression. Cell. 100:387-390.

Dombkowski, AA (2003) Disulfide by Design: a computational method for the rational design of disulfide bonds in proteins. Bioinformatics. 19:1852-1853.

Draskovic, P, Saiardi, A, Bhandari, R, Burton, A, Ilc, G, Kovacevic, M, Snyder, SH, Podobnik, M (2008) Inositol hexakisphosphate kinase products contain diphosphate and triphosphate groups. Chem Biol. 15:274-286.

Eckmann, L, Rudolf, MT, Ptasznik, A, Schultz, C, Jiang, T, Wolfson, N, Tsien, R, Fierer, J, Shears, SB, Kagnoff, MF, Traynor-Kaplan, AE (1997) D-myo-Inositol 1,4,5,6-tetrakisphosphate produced in human intestinal epithelial cells in response to Salmonella invasion inhibits phosphoinositide 3-kinase signaling pathways. Proc Natl Acad Sci U S A. 94:14456-14460.

Efanov, AM, Zaitsev, SV, Berggren, PO (1997) Inositol hexakisphosphate stimulates non-Ca2+-mediated and primes Ca2+-mediated exocytosis of insulin by activation of protein kinase C. Proc Natl Acad Sci U S A. 94:4435-4439.

Emsley, P, Cowtan, K (2004) Coot: model-building tools for molecular graphics. Acta Crystallogr D Biol Crystallogr. 60:2126-2132.

Endo-Streeter, S, Tsui, MK, Odom, AR, Block, J, York, JD (2012) Structural studies and protein engineering of inositol phosphate multikinase. J Biol Chem. 287:35360-35369.

Feng, Y, Wente, SR, Majerus, PW (2001) Overexpression of the inositol phosphatase SopB in human 293 cells stimulates cellular chloride influx and inhibits nuclear mRNA export. Proc Natl Acad Sci U S A. 98:875-879.

Fukuda, M, Mikoshiba, K (1996) Structure-function relationships of the mouse Gap1m. Determination of the inositol 1,3,4,5-tetrakisphosphate-binding domain. J Biol Chem. 271:18838-18842.

Gao, Y, Wang, HY (2006) Casein kinase 2 Is activated and essential for Wnt/beta-catenin signaling. J Biol Chem. 281:18394-18400.

Gao, Y, Wang, HY (2007) Inositol pentakisphosphate mediates Wnt/beta-catenin signaling. J Biol Chem. 282:26490-26502.

Glennon, MC, Shears, SB (1993) Turnover of inositol pentakisphosphates, inositol hexakisphosphate and diphosphoinositol polyphosphates in primary cultured hepatocytes. Biochem J. 293:583-590.

Gokhale, NA, Zaremba, A, Shears, SB (2011) Receptor-dependent compartmentalization of PPIP5K1, a kinase with a cryptic polyphosphoinositide binding domain. Biochem J. 434:415-426.

Gonzalez, B, Schell, MJ, Letcher, AJ, Veprintsev, DB, Irvine, RF, Williams, RL (2004) Structure of a human inositol 1,4,5-trisphosphate 3-kinase: substrate binding reveals why it is not a phosphoinositide 3-kinase. Mol Cell. 15:689-701.

Gonzalez, B, Banos-Sanz, JI, Villate, M, Brearley, CA, Sanz-Aparicio, J (2010) Inositol 1,3,4,5,6-pentakisphosphate 2-kinase is a distant IPK member with a singular inositide binding site for axial 2-OH recognition. Proc Natl Acad Sci U S A. 107:9608-9613.

Goodison, WV, Frisardi, V, Kehoe, PG (2012) Calcium channel blockers and Alzheimer's disease: potential relevance in treatment strategies of metabolic syndrome. J Alzheimers Dis. 30 Suppl 2:S269-282.

Gosein, V, Leung, TF, Krajden, O, Miller, GJ (2012) Inositol phosphate-induced stabilization of inositol 1,3,4,5,6-pentakisphosphate 2-kinase and its role in substrate specificity. Protein Sci. 21:737-742.

Gosein, V, Miller, GJ (2013) Roles of phosphate recognition in inositol 1,3,4,5,6-pentakisphosphate 2-kinase (IPK1) substrate binding and activation. J Biol Chem. 288:26908-26913.

Gu, M, Raina, K, Agarwal, C, Agarwal, R (2010) Inositol hexaphosphate downregulates both constitutive and ligand-induced mitogenic and cell survival signaling, and causes caspase-mediated apoptotic death of human prostate carcinoma PC-3 cells. Mol Carcinog. 49:1-12.

Guse, AH, Emmrich, F (1991) T-cell receptor-mediated metabolism of inositol polyphosphates in Jurkat T-lymphocytes. Identification of a D-myo-inositol 1,2,3,4,6-pentakisphosphate-2-phosphomonoesterase activity, a D-myo-inositol 1,3,4,5,6-pentakisphosphate-1/3-phosphatase activity and a D/L-myo-inositol 1,2,4,5,6-pentakisphosphate-1/3-kinase activity. J Biol Chem. 266:24498-24502.

Hanakahi, LA, Bartlet-Jones, M, Chappell, C, Pappin, D, West, SC (2000) Binding of inositol phosphate to DNA-PK and stimulation of double-strand break repair. Cell. 102:721-729.

Hawkins, PT, Poyner, DR, Jackson, TR, Letcher, AJ, Lander, DA, Irvine, RF (1993) Inhibition of iron-catalysed hydroxyl radical formation by inositol polyphosphates: a possible physiological function for myo-inositol hexakisphosphate. Biochem J. 294:929-934.

He, Y, Swaminathan, A, Lopes, JM (2012) Transcription regulation of the Saccharomyces cerevisiae PHO5 gene by the Ino2p and Ino4p basic helix-loop-helix proteins. Mol Microbiol. 83:395-407.

Hermosura, MC, Takeuchi, H, Fleig, A, Riley, AM, Potter, BV, Hirata, M, Penner, R (2000) InsP4 facilitates store-operated calcium influx by inhibition of InsP3 5-phosphatase. Nature. 408:735-740.

Heslop, JP, Irvine, RF, Tashjian, AH, Jr., Berridge, MJ (1985) Inositol tetrakis- and pentakisphosphates in GH4 cells. J Exp Biol. 119:395-401.

Hill, TD, Dean, NM, Boynton, AL (1988) Inositol 1,3,4,5-tetrakisphosphate induces Ca2+ sequestration in rat liver cells. Science. 242:1176-1178.

Hilton, JM, Plomann, M, Ritter, B, Modregger, J, Freeman, HN, Falck, JR, Krishna, UM, Tobin, AB (2001) Phosphorylation of a synaptic vesicle-associated protein by an inositol hexakisphosphate-regulated protein kinase. J Biol Chem. 276:16341-16347.

Ho, MW, Kaetzel, MA, Armstrong, DL, Shears, SB (2001) Regulation of a human chloride channel. a paradigm for integrating input from calcium, type ii calmodulin-dependent protein kinase, and inositol 3,4,5,6-tetrakisphosphate. J Biol Chem. 276:18673-18680.

Ho, MW, Yang, X, Carew, MA, Zhang, T, Hua, L, Kwon, YU, Chung, SK, Adelt, S, Vogel, G, Riley, AM, Potter, BV, Shears, SB (2002) Regulation of Ins(3,4,5,6)P(4) signaling by a reversible kinase/phosphatase. Curr Biol. 12:477-482.

Ho, MWY, Shears, SB (2002) Regulation of calcium-activated chloride channels by inositol 3,4,5,6-tetrakisphosphate. In Current Topics in Membranes. C. M. Fuller. London, Academic Press. 53:345-363.

Holmes, W, Jogl, G (2006) Crystal structure of inositol phosphate multikinase 2 and implications for substrate specificity. J Biol Chem. 281:38109-38116.

Hoy, M, Efanov, AM, Bertorello, AM, Zaitsev, SV, Olsen, HL, Bokvist, K, Leibiger, B, Leibiger, IB, Zwiller, J, Berggren, PO, Gromada, J (2002) Inositol hexakisphosphate promotes dynamin I- mediated endocytosis. Proc Natl Acad Sci U S A. 99:6773-6777.

Huang, YH, Sauer, K (2010) Lipid signaling in T-cell development and function. Cold Spring Harb Perspect Biol. 2:a002428.

Huse, M, Kuriyan, J (2002) The conformational plasticity of protein kinases. Cell. 109:275-282.

Irvine, RF (1986) Calcium transients: mobilization of intracellular Ca2+. Br Med Bull. 42:369-374.

Irvine, RF, Letcher, AJ, Heslop, JP, Berridge, MJ (1986) The inositol tris/tetrakisphosphate pathway--demonstration of Ins(1,4,5)P3 3-kinase activity in animal tissues. Nature. 320:631-634.

Irvine, RF, Moor, RM (1987) Inositol(1,3,4,5)tetrakisphosphate-induced activation of sea urchin eggs requires the presence of inositol trisphosphate. Biochem Biophys Res Commun. 146:284-290.

Irvine, RF (1992) Is inositol tetrakisphosphate the second messenger that controls Ca2+ entry into cells? Adv Second Messenger Phosphoprotein Res. 26:161-185.

Irvine, RF, Schell, MJ (2001) Back in the water: the return of the inositol phosphates. Nat Rev Mol Cell Biol. 2:327-338.

Irvine, RF (2005) Inositide evolution - towards turtle domination? J Physiol. 566:295-300.

Isaacks, RE, Harkness, DR, Witham, PR (1978) Relationship between the major phosphorylated metabolic intermediates and oxygen affinity of whole blood in the loggerhead (Caretta caretta) and the Green Sea Turtle (Chelonia mydas) during development. Dev Biol. 62:344-353.

Isaacks, RE, Lai, LL, Goldman, PH, Kim, CY (1987) Studies on avian erythrocyte metabolism. XVI. Accumulation of 2,3-bisphosphoglycerate with shifts in oxygen affinity of chicken erythrocytes. Arch Biochem Biophys. 257:177-185.

Ismailov, II, Fuller, CM, Berdiev, BK, Shlyonsky, VG, Benos, DJ, Barrett, KE (1996) A biologic function for an "orphan" messenger: D-myo-inositol 3,4,5,6-tetrakisphosphate selectively blocks epithelial calcium-activated chloride channels. Proc Natl Acad Sci U S A. 93:10505-10509.

IUPAC (1976) IUPAC Commission on the Nomenclature of Organic Chemistry (CNOC) and IUPAC-IUB Commission on Biochemical Nomenclature (CBN). Nomenclature of cyclitols. Recommendations, 1973. Biochem J. 153:23-31.

Ives, EB, Nichols, J, Wente, SR, York, JD (2000) Biochemical and functional characterization of inositol 1,3,4,5, 6-pentakisphosphate 2-kinases. J Biol Chem. 275:36575-36583.

Ivorra, I, Gigg, R, Irvine, RF, Parker, I (1991) Inositol 1,3,4,6-tetrakisphosphate mobilizes calcium in Xenopus oocytes with high potency. Biochem J. 273:317-321.

Jackson, S, Al-Saigh, S, Schultz, C, Junop, M (2011) Inositol pentakisphosphate isomers bind PH domains with varying specificity and inhibit phosphoinositide interactions. BMC Struct Biol. 11:11.

Jagadeesh, S, Banerjee, PP (2006) Inositol hexaphosphate represses telomerase activity and translocates TERT from the nucleus in mouse and human prostate cancer cells via the deactivation of Akt and PKCalpha. Biochem Biophys Res Commun. 349:1361-1367.

Jammi, NV, Whitby, LR, Beal, PA (2003) Small molecule inhibitors of the RNA-dependent protein kinase. Biochem Biophys Res Commun. 308:50-57.

Jia, Y, Subramanian, KK, Erneux, C, Pouillon, V, Hattori, H, Jo, H, You, J, Zhu, D, Schurmans, S, Luo, HR (2007) Inositol 1,3,4,5-tetrakisphosphate negatively regulates phosphatidylinositol-3,4,5- trisphosphate signaling in neutrophils. Immunity. 27:453-467.

Kamimura, J, Wakui, K, Kadowaki, H, Watanabe, Y, Miyake, K, Harada, N, Sakamoto, M, Kinoshita, A, Yoshiura, K, Ohta, T, Kishino, T, Ishikawa, M, Kasuga, M, Fukushima, Y, Niikawa, N, Matsumoto, N (2004) The IHPK1 gene is disrupted at the 3p21.31 breakpoint of t(3;9) in a family with type 2 diabetes mellitus. J Hum Genet. 49:360-365.

Karni, R, Mizrachi, S, Reiss-Sklan, E, Gazit, A, Livnah, O, Levitzki, A (2003) The pp60c-Src inhibitor PP1 is non-competitive against ATP. FEBS Letters. 537:47-52.

Kase, H, Iwahashi, K, Nakanishi, S, Matsuda, Y, Yamada, K, Takahashi, M, Murakata, C, Sato, A, Kaneko, M (1987) K-252 compounds, novel and potent inhibitors of protein kinase C and cyclic nucleotide-dependent protein kinases. Biochem Biophys Res Commun. 142:436-440.

Kavran, JM, Klein, DE, Lee, A, Falasca, M, Isakoff, SJ, Skolnik, EY, Lemmon, MA (1998) Specificity and promiscuity in phosphoinositide binding by pleckstrin homology domains. J Biol Chem. 273:30497-30508.

Kim, JH, Kim, SI, Song, KS (2001) Prolyl endopeptidase inhibitors from green tea. Arch Pharm Res. 24:292-296.

Kim, W, Kim, M, Jho, EH (2013) Wnt/beta-catenin signalling: from plasma membrane to nucleus. Biochem J. 450:9-21.

Knighton, DR, Zheng, JH, Ten Eyck, LF, Xuong, NH, Taylor, SS, Sowadski, JM (1991) Structure of a peptide inhibitor bound to the catalytic subunit of cyclic adenosine monophosphate-dependent protein kinase. Science. 253:414-420.

Komander, D, Fairservice, A, Deak, M, Kular, GS, Prescott, AR, Peter Downes, C, Safrany, ST, Alessi, DR, van Aalten, DM (2004) Structural insights into the regulation of PDK1 by phosphoinositides and inositol phosphates. EMBO J. 23:3918-3928.

Larsson, O, Barker, CJ, Sjoholm, A, Carlqvist, H, Michell, RH, Bertorello, A, Nilsson, T, Honkanen, RE, Mayr, GW, Zwiller, J, Berggren, PO (1997) Inhibition of phosphatases and increased Ca2+ channel activity by inositol hexakisphosphate. Science. 278:471-474.

Laussmann, T, Eujen, R, Weisshuhn, CM, Thiel, U, Vogel, G (1996) Structures of diphospho-myo-inositol pentakisphosphate and bisdiphospho-myo-inositol

tetrakisphosphate from Dictyostelium resolved by NMR analysis. Biochem J. 315:715-720.

Lea, WA, Simeonov, A (2012) Differential scanning fluorometry signatures as indicators of enzyme inhibitor mode of action: case study of glutathione S-transferase. PLoS One. 7:e36219.

Lemmon, MA (2007) Pleckstrin homology (PH) domains and phosphoinositides. Biochem Soc Symp. 81-93.

Leung, AY, Wong, PY, Gabriel, SE, Yankaskas, JR, Boucher, RC (1995) cAMP- but not Ca(2+)-regulated Cl- conductance in the oviduct is defective in mouse model of cystic fibrosis. Am J Physiol. 268:C708-712.

Lewis, KC, Selzer, T, Shahar, C, Udi, Y, Tworowski, D, Sagi, I (2008) Inhibition of pectin methyl esterase activity by green tea catechins. Phytochemistry. 69:2586-2592.

Lin, H, Fridy, PC, Ribeiro, AA, Choi, JH, Barma, DK, Vogel, G, Falck, JR, Shears, SB, York, JD, Mayr, GW (2009) Structural analysis and detection of biological inositol pyrophosphates reveal that the family of VIP/diphosphoinositol pentakisphosphate kinases are 1/3-kinases. J Biol Chem. 284:1863-1872.

Loewus, FA, Murthy, PPN (2000) myo-Inositol metabolism in plants. Plant Science. 150:1-19.

Luckhoff, A, Clapham, DE (1992) Inositol 1,3,4,5-tetrakisphosphate activates an endothelial Ca(2+)-permeable channel. Nature. 355:356-358.

Macbeth, MR, Schubert, HL, Vandemark, AP, Lingam, AT, Hill, CP, Bass, BL (2005) Inositol hexakisphosphate is bound in the ADAR2 core and required for RNA editing. Science. 309:1534-1539.

MacDonald, BT, Tamai, K, He, X (2009) Wnt/beta-catenin signaling: components, mechanisms, and diseases. Dev Cell. 17:9-26.

Madhusudan, Trafny, EA, Xuong, NH, Adams, JA, Ten Eyck, LF, Taylor, SS, Sowadski, JM (1994) cAMP-dependent protein kinase: crystallographic insights into substrate recognition and phosphotransfer. Protein Sci. 3:176-187.

Madhusudan, Akamine, P, Xuong, NH, Taylor, SS (2002) Crystal structure of a transition state mimic of the catalytic subunit of cAMP-dependent protein kinase. Nat Struct Biol. 9:273-277.

Maffucci, T, Piccolo, E, Cumashi, A, Iezzi, M, Riley, AM, Saiardi, A, Godage, HY, Rossi, C, Broggini, M, Iacobelli, S, Potter, BV, Innocenti, P, Falasca, M (2005) Inhibition of the phosphatidylinositol 3-kinase/Akt pathway by inositol pentakisphosphate results in antiangiogenic and antitumor effects. Cancer Res. 65:8339-8349.

Majerus, PW (1992) Inositol phosphate biochemistry. Annu Rev Biochem. 61:225-250.

Manning, BD, Cantley, LC (2007) AKT/PKB signaling: navigating downstream. Cell. 129:1261-1274.

Marechal, Y, Pesesse, X, Jia, Y, Pouillon, V, Perez-Morga, D, Daniel, J, Izui, S, Cullen, PJ, Leo, O, Luo, HR, Erneux, C, Schurmans, S (2007) Inositol 1,3,4,5-tetrakisphosphate controls proapoptotic Bim gene expression and survival in B cells. Proc Natl Acad Sci U S A. 104:13978-13983.

Mayr, GW, Windhorst, S, Hillemeier, K (2005) Antiproliferative plant and synthetic polyphenolics are specific inhibitors of vertebrate inositol-1,4,5-trisphosphate 3-kinases and inositol polyphosphate multikinase. J Biol Chem. 280:13229-13240.

McConnell, FM, Stephens, LR, Shears, SB (1991) Multiple isomers of inositol pentakisphosphate in Epstein-Barr-virus- transformed (T5-1) B-lymphocytes. Identification of inositol 1,3,4,5,6-pentakisphosphate, D-inositol 1,2,4,5,6-pentakisphosphate and L-inositol 1,2,4,5,6-pentakisphosphate. Biochem J. 280:323-329.

Menniti, FS, Miller, RN, Putney, JW, Jr., Shears, SB (1993) Turnover of inositol polyphosphate pyrophosphates in pancreatoma cells. J Biol Chem. 268:3850-3856.

Merchant, ML, Perkins, BA, Boratyn, GM, Ficociello, LH, Wilkey, DW, Barati, MT, Bertram, CC, Page, GP, Rovin, BH, Warram, JH, Krolewski, AS, Klein, JB (2009) Urinary peptidome may predict renal function decline in type 1 diabetes and microalbuminuria. J Am Soc Nephrol. 20:2065-2074.

Meurs, EF, Galabru, J, Barber, GN, Katze, MG, Hovanessian, AG (1993) Tumor suppressor function of the interferon-induced double-stranded RNA-activated protein kinase. Proc Natl Acad Sci U S A. 90:232-236.

Michell, RH, Kirk, CJ, Jones, LM, Downes, CP, Creba, JA (1981) The stimulation of inositol lipid metabolism that accompanies calcium mobilization in stimulated cells: defined characteristics and unanswered questions. Philos Trans R Soc Lond B Biol Sci. 296:123-138.

Millard, CJ, Watson, PJ, Celardo, I, Gordiyenko, Y, Cowley, SM, Robinson, CV, Fairall, L, Schwabe, JW (2013) Class I HDACs share a common mechanism of regulation by inositol phosphates. Mol Cell. 51:57-67.

Miller, AL, Suntharalingam, M, Johnson, SL, Audhya, A, Emr, SD, Wente, SR (2004) Cytoplasmic inositol hexakisphosphate production is sufficient for mediating the Gle1-mRNA export pathway. J Biol Chem. 279:51022-51032.

Miller, GJ, Hurley, JH (2004) Crystal structure of the catalytic core of inositol 1,4,5-trisphosphate 3-kinase. Mol Cell. 15:703-711.

Miller, GJ, Wilson, MP, Majerus, PW, Hurley, JH (2005) Specificity determinants in inositol polyphosphate synthesis: crystal structure of inositol 1,3,4-trisphosphate 5/6-kinase. Mol Cell. 18:201-212.

Mitchell, J, Wang, X, Zhang, G, Gentzsch, M, Nelson, DJ, Shears, SB (2008) An expanded biological repertoire for Ins(3,4,5,6)P4 through its modulation of ClC-3 function. Curr Biol. 18:1600-1605.

Modiano, G, Bombieri, C, Ciminelli, BM, Belpinati, F, Giorgi, S, Georges, M, Scotet, V, Pompei, F, Ciccacci, C, Guittard, C, Audrezet, MP, Begnini, A, Toepfer, M, Macek, M, Ferec, C, Claustres, M, Pignatti, PF (2005) A large-scale study of the random variability of a coding sequence: a study on the CFTR gene. Eur J Hum Genet. 13:184-192.

Monserrate, JP, York, JD (2010) Inositol phosphate synthesis and the nuclear processes they affect. Curr Opin Cell Biol. 22:365-373.

Morrison, BH, Bauer, JA, Kalvakolanu, DV, Lindner, DJ (2001) Inositol hexakisphosphate kinase 2 mediates growth suppressive and apoptotic effects of interferon-beta in ovarian carcinoma cells. J Biol Chem. 276:24965-24970.

Morrison, BH, Bauer, JA, Hu, J, Grane, RW, Ozdemir, AM, Chawla-Sarkar, M, Gong, B, Almasan, A, Kalvakolanu, DV, Lindner, DJ (2002) Inositol hexakisphosphate kinase 2 sensitizes ovarian carcinoma cells to multiple cancer therapeutics. Oncogene. 21:1882-1889.

Morrison, BH, Haney, R, Lamarre, E, Drazba, J, Prestwich, GD, Lindner, DJ (2009) Gene deletion of inositol hexakisphosphate kinase 2 predisposes to aerodigestive tract carcinoma. Oncogene. 28:2383-2392.

Mosblech, A, Thurow, C, Gatz, C, Feussner, I, Heilmann, I (2011) Jasmonic acid perception by COI1 involves inositol polyphosphates in Arabidopsis thaliana. Plant J. 65:949-957.

Mulugu, S, Bai, W, Fridy, PC, Bastidas, RJ, Otto, JC, Dollins, DE, Haystead, TA, Ribeiro, AA, York, JD (2007) A conserved family of enzymes that phosphorylate inositol hexakisphosphate. Science. 316:106-109.

Murphy, AM, Otto, B, Brearley, CA, Carr, JP, Hanke, DE (2008) A role for inositol hexakisphosphate in the maintenance of basal resistance to plant pathogens. Plant J. 56:638-652.

Murthy, PP (2006) Structure and nomenclature of inositol phosphates, phosphoinositides, and glycosylphosphatidylinositols. Subcell Biochem. 39:1-19.

Nagata, E, Luo, HR, Saiardi, A, Bae, BI, Suzuki, N, Snyder, SH (2005) Inositol hexakisphosphate kinase-2, a physiologic mediator of cell death. J Biol Chem. 280:1634-1640.

Nalaskowski, MM, Deschermeier, C, Fanick, W, Mayr, GW (2002) The human homologue of yeast ArgRIII protein is an inositol phosphate multikinase with predominantly nuclear localization. Biochem J. 366:549-556.

Norris, FA, Ungewickell, E, Majerus, PW (1995) Inositol hexakisphosphate binds to clathrin assembly protein 3 (AP-3/AP180) and inhibits clathrin cage assembly in vitro. J Biol Chem. 270:214-217.

Norris, FA, Wilson, MP, Wallis, TS, Galyov, EE, Majerus, PW (1998) SopB, a protein required for virulence of Salmonella dublin, is an inositol phosphate phosphatase. Proc Natl Acad Sci U S A. 95:14057-14059.

Odom, AR, Stahlberg, A, Wente, SR, York, JD (2000) A role for nuclear inositol 1,4,5-trisphosphate kinase in transcriptional control. Science. 287:2026-2029.

Oliver, KG, Putney, JW, Jr., Obie, JF, Shears, SB (1992) The interconversion of inositol 1,3,4,5,6-pentakisphosphate and inositol tetrakisphosphates in AR4-2J cells. J Biol Chem. 267:21528-21534.

Otto, JC, Mulugu, S, Fridy, PC, Chiou, ST, Armbruster, BN, Ribeiro, AA, York, JD (2007) Biochemical analysis of inositol phosphate kinases. Methods Enzymol. 434:171-185.

Otwinowski, Z, Minor, M (1997) Processing of X-ray Diffraction Data Collected in Oscillation Mode. Methods Enzymol. J. Carter, C.W. and R. M. Sweet. New York, Academic Press. 276:307-326.

Ozkirimli, E, Post, CB (2006) Src kinase activation: A switched electrostatic network. Protein Sci. 15:1051-1062.

Padmanabhan, U, Dollins, DE, Fridy, PC, York, JD, Downes, CP (2009) Characterization of a selective inhibitor of inositol hexakisphosphate kinases: use in defining biological roles and metabolic relationships of inositol pyrophosphates. J Biol Chem. 284:10571-10582.

Pattni, K, Banting, G (2004) Ins(1,4,5)P3 metabolism and the family of IP3-3Kinases. Cell Signal. 16:643-654.

Petersen, OH (1992) Stimulus-secretion coupling: cytoplasmic calcium signals and the control of ion channels in exocrine acinar cells. J Physiol. 448:1-51.

Phillippy, BQ, Ullah, AH, Ehrlich, KC (1994) Purification and some properties of inositol 1,3,4,5,6-Pentakisphosphate 2-kinase from immature soybean seeds. J Biol Chem. 269:28393-28399.

Piccolo, E, Vignati, S, Maffucci, T, Innominato, PF, Riley, AM, Potter, BV, Pandolfi, PP, Broggini, M, Iacobelli, S, Innocenti, P, Falasca, M (2004) Inositol pentakisphosphate promotes apoptosis through the PI 3-K/Akt pathway. Oncogene. 23:1754-1765.

Pittet, D, Schlegel, W, Lew, DP, Monod, A, Mayr, GW (1989) Mass changes in inositol tetrakis- and pentakisphosphate isomers induced by chemotactic peptide stimulation in HL-60 cells. J Biol Chem. 264:18489-18493.

Posternak, S (1919) Sur la synthese de l'ether hexaphosphorique de l'inosite avec le principe phosphoorganique de reserve des plantes vertes. Comptes Rendus de l'Académie des Sciences. 169:138-140.

Posternak, T (1965) The Cyclitols. San Francisco, CA, Holden-Day, Inc.

Pouillon, V, Hascakova-Bartova, R, Pajak, B, Adam, E, Bex, F, Dewaste, V, Van Lint, C, Leo, O, Erneux, C, Schurmans, S (2003) Inositol 1,3,4,5-tetrakisphosphate is essential for T lymphocyte development. Nat Immunol. 4:1136-1143.

Putney, JW, Jr. (1992) Inositol phosphates and calcium entry. Adv Second Messenger Phosphoprotein Res. 26:143-160.

Ranjith-Kumar, CT, Lai, Y, Sarisky, RT, Cheng Kao, C (2010) Green tea catechin, epigallocatechin gallate, suppresses signaling by the dsRNA innate immune receptor RIG-I. PLoS One. 5:e12878.

Resnick, AC, Saiardi, A (2008) Inositol polyphosphate multikinase: metabolic architect of nuclear inositides. Front Biosci. 13:856-866.

Riera, M, Fuster, JF, Palacios, L (1991) Role of erythrocyte organic phosphates in blood oxygen transport in anemic quail. Am J Physiol. 260:R798-803.

Rosen, SA, Gaffney, PR, Spiess, B, Gould, IR (2012) Understanding the relative affinity and specificity of the pleckstrin homology domain of protein kinase B for inositol phosphates. Phys Chem Chem Phys. 14:929-936.

Rudolf, MT, Dinkel, C, Traynor-Kaplan, AE, Schultz, C (2003) Antagonists of myo-inositol 3,4,5,6-tetrakisphosphate allow repeated epithelial chloride secretion. Bioorg Med Chem. 11:3315-3329.

Ruzzene, M, Di Maira, G, Tosoni, K, Pinna, LA (2010) Assessment of CK2 constitutive activity in cancer cells. Methods Enzymol. 484:495-514.

Saiardi, A, Erdjument-Bromage, H, Snowman, AM, Tempst, P, Snyder, SH (1999) Synthesis of diphosphoinositol pentakisphosphate by a newly identified family of higher inositol polyphosphate kinases. Curr Biol. 9:1323-1326.

Saiardi, A, Caffrey, JJ, Snyder, SH, Shears, SB (2000a) Inositol polyphosphate multikinase (ArgRIII) determines nuclear mRNA export in Saccharomyces cerevisiae. FEBS Lett. 468:28-32.

Saiardi, A, Caffrey, JJ, Snyder, SH, Shears, SB (2000b) The inositol hexakisphosphate kinase family. Catalytic flexibility and function in yeast vacuole biogenesis. J Biol Chem. 275:24686-24692.

Saiardi, A, Nagata, E, Luo, HR, Sawa, A, Luo, X, Snowman, AM, Snyder, SH (2001a) Mammalian inositol polyphosphate multikinase synthesizes inositol 1,4,5-trisphosphate and an inositol pyrophosphate. Proc Natl Acad Sci U S A. 98:2306-2311.

Saiardi, A, Nagata, E, Luo, HR, Snowman, AM, Snyder, SH (2001b) Identification and characterization of a novel inositol hexakisphosphate kinase. J Biol Chem. 276:39179-39185.

Saiardi, A, Sciambi, C, McCaffery, JM, Wendland, B, Snyder, SH (2002) Inositol pyrophosphates regulate endocytic trafficking. Proc Natl Acad Sci U S A. 99:14206-14211.

Saiardi, A, Bhandari, R, Resnick, AC, Snowman, AM, Snyder, SH (2004) Phosphorylation of proteins by inositol pyrophosphates. Science. 306:2101-2105.

Saiardi, A, Resnick, AC, Snowman, AM, Wendland, B, Snyder, SH (2005) Inositol pyrophosphates regulate cell death and telomere length through phosphoinositide 3-kinase-related protein kinases. Proc Natl Acad Sci U S A. 102:1911-1914.

Saiardi, A, Cockcroft, S (2008) Human ITPK1: a reversible inositol phosphate kinase/phosphatase that links receptor-dependent phospholipase C to Ca2+-activated chloride channels. Sci Signal. 1:pe5.

Sain, N, Krishnan, B, Ormerod, MG, De Rienzo, A, Liu, WM, Kaye, SB, Workman, P, Jackman, AL (2006) Potentiation of paclitaxel activity by the HSP90 inhibitor 17-allylamino-17-demethoxygeldanamycin in human ovarian carcinoma cell lines with high levels of activated AKT. Mol Cancer Ther. 5:1197-1208.

Sarmah, B, Latimer, AJ, Appel, B, Wente, SR (2005) Inositol polyphosphates regulate zebrafish left-right asymmetry. Dev Cell. 9:133-145.

Sarmah, B, Winfrey, VP, Olson, GE, Appel, B, Wente, SR (2007) A role for the inositol kinase Ipk1 in ciliary beating and length maintenance. Proc Natl Acad Sci U S A. 104:19843-19848.

Sarmah, B, Wente, SR (2009) Dual functions for the Schizosaccharomyces pombe inositol kinase Ipk1 in nuclear mRNA export and polarized cell growth. Eukaryot Cell. 8:134-146.

Sauer, K, Cooke, MP (2010) Regulation of immune cell development through soluble inositol-1,3,4,5-tetrakisphosphate. Nat Rev Immunol. 10:257-271.

Schell, MJ, Letcher, AJ, Brearley, CA, Biber, J, Murer, H, Irvine, RF (1999) PiUS (Pi uptake stimulator) is an inositol hexakisphosphate kinase. FEBS Lett. 461:169-172.

Schell, MJ (2010) Inositol trisphosphate 3-kinases: focus on immune and neuronal signaling. Cell Mol Life Sci. 67:1755-1778.

Schneider, CA, Rasband, WS, Eliceiri, KW (2012) NIH Image to ImageJ: 25 years of image analysis. Nat Methods. 9:671-675.

Shames, DS, Minna, JD (2008) IP6K2 is a client for HSP90 and a target for cancer therapeutics development. Proceedings of the National Academy of Sciences. 105:1389-1390.

Shamsuddin, AM, Yang, GY (1995) Inositol hexaphosphate inhibits growth and induces differentiation of PC-3 human prostate cancer cells. Carcinogenesis. 16:1975-1979.

Sharma, G, Singh, RP, Agarwal, R (2003) Growth inhibitory and apoptotic effects of inositol hexaphosphate in transgenic adenocarcinoma of mouse prostate (TRAMP-C1) cells. Int J Oncol. 23:1413-1418.

Shears, S (2010) The long-awaited demonstration of protein pyrophosphorylation by IP7 in vivo? Proc Natl Acad Sci U S A. 107:E17; author reply E18.

Shears, SB, Parry, JB, Tang, EK, Irvine, RF, Michell, RH, Kirk, CJ (1987) Metabolism of D-myo-inositol 1,3,4,5-tetrakisphosphate by rat liver, including the synthesis of a novel isomer of myo-inositol tetrakisphosphate. Biochem J. 246:139-147.

Shears, SB (1998) The versatility of inositol phosphates as cellular signals. Biochim Biophys Acta. 1436:49-67.

Shears, SB (2001) Assessing the omnipotence of inositol hexakisphosphate. Cell Signal. 13:151-158.

Shears, SB (2004) How versatile are inositol phosphate kinases? Biochem J. 377:265-280.

Shears, SB, Ganapathi, SB, Gokhale, NA, Schenk, TM, Wang, H, Weaver, JD, Zaremba, A, Zhou, Y (2012) Defining signal transduction by inositol phosphates. Subcell Biochem. 59:389-412.

Shen, X, Xiao, H, Ranallo, R, Wu, WH, Wu, C (2003) Modulation of ATP-dependent chromatin-remodeling complexes by inositol polyphosphates. Science. 299:112-114.

Shi, Y, Azab, AN, Thompson, MN, Greenberg, ML (2006) Inositol phosphates and phosphoinositides in health and disease. Subcell Biochem. 39:265-292.

Sicheri, F, Moarefi, I, Kuriyan, J (1997) Crystal structure of the Src family tyrosine kinase Hck. Nature. 385:602-609.

Slusarski, DC, Corces, VG, Moon, RT (1997) Interaction of Wnt and a Frizzled homologue triggers G-protein-linked phosphatidylinositol signalling. Nature. 390:410-413.

Smith, PM, Harmer, AR, Letcher, AJ, Irvine, RF (2000) The effect of inositol 1,3,4,5-tetrakisphosphate on inositol trisphosphate-induced Ca2+ mobilization in freshly isolated and cultured mouse lacrimal acinar cells. Biochem J. 347:77-82.

Solyakov, L, Cain, K, Tracey, BM, Jukes, R, Riley, AM, Potter, BV, Tobin, AB (2004) Regulation of casein kinase-2 (CK2) activity by inositol phosphates. J Biol Chem. 279:43403-43410.

Song, DH, Dominguez, I, Mizuno, J, Kaut, M, Mohr, SC, Seldin, DC (2003) CK2 phosphorylation of the armadillo repeat region of beta-catenin potentiates Wnt signaling. J Biol Chem. 278:24018-24025.

Soon, FF, Suino-Powell, KM, Li, J, Yong, EL, Xu, HE, Melcher, K (2012) Abscisic acid signaling: thermal stability shift assays as tool to analyze hormone perception and signal transduction. PLoS One. 7:e47857.

Spiers, ID, Barker, CJ, Chung, SK, Chang, YT, Freeman, S, Gardiner, JM, Hirst, PH, Lambert, PA, Michell, RH, Poyner, DR, Schwalbe, CH, Smith, AW, Solomons, KR (1996) Synthesis and iron binding studies of myo-inositol 1,2,3-trisphosphate and (+/-)-myo-inositol 1,2-bisphosphate, and iron binding studies of all myo-inositol tetrakisphosphates. Carbohydr Res. 282:81-99.

Steger, DJ, Haswell, ES, Miller, AL, Wente, SR, O'Shea, EK (2003) Regulation of chromatin remodeling by inositol polyphosphates. Science. 299:114-116.

Stephens, L, Radenberg, T, Thiel, U, Vogel, G, Khoo, KH, Dell, A, Jackson, TR, Hawkins, PT, Mayr, GW (1993) The detection, purification, structural characterization, and metabolism of diphosphoinositol pentakisphosphate(s) and bisdiphosphoinositol tetrakisphosphate(s). J Biol Chem. 268:4009-4015.

Stephens, L, Anderson, K, Stokoe, D, Erdjument-Bromage, H, Painter, GF, Holmes, AB, Gaffney, PR, Reese, CB, McCormick, F, Tempst, P, Coadwell, J, Hawkins, PT (1998) Protein kinase B kinases that mediate phosphatidylinositol 3,4,5-trisphosphate-dependent activation of protein kinase B. Science. 279:710-714.

Stephens, LR, Hawkins, PT, Morris, AJ, Downes, PC (1988) L-myo-inositol 1,4,5,6-tetrakisphosphate (3-hydroxy)kinase. Biochem J. 249:283-292.

Stephens, LR, Hawkins, PT, Stanley, AF, Moore, T, Poyner, DR, Morris, PJ, Hanley, MR, Kay, RR, Irvine, RF (1991) myo-inositol pentakisphosphates.

Structure, biological occurrence and phosphorylation to myo-inositol hexakisphosphate. Biochem J. 275:485-499.

Stevenson-Paulik, J, Odom, AR, York, JD (2002) Molecular and biochemical characterization of two plant inositol polyphosphate 6-/3-/5-kinases. J Biol Chem. 277:42711-42718.

Stokoe, D, Stephens, LR, Copeland, T, Gaffney, PR, Reese, CB, Painter, GF, Holmes, AB, McCormick, F, Hawkins, PT (1997) Dual role of phosphatidylinositol-3,4,5-trisphosphate in the activation of protein kinase B. Science. 277:567-570.

Streb, H, Irvine, RF, Berridge, MJ, Schulz, I (1983) Release of Ca2+ from a nonmitochondrial intracellular store in pancreatic acinar cells by inositol-1,4,5-trisphosphate. Nature. 306:67-69.

Stutzmann, GE (2005) Calcium dysregulation, IP3 signaling, and Alzheimer's disease. Neuroscientist. 11:110-115.

Sun, Y, Thompson, M, Lin, G, Butler, H, Gao, Z, Thornburgh, S, Yau, K, Smith, DA, Shukla, VK (2007) Inositol 1,3,4,5,6-pentakisphosphate 2-kinase from maize: molecular and biochemical characterization. Plant Physiol. 144:1278-1291.

Sweetman, D, Johnson, S, Caddick, SE, Hanke, DE, Brearley, CA (2006) Characterization of an Arabidopsis inositol 1,3,4,5,6-pentakisphosphate 2-kinase (AtIPK1). Biochem J. 394:95-103.

Szijgyarto, Z, Garedew, A, Azevedo, C, Saiardi, A (2011) Influence of inositol pyrophosphates on cellular energy dynamics. Science. 334:802-805.

Szwergold, BS, Graham, RA, Brown, TR (1987) Observation of inositol pentakis- and hexakis-phosphates in mammalian tissues by 31P NMR. Biochem Biophys Res Commun. 149:874-881.

Tan, X, Calderon-Villalobos, LI, Sharon, M, Zheng, C, Robinson, CV, Estelle, M, Zheng, N (2007) Mechanism of auxin perception by the TIR1 ubiquitin ligase. Nature. 446:640-645.

Tan, Z, Bruzik, KS, Shears, SB (1997) Properties of the inositol 3,4,5,6-tetrakisphosphate 1-kinase purified from rat liver. Regulation of enzyme activity by inositol 1,3,4-trisphosphate. J Biol Chem. 272:2285-2290.

Tantivejkul, K, Vucenik, I, Eiseman, J, Shamsuddin, AM (2003) Inositol hexaphosphate (IP6) enhances the anti-proliferative effects of adriamycin and tamoxifen in breast cancer. Breast Cancer Res Treat. 79:301-312.

Taylor, RC, Cullen, SP, Martin, SJ (2008) Apoptosis: controlled demolition at the cellular level. Nat Rev Mol Cell Biol. 9:231-241.

Ten Eyck, LF, Taylor, SS, Kornev, AP (2008) Conserved spatial patterns across the protein kinase family. Biochim Biophys Acta. 1784:238-243.

Theibert, AB, Estevez, VA, Ferris, CD, Danoff, SK, Barrow, RK, Prestwich, GD, Snyder, SH (1991) Inositol 1,3,4,5-tetrakisphosphate and inositol hexakisphosphate receptor proteins: isolation and characterization from rat brain. Proc Natl Acad Sci U S A. 88:3165-3169.

Ubersax, JA, Ferrell, JE, Jr. (2007) Mechanisms of specificity in protein phosphorylation. Nat Rev Mol Cell Biol. 8:530-541.

Vajanaphanich, M, Schultz, C, Rudolf, MT, Wasserman, M, Enyedi, P, Craxton, A, Shears, SB, Tsien, RY, Barrett, KE, Traynor-Kaplan, A (1994) Long-term uncoupling of chloride secretion from intracellular calcium levels by Ins(3,4,5,6)P4. Nature. 371:711-714.

Val, AL, Affonso, EG, Souza, RHD, Dealmeidaval, VMF, Demoura, MAF (1992) Inositol pentaphosphate in the erythrocytes of an Amazonian fish, the Pirarucu (Arapaima gigas). Canadian Journal of Zoology. 70:852-855.

Verbsky, JW, Wilson, MP, Kisseleva, MV, Majerus, PW, Wente, SR (2002) The synthesis of inositol hexakisphosphate. Characterization of human inositol 1,3,4,5,6-pentakisphosphate 2-kinase. J Biol Chem. 277:31857-31862.

Verbsky, JW, Chang, SC, Wilson, MP, Mochizuki, Y, Majerus, PW (2005a) The pathway for the production of inositol hexakisphosphate in human cells. J Biol Chem. 280:1911-1920.

Verbsky, JW, Lavine, K, Majerus, PW (2005b) Disruption of the mouse inositol 1,3,4,5,6-pentakisphosphate 2-kinase gene, associated lethality, and tissue distribution of 2-kinase expression. Proc Natl Acad Sci U S A. 102:8448-8453.

Verbsky, JW, Majerus, PW (2005) Increased levels of inositol hexakisphosphate (InsP6) protect HEK293 cells from tumor necrosis factor (alpha)- and Fas-induced apoptosis. J Biol Chem. 280:29263-29268.

Vucenik, I, Shamsuddin, AM (2003) Cancer inhibition by inositol hexaphosphate (IP6) and inositol: from laboratory to clinic. J Nutr. 133:3778S-3784S.

Vucenik, I, Shamsuddin, AM (2006) Protection against cancer by dietary IP6 and inositol. Nutr Cancer. 55:109-125.

Wang, H, Falck, JR, Hall, TM, Shears, SB (2012) Structural basis for an inositol pyrophosphate kinase surmounting phosphate crowding. Nat Chem Biol. 8:111-116.

Watson, PJ, Fairall, L, Santos, GM, Schwabe, JW (2012) Structure of HDAC3 bound to co-repressor and inositol tetraphosphate. Nature. 481:335-340.

Wilson, MP, Majerus, PW (1996) Isolation of inositol 1,3,4-trisphosphate 5/6-kinase, cDNA cloning and expression of the recombinant enzyme. J Biol Chem. 271:11904-11910.

Wilson, MP, Sun, Y, Cao, L, Majerus, PW (2001) Inositol 1,3,4-trisphosphate 5/6-kinase is a protein kinase that phosphorylates the transcription factors c-Jun and ATF-2. J Biol Chem. 276:40998-41004.

Wilson, MS, Livermore, TM, Saiardi, A (2013) Inositol pyrophosphates: between signalling and metabolism. Biochem J. 452:369-379.

Worley, PF, Baraban, JM, Snyder, SH (1989) Inositol 1,4,5-trisphosphate receptor binding: autoradiographic localization in rat brain. J Neurosci. 9:339-346.

Xie, W, Kaetzel, MA, Bruzik, KS, Dedman, JR, Shears, SB, Nelson, DJ (1996) Inositol 3,4,5,6-tetrakisphosphate inhibits the calmodulin-dependent protein kinase II-activated chloride conductance in T84 colonic epithelial cells. J Biol Chem. 271:14092-14097.

Xie, W, Solomons, KR, Freeman, S, Kaetzel, MA, Bruzik, KS, Nelson, DJ, Shears, SB (1998) Regulation of Ca2+-dependent Cl- conductance in a human colonic epithelial cell line (T84): cross-talk between Ins(3,4,5,6)P4 and protein phosphatases. J Physiol. 510:661-673.

Yang, L, Reece, J, Gabriel, SE, Shears, SB (2006) Apical localization of ITPK1 enhances its ability to be a modifier gene product in a murine tracheal cell model of cystic fibrosis. J Cell Sci. 119:1320-1328.

Yang, X, Shears, SB (2000) Multitasking in signal transduction by a promiscuous human Ins(3,4,5,6)P(4) 1-kinase/Ins(1,3,4)P(3) 5/6-kinase. Biochem J. 351:551-555.

Ye, W, Ali, N, Bembenek, ME, Shears, SB, Lafer, EM (1995) Inhibition of clathrin assembly by high affinity binding of specific inositol polyphosphates to the synapse-specific clathrin assembly protein AP-3. J Biol Chem. 270:1564-1568.

York, JD, Odom, AR, Murphy, R, Ives, EB, Wente, SR (1999) A phospholipase C-dependent inositol polyphosphate kinase pathway required for efficient messenger RNA export. Science. 285:96-100.

Zhou, D, Chen, LM, Hernandez, L, Shears, SB, Galan, JE (2001) A Salmonella inositol polyphosphatase acts in conjunction with other bacterial effectors to promote host cell actin cytoskeleton rearrangements and bacterial internalization. Mol Microbiol. 39:248-259.